
DATA-DRIVEN PARTICLE DYNAMICS: STRUCTURE-PRESERVING COARSE-GRAINING FOR EMERGENT BEHAVIOR IN NON-EQUILIBRIUM SYSTEMS

Quercus Hernández¹, Max Win¹, Thomas O'Connor², Paulo E. Arratia¹, and Nathaniel Trask¹

¹School of Engineering and Applied Science, University of Pennsylvania, 220 South 33rd Street, Philadelphia, PA 19104, USA.

²Department of Materials Science and Engineering, Carnegie Mellon University, Pittsburgh, PA, USA.

August 19, 2025

ABSTRACT

Multiscale systems are ubiquitous in science and technology, but are notoriously challenging to simulate as short spatiotemporal scales must be appropriately linked to emergent bulk physics. When expensive high-dimensional dynamical systems are coarse-grained into low-dimensional models, the entropic loss of information leads to emergent physics which are dissipative, history-dependent, and stochastic. To machine learn coarse-grained dynamics from time-series observations of particle trajectories, we propose a framework using the metriplectic bracket formalism that preserves these properties by construction; most notably, the framework guarantees discrete notions of the first and second laws of thermodynamics, conservation of momentum, and a discrete fluctuation-dissipation balance crucial for capturing non-equilibrium statistics. We introduce the mathematical framework abstractly before specializing to a particle discretization. As labels are generally unavailable for entropic state variables, we introduce a novel self-supervised learning strategy to identify emergent structural variables. We validate the method on benchmark systems and demonstrate its utility on two challenging examples: (1) coarse-graining star polymers at challenging levels of coarse-graining while preserving non-equilibrium statistics, and (2) learning models from high-speed video of colloidal suspensions that capture coupling between local rearrangement events and emergent stochastic dynamics. We provide open-source implementations in both PyTorch and LAMMPS, enabling large-scale inference and extensibility to diverse particle-based systems.

1 Introduction

Multiscale phenomena governing systems from quantum materials to geophysical flows arise from emergent behaviors across widely separated length and time scales. For example, quantum effects govern ferromagnetic ordering in magnetic materials [1], while topological entanglement leads to anomalous diffusion in polymer melts [2]. At geological length scales, the bulk evolution of soil landscapes can be tied to microstructural events such as jamming transitions in dense suspensions [3, 4]. Bridging these disparate scales is an outstanding challenge for multiscale simulation, as simulation strategies must find a way to avoid resolving prohibitively short time-scales, often by introducing a "coarse-grained" representation of unresolved processes. For example, resolution of electron motion by density functional theory (DFT) (timesteps of 10^{-15} s) or vibrational motion by molecular dynamics (MD) (timesteps of 10^{-12} s) would mandate

$10^{12} - 10^{15}$ timestep simulations to resolve $O(1)$ s engineering timescales. Coarse-grained MD has generally served as an empirical technique to hypothesize models that replace clusters or degrees of freedom (DOFs) with a single effective macroparticle with modified equations of motion, obtaining a model of decreased fidelity that is nonetheless able to capture aspects of emergent physics without explicit resolution of stiff dynamics. While best exemplified in the molecular setting, coarse-grained models can be found at continuum scales as well, e.g. large-eddy simulations filtering out high-frequency modes of turbulence, or projection-based reduced order models using principal component analysis to identify finite element simulators that can be run in real time.

Several frameworks offer mathematical formalisms for deriving and analyzing coarse-grained dynamics. The Mori-Zwanzig (MZ) formalism [5, 6, 7, 8] provides a theory to analyze the projection of full-order dynamics onto coarse-grained variables. This formalism rigorously shows how coarse-

graining induces three terms: a mean-field coarsened dynamics; a non-Markovian/history-dependent dissipative memory kernel; and a stochastic term accounting for work done by unresolved physics. Although the full-order system may be reversible, MZ establishes the need to rigorously treat non-Markovian stochasticity and dissipation in a consistent manner; the work done on the system by fluctuations must exactly balance the dissipation from memory to ensure energy is conserved. This is an example of *detailed fluctuation-dissipation balance* [9, 10]. In non-equilibrium systems, this provides a probabilistic formalism for modeling the transfer of energy from unresolved non-equilibrium fluctuations and resolved state variables via dissipative mechanisms.

While a flurry of works have aimed to employ machine learning (ML) dimension reduction to coarse-grained systems, these techniques have been primarily successful in *supervised* contexts. In molecular systems, this is described as *force-matching*; a data-driven MD can be identified which maps local atom configuration to the same potential prescribed by a more costly DFT calculation [11]. AlphaFold [12], perhaps the current most successful technique, maps directly from a protein sequence to a final configuration as a regression without modeling the interim dynamical process. As regression-based techniques, "black-box" supervised learning models suffer from an inability to perform out-of-distribution inference and do not generally "see" the notions of structure prescribed by MZ, although many are increasingly considering other notions of structure-preservation (e.g. equivariant/invariant embeddings, permutation invariance).

2 Prior literature

2.1 Force matching

In computational materials science, force matching is a powerful technique employed to construct accurate and efficient interatomic potentials by parameterizing a pair potential and minimizing the difference between the predicted forces and those computed from high-fidelity quantum mechanical calculations. Graph Neural Networks have attracted attention as a potential architecture, as short-range particle interactions are naturally interpreted as interactions on epsilon-ball graphs. Traditional message passing GNNs [13, 14, 15] were soon upgraded with equivariant [16, 17, 18, 19] and invariant [20, 21, 22] feature processing. Due to the increasing popularity of large language models, attention-based Transformer architectures [23] have also been explored for molecule property prediction [24, 25, 26]. Generative diffusion-based algorithms [27, 28] have been proven to be effective for generative protein docking models.

The main disadvantage of force matching methods is that they rely on prior knowledge of *ab initio* calculations based on costly quantum mechanics simulations, and are often tested over small molecule benchmark datasets. Secondly, they provide no model for the emergent statistical behavior, typically "fitting to the mean" of a bottom-up forcing, precluding fitting models "top-down" from continuum observations. As a result,

successes have primarily focused on up-scaling DFT to MD without accessing mesoscale or continuum scale data sources.

2.2 Coarse-graining models

Traditional coarse-graining methods aim to reduce the dimensionality of the simulation so that computational cost is dramatically decreased. Early particle models include dissipative particle dynamics (DPD) [29] or smoothed-dissipative particle dynamics (SDPD) [30]. These methods model the conservative, dissipative, and noise terms arising from the unresolved degrees of freedom of the system empirically, often using the MZ formalism for justification. Many extensions of DPD/SDPD may be found in the literature [31], including to multiphase flows [32], free surface flows [33] or many-body interactions [34].

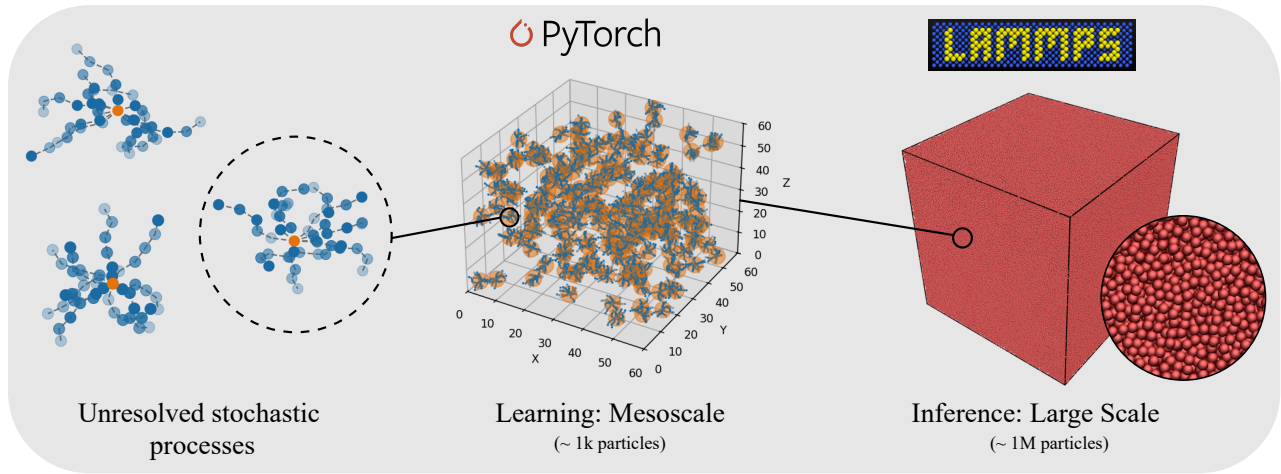
Machine learning models have also recently emerged trying to emulate the same principles. Bottleneck architectures such as autoencoders [35, 36, 37] are a popular choice due to their simplicity. Graph neural networks are also a common choice [38, 39], as they can include aggregation functions over graph substructures in a U-Net Graph-Autoencoder approach. However, none of the mentioned works incorporate physical structure governing non-equilibrium statistics into the architecture, and typically fit to the mean of data. The current work can be viewed as a hybrid method, mimicking the mathematical structure of SDPD, but replacing traditional discretizations of known physics with machine-learnable notions of volume, energy, and dissipation brackets that can capture arbitrary fluctuating physics from data.

2.3 Structure-preserving algorithms

Apart from purely data-driven approaches, a parallel research direction focuses on embedding physical structure into learned dynamics, drawing from variational mechanics. These efforts include learning Lagrangian [40] or Hamiltonian [41, 42, 43] principles to recover conservative systems that inherently respect symplectic structure and energy conservation. This perspective has been extended to dissipative dynamics via generalized variational principles [44, 45, 46], as well as through soft [47, 48] or hard constraints [49, 50, 51], and Onsager-based single-bracket formulations [52, 53].

In this work, we adopt the metriplectic formalism (also known with small technical distinction as GENERIC [54, 55]) as a principled alternative to Mori–Zwanzig projection. Metriplectic dynamics generalize Hamiltonian mechanics by introducing a second bracket that enforces entropy production alongside energy conservation. Though metriplectic systems can be derived from the Mori–Zwanzig theory [56], their algebraic bracket structure maps more naturally onto automatic differentiation and neural architectures. While Lagrangian and Hamiltonian neural networks are well established [40, 41, 42, 43], metriplectic learning has seen limited adoption: existing methods either rely on penalty-based constraints that fail to preserve structure exactly [47, 48], or require expensive bracket construction that limits scalability to small systems [49, 50, 51].

A Coarse-grained acceleration of multibody physics



B Structure-preserving model direct from experiments

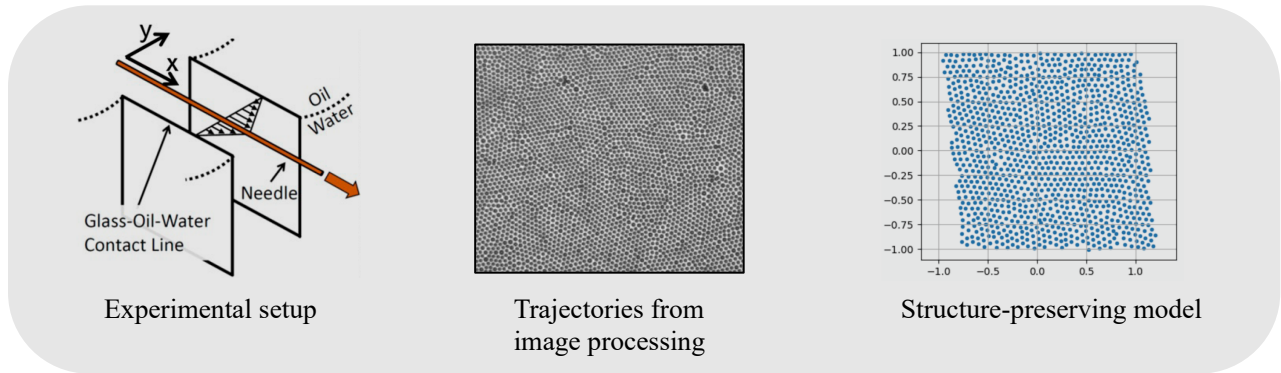


Figure 1: Exemplar applications using data-driven particle dynamics to bridge scales in simulated (top) and experimental (bottom) datasets. (A) Detailed simulation of polymers fully resolve stochastic fluctuations (left), in-silico experiments of a small domain supervise model discovery (middle), yielding a data-driven model for non-equilibrium bulk response solved in a massive parallel simulator (right). (B) A 2D suspension in an oscillatory shear flow provides a rich multiphysics/multiscale exemplar incorporating lubrication, electrostatics, contact, and stochasticity (left). Trajectories of particle data are extracted using computer vision techniques, providing complete but noisy data to supervise model collection (center), ultimately yielding a model which predicts linkages between structure and emergent dynamics (right).

Here, we introduce a scalable metriplectic architecture based on localized pairwise particle interactions, achieving linear $O(N)$ complexity and enabling integration with large-scale particle simulators such as LAMMPS. The open-source implementation (<https://github.com/PIMILab>) represents the first demonstration of scalable, learned metriplectic dynamics.

Our framework is notable in two respects. First, it is *interpretable*: it consists of small subnetworks that predict physically meaningful quantities such as temperature, pressure, energy, and entropy, which can be either supervised or inferred post hoc. Second, it addresses a core challenge in coarse-grained modeling: internal variables describing unresolved states (e.g., entropy) are typically unmeasurable in experiments [57, 35]. We resolve this via a *self-supervised* learning strategy that discovers both latent variables and their dy-

namics in a thermodynamically consistent manner. In concert, this framework produces scalable models that are able to learn emergent physics tied to stochastic unresolved phenomena.

3 Results

We apply the methodology to three test cases. First, we learn a coarse-grained model of an ideal gas and demonstrate that it preserves statistics under extrapolation to unseen boundary conditions, traditionally a major challenge for deep-learning approaches. Second, we push the coarse-graining further by modeling two star polymer systems with increasing chain length. In every molecular dynamics scenario, we roll out the simulations far beyond the training horizon to evaluate position and velocity correlation statistics. Comparisons

are benchmarked against a "black-box" Graph Network-based Solver [58] (GNS), the same model with a stochastic forcing and maximum-likelihood loss to better treat statistics [59] (GNS-SDE), and a vanilla DPD model with optimal parameters calibrated by gradient descent (DPD); see Appendix F for details. Finally, we show that the framework may incorporate other kinds of physics by introducing mechanical strain energy as an additional energetic contribution, allowing us to consider viscoelastic materials and dense electrokinetic suspension systems.

3.1 Introductory toy problem: Ideal gas

We first consider an ideal gas in a 3D periodic box over three different forcings to demonstrate out-of-distribution generalization, sketched in Fig. 2. Training is performed for vortex forcing (TAYLOR-GREEN, [60]), while inference is tested under configurations unseen during training for an unforced system (SELF-DIFFUSION) and shear forcing via Lees-Edwards boundary conditions (SHEAR FLOW, [61]).

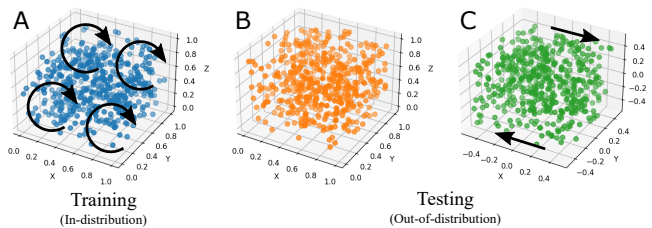


Figure 2: IDEAL GAS datasets. Flow configurations for (A) TAYLOR-GREEN training dataset, and (B) SELF DIFFUSION and (C) SHEAR FLOW testing datasets. We confirm generalization of non-equilibrium statistics in (B) and (C) despite distinct flow conditions held out during training.

Table 1 and Fig. 9 demonstrate good agreement between the proposed methodology and spatial statistics. On the other hand, both GNS and GNS-SDE fail to capture the statistics of the flow or offer an improvement relative to DPD; they predict a nearly flat RDF, meaning that the prediction lacks spatial structure and correlations. Both the VACF and MSD deviate from the ground truth by orders of magnitude, which suggests that they overestimate the velocity and dissipation. Similarly, the deviation in the MSD shows an overestimation of the diffusion regime, totally misrepresenting the stochastic dynamics of the system. This highlights the major qualitative impact physical structure preservation has on even simple systems, and that "black-box" techniques are poor candidates for coarse-graining. Without any ML, the well-calibrated DPD model outperforms these methods with drastically fewer parameters.

Now we test the same model under two different periodic boundary conditions without any additional training. The results for both tests are shown in Table 1. We can observe that our method maintains its performance under extrapolation to unseen flows while the traditional GNN methods diverge in longer rollouts.

Table 1: L2 relative error (\downarrow) of correlation metrics for the IDEAL GAS interpolation and extrapolation experiments and STAR POLYMER examples.

		VACF	RDF	MSD
TAYLOR-GREEN	GNS	1.09e4	3.27e-1	2.24e4
	GNS-SDE	8.23e4	3.40e-1	1.70e5
	DPD	3.25e-1	4.41e-2	2.66e-1
	Ours	5.18e-2	9.82e-3	7.73e-2
SELF-DIFFUSION	GNS	1.02e4	3.15e-1	1.94e4
	GNS-SDE	6.46e4	3.27e-1	1.23e5
	DPD	4.52e-1	4.44e-2	4.65e-1
	Ours	4.19e-2	1.59e-2	4.54e-2
SHEAR FLOW	GNS	7.59e5	3.43e-1	3.45e-1
	GNS-SDE	1.47e5	2.94e-1	3.74e-1
	DPD	2.18e-1	3.68e-2	4.64e-2
	Ours	7.94e-2	1.12e-2	3.76e-2
STAR POLYMER 11	GNS	1.25e6	4.29e-1	2.09e6
	GNS-SDE	3.87e5	4.27e-1	6.45e5
	DPD	6.66e-1	2.26e-1	9.51e-1
	Ours	9.89e-2	1.99e-2	4.73e-2
STAR POLYMER 51	GNS	1.27e1	2.13e-1	2.12e1
	GNS-SDE	7.97e6	2.23e-1	1.61e7
	DPD	4.00e0	9.64e-2	7.63e0
	Ours	1.41e-1	5.28e-2	5.32e-2

We have also included two additional tests to provide visual intuition of our algorithm's performance in inference; these cases have not been held out during training. Fig. 10 shows how the proposed method achieves the correct average velocity shear profile with respect to the reference solution for the SHEAR FLOW dataset. Fig. 11 shows the inferred SELF-DIFFUSION mixing of a domain scaled up to $L = 2$.

3.2 Challenging coarse graining experiment: Star polymer

The next consider a star polymer melt in a 3D periodic box. Each polymer is composed of a core atom and 10 arms bonded by a FENE potential, whereas the interaction between polymers is modeled by a Lennard-Jones potential. Two different internal configurations are considered: 1 and 5 beads per arm, which results in less and higher coarse-graining levels (Fig. 3). The fully resolved datasets are generated using LAMMPS [62] and then coarse-grained by computing the center of mass position and velocity of each polymer. The results are shown in Table 1 and Fig. 4. We observe that, similar to the previous dataset, the correct statistics are obtained.

3.3 Weak scaling study

Table 2 shows the per timestep performance of the tested models in a serial implementation. The models have been optimized with the TorchScript compiler and run on a single GPU over a $T = 2000$ timestep run. As expected, the vanilla DPD model exhibits the highest computational efficiency among the models evaluated, primarily due to its minimal architecture with only four trainable parameters. Our method is within a factor of two of GNS/GNS-SDE, as we employ multiple in-

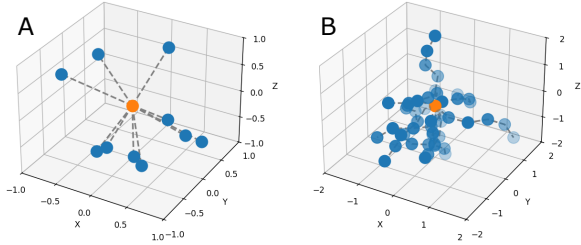


Figure 3: Representative star polymers coarse grained into a single data-driven particle in STAR POLYMER datasets. (A) STAR POLYMER 11 with 1 core, 10 arms and 1 bead per arm. (B) STAR POLYMER 51 with 1 core, 10 arms and 5 beads per arm.

ternal neural networks. Importantly, all coarse-grained models achieve significantly faster runtimes than the fully resolved dynamics, demonstrating the computational benefits of coarse-graining.

Table 2: Time performance (mean \pm std) in ms/step (\downarrow) for the evaluated methods and the fully resolved dynamics (full-order).

	IDEAL GAS	STAR POLYMER 11	STAR POLYMER 51
GNS	1.32 ± 0.04	1.93 ± 0.03	2.51 ± 0.02
GNS-SDE	2.57 ± 0.02	3.75 ± 0.04	4.99 ± 0.04
DPD	0.17 ± 0.00	0.18 ± 0.00	0.17 ± 0.00
Ours	5.98 ± 0.05	6.12 ± 0.06	6.00 ± 0.08
Full-order	-	21.87	74.40

Given a trained model, we provide code to perform inference in LAMMPS [62] as a custom pair style. LAMMPS is an exascale code, and thus provides a means of taking models trained on small systems and performing inference on arbitrarily large numbers of particles. In Fig. 5 we analyze weak scaling performance up to 8 million coarse-grained particles over 64 processors.

4 Extension to general physics problems

The above choice of energy is appropriate for a fluid-like system which stores energy only via dilatation. We now demonstrate how broader classes of physics may be considered by extending the definition of potential energy functional to handle additional inputs by adding a tensorial strain energy dependence appropriate for solid systems. This allows the model to account for reversible effects stored elastically as shear stresses, which are not present in fluids. The derivation of dissipative and noise terms is independent of this addition and remains unchanged; this case serves as an example for how to add additional reversible physics in the framework.

4.1 Viscoelastic solid

We consider next a viscoelastic material under shear to demonstrate the capture of strain energy (Fig. 6 and 7). The predic-

tions of the model are in good agreement with the reference finite element solution, up to a large 50% strain. The model is also able to complete a full cycle starting from rest and returning to its original configuration after a relaxation period.

4.2 Measured dataset: jammed colloidal system

Finally, we consider an experimental dataset of particle trajectories extracted from a jammed two-dimensional (2D) monolayer of repulsive microspheres in suspension under a cyclic shear forcing [63]. The system consists of sulfate latex particles adsorbed at a water-decane interface, forming a soft jammed material due to electrostatic dipole-dipole repulsion. The material is sheared using an interfacial stress rheometer (ISR), where a magnetized needle applies oscillatory shear stress within a confined channel [63, 64]. High-resolution optical microscopy is used to capture the positions of each particle, processed with a computer vision particle tracking algorithm, and velocities are obtained with finite differences. This system integrates fluid, electrostatic, solid-like behavior of jammed polycrystals, and contact physics, highlighting the broad applicability of the framework.

We can observe in Fig. 7 that the RDF statistics are faithfully predicted, showing that the model can capture the relative structure rearrangements of the material. We have performed additional metrics to evaluate the prediction of dynamical properties, based on the non-affine displacement (D_{\min}^2) clusters [65]. As shown in Fig. 12, we can predict the hyperbolic motion of dislocations, the local rearrangements of clusters of particles and the average trend of the dislocation distribution with different time lags in a full cycle. In Fig. 12 we compare the statistics of the same dislocation metric histograms of both the reference and the predicted simulations and we observe that, up to a constant factor of 20%, the model can reproduce the statistics of local non-affine rearrangements. The model is mechanically resolving the force dipole driving displacement events but underestimating the magnitude of the interaction. As highlighted in [64] and citing work, the prediction of the mechanism driving dislocation dynamics has proven elusive to the community, and it is remarkable that the mechanism (a rare event) emerges from a training of top-down statistics.

5 Discussion

We have presented a deep learning methodology to construct physical models of conservative, dissipative, and stochastic effects which are consistent with the laws of thermodynamics and satisfy the fluctuation-dissipation theorem. The model is supervised by time-series data for position and velocity only, with a self-supervised technique identifying emergent entropic variables that govern dissipative physics. The technique successfully captures the coarse-grained response of molecular systems using only top-down information, providing a new alternative to traditional bottom-up models extracted from density functional theory. We have further demonstrated that diverse physics may be handled by modifying the internal energy

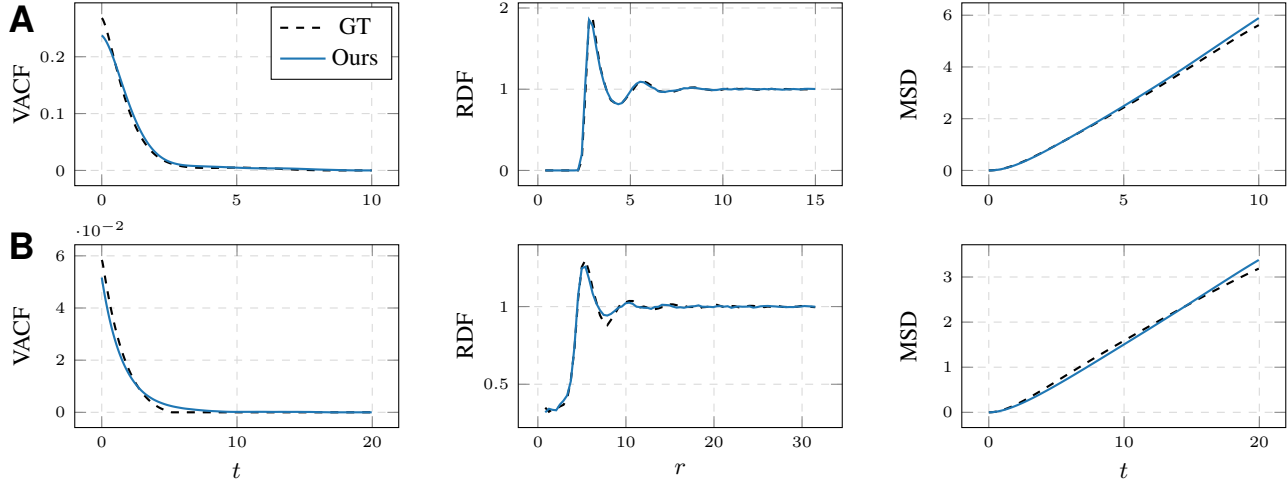


Figure 4: Correlation metrics for the (A) STAR POLYMER 11 and (B) STAR POLYMER 51 datasets, establishing recovery of structure and dissipative response.

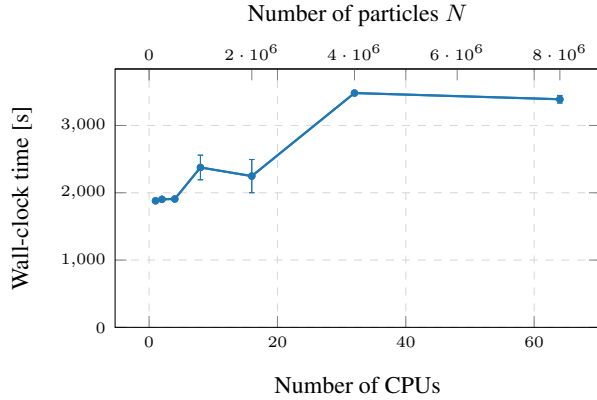


Figure 5: Computation time required for a fixed number of CPUs per processor without GPU acceleration. A flat curve denotes weak scaling, demonstrating that systems of arbitrary size may be considered by scaling CPUs.

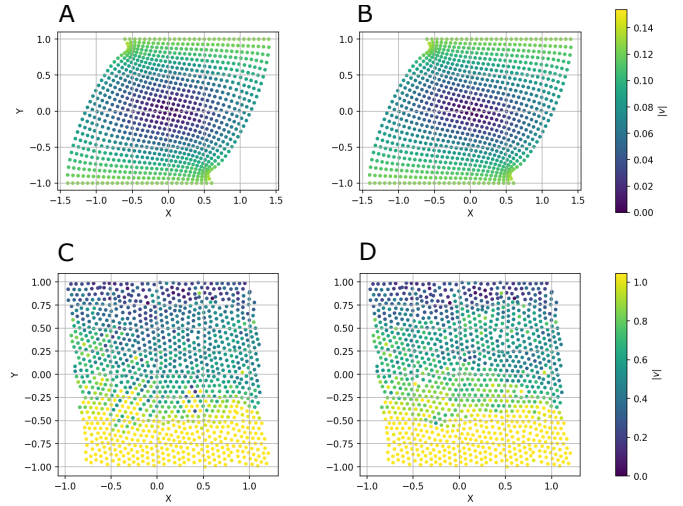


Figure 6: Intermediate snapshot from the VISCOELASTIC and NEEDLE datasets. Color encodes velocity magnitude. (A) and (C) Prediction rollout of the neural network. (B) and (D) Ground truth reference solution.

functional, allowing us to capture viscoelasticity and electrokinetic suspensions in a common framework.

The presented methodology is mostly agnostic to the architectural choice of the machine-learnable quantities. The algorithm could be improved with more sophisticated architectures such as cross-attention [66] or conditioning over parametric variables such as differing molecule types. One might also use, e.g. graph autoencoders to directly map from microstructure configuration to the emergent entropy variable rather than using self-supervised learning [67, 68]. We have chosen to demonstrate the framework with simple dense network architectures to highlight the significance of structure-preservation without relying on large datasets or transformers which may not be tractable to curate in data-sparse experimental settings.

6 Materials and Methods

Let \boldsymbol{x} be a set of a dynamical system state variables. In metriplectic dynamics, the deterministic evolution of \boldsymbol{x} is given by

$$d\boldsymbol{x} = \left[\boldsymbol{L} \frac{\partial E}{\partial \boldsymbol{x}} + \boldsymbol{M} \frac{\partial S}{\partial \boldsymbol{x}} + k_B \frac{\partial}{\partial \boldsymbol{x}} \cdot \boldsymbol{M} \right] dt + d\tilde{\boldsymbol{x}}. \quad (1)$$

where $E(\boldsymbol{x})$ and $S(\boldsymbol{x})$ are functionals prescribing generalized energy and entropy of the system, $\boldsymbol{L}(\boldsymbol{x}) = -\boldsymbol{L}^T$ is a skew-symmetric Poisson matrix and $\boldsymbol{M}(\boldsymbol{x}) = \boldsymbol{M}^T$ is a symmetric positive semi-definite friction matrix. These two terms prescribe the reversible and irreversible dynamics of the system,

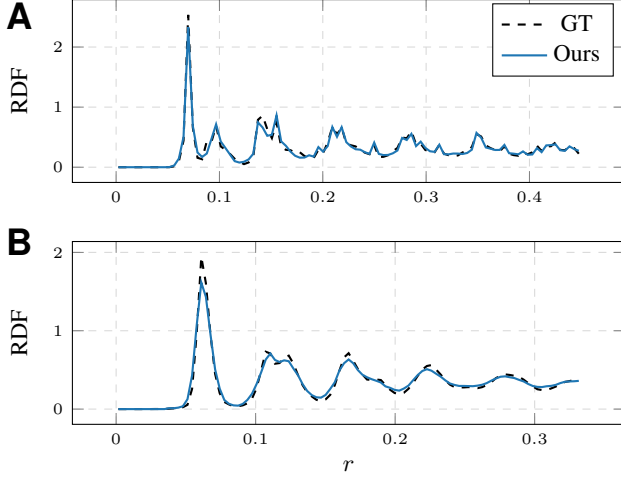


Figure 7: Radial Distribution Function for the (A) VISCOELASTIC and (B) NEEDLE datasets, indicating the correct prediction of structural statistics.

respectively. By imposing the degeneracy conditions,

$$\mathbf{L}\nabla S = \mathbf{M}\nabla E = \mathbf{0},$$

the dynamics satisfy the following discrete versions of the first and second laws of thermodynamics independent of the choice of state variables; these degeneracy conditions are challenging to impose in machine learning contexts. The stochastic effects $d\tilde{\mathbf{x}}$ are directly related to the dissipative effects via the fluctuation-dissipation theorem [9, 10]:

$$d\tilde{\mathbf{x}}d\tilde{\mathbf{x}}^T = 2k_B\mathbf{M}dt, \quad (2)$$

where k_B is the Boltzmann constant, meaning that $d\tilde{\mathbf{x}}$ is an infinitesimal of order $1/2$. Intuitively, the extra mechanical work induced by random fluctuation should be balanced with the dissipation forces to maintain thermodynamical equilibrium. We prove in the SI conservation properties and fluctuation-dissipation principles for dynamics of this class.

Proposition 6.1. *Eq. (1) satisfies energy conservation $dE = 0$ if $\mathbf{M}\nabla E = \mathbf{0}$ and $d\tilde{\mathbf{x}} \cdot \nabla E = 0$.*

Proof. See proof in Appendix B.1. \square

We next demonstrate a general construction for metriplectic dynamics as a dissipative/stochastic perturbation of an arbitrary non-canonical Hamiltonian system. While we later specialize this to particles, the technique can be applied to any discrete system (e.g. finite element simulations or circuit models). Assume that the state \mathbf{x} can be partitioned into reversible and irreversible variables $\mathbf{x} = (\mathbf{x}_{\text{rev}}, \mathbf{x}_{\text{irr}})$ such that in the absence of irreversibility

$$d\mathbf{x}_{\text{rev}} = \mathbf{L}_{\text{rev}} \frac{\partial E}{\partial \mathbf{x}_{\text{rev}}} dt,$$

or in other words, $\mathbf{L}_{\text{rev}} = -\mathbf{L}_{\text{rev}}^T$ prescribes non-canonical Hamiltonian dynamics for \mathbf{x}_{rev} . Under the further assumption that the reversible state can be written in terms of generalized

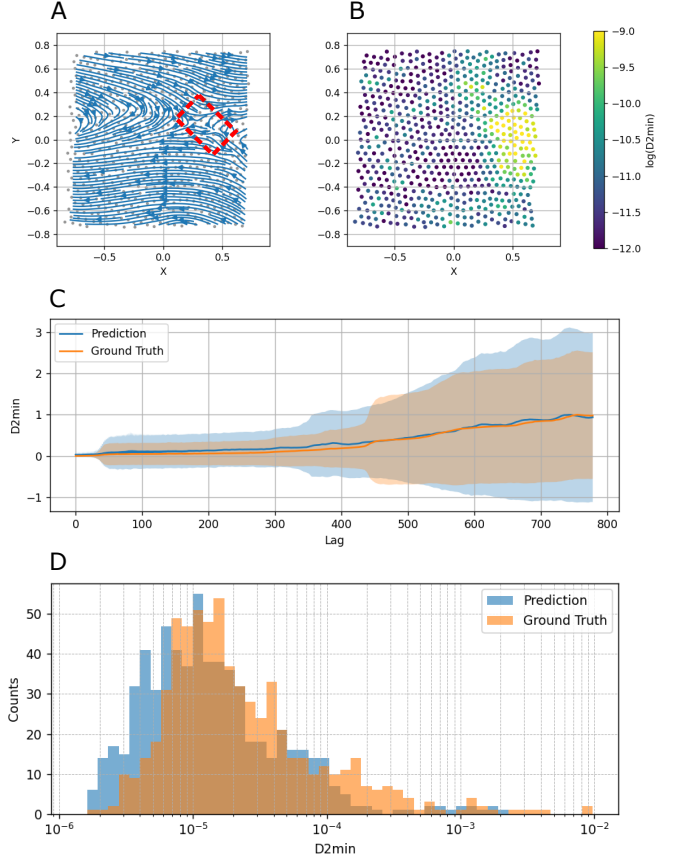


Figure 8: Dynamical properties of the network predictions on the NEEDLE dataset for a domain crop. (A) Streamlines computed from displacements for a lag of 200 snapshots of the first cycle. The red square identifies a hyperbolic motion of a dislocation event fully predicted by the neural network. Predicting the force dipole driving the displacement hopping has been a major challenge for the rheology community. (B) Non-affine squared displacement field (D_{\min}^2), where the hotspots represent non-affine deformation clusters, highlighting that the learned model is able to identify dislocation events. (C) Normalized mean and standard deviation of D_{\min}^2 for different lag times on a peak-to-peak cycle. While the magnitude of the force dipole driving the displacement is underestimated, after normalization we observe qualitative agreement with experiment. (D) Histogram of non-affine displacements for lag 150.

position-momentum coordinates such that $\mathbf{x}_{\text{rev}} = (\mathbf{q}, \mathbf{p})$ and $\mathbf{x} = (\mathbf{q}, \mathbf{p}, \mathbf{x}_{\text{irr}})$, we define the Poisson matrix as a block system

$$\mathbf{L} = \begin{bmatrix} \mathbf{L}_{\text{rev}} & \mathbf{0} \\ \mathbf{0} & \mathbf{0} \end{bmatrix}$$

If we assume that the entropic variable depends only on the irreversible state $S(\mathbf{x}_{\text{irr}})$ then the degeneracy condition $\mathbf{L}\nabla S = \mathbf{0}$ holds trivially. To construct noise and dissipation compatible with the other degeneracy conditions $\mathbf{M}\nabla E = \mathbf{0}$ and $d\tilde{\mathbf{x}} \cdot \nabla E = 0$, we express the noise based on the Cholesky

decomposition of $M = QQ^T$ as $d\tilde{x} = QdW$. We enforce the degeneracy condition via the ansatz,

$$Q_{ji} = C_{ijk} \frac{\partial E}{\partial x_k},$$

where C_{ijk} is a sparse 3-tensor with the skew-symmetry $C_{ijk} = -C_{ikj}$. See Proposition B.4 for the detailed derivation specifying a precise functional form.

With the degeneracy conditions satisfied, we have thus arrived at a construction for a metriplectic system. We construct metriplectic ML architectures via the following "metriplectic cookbook":

1. Select reversible \mathbf{x}_{rev} and irreversible variables \mathbf{x}_{irr} such that $\mathbf{x} = (\mathbf{x}_{\text{rev}}, \mathbf{x}_{\text{irr}})$.
2. Develop parameterized energies and entropies, assuming functional dependencies $E(\mathbf{x}_{\text{rev}}, \mathbf{x}_{\text{irr}})$ and $S(\mathbf{x}_{\text{irr}})$.
3. Develop a parametrization of $d\tilde{x}$ (and consequently M) consistent with the fluctuation-dissipation theorem.
4. Use the metriplectic Eq. (1) to determine the dynamical equations.
5. Use maximum likelihood to fit the architecture to experimental data, using a marginal distribution over subsets of degrees of freedom to minibatch and maintain $O(1)$ training.
6. Introduce a self-supervised "teacher network" to identify unobservable \mathbf{x}_{irr} labels during training.

6.1 Data-driven particle dynamics

Consider now a collection of N particles with positions \mathbf{r}_i and velocities $\mathbf{v}_i = \frac{d\mathbf{r}_i}{dt}$ for $i \in V = \{1, \dots, N\}$. We introduce energy and entropy functionals

$$E = \sum_i \left[\frac{1}{2} m_i v_i^2 + U_i \right], \quad S = \sum_i S_i,$$

where: $m_i = m$ is a particle mass, assumed to be constant; S_i is a per particle entropy; $U_i = U(\mathcal{V}_i, S_i)$ is a function prescribing per particle internal energy; and $\mathcal{V}_i(\mathbf{r}_1, \dots, \mathbf{r}_N)$ is a per particle volume which will be prescribed as a function of neighboring particle positions. We identify this with the general framework of the previous section by selecting generalized position and momentum $(\mathbf{q}_i, \mathbf{p}_i)$ as $\mathbf{x}_{\text{rev},i} = (\mathbf{r}_i, \mathbf{v}_i)$ and selecting entropy as the irreversible variable $\mathbf{x}_{\text{irr},i} = S_i$.

Recall the first law of thermodynamics $dU = TdS - PdV$, from which we may define per particle temperature and pressure as partials of U

$$T_i = \frac{\partial U_i}{\partial S_i}, \quad P_i = -\frac{\partial U_i}{\partial \mathcal{V}_i}.$$

For these choices, the gradients of energy and entropy are given by

$$\frac{\partial E}{\partial \mathbf{x}_i} = \begin{bmatrix} \frac{\partial U}{\partial \mathbf{r}_i} \\ m_i \mathbf{v}_i \\ T_i \end{bmatrix}, \quad \frac{\partial S}{\partial \mathbf{x}_i} = \begin{bmatrix} \mathbf{0} \\ \mathbf{0} \\ 1 \end{bmatrix}.$$

Substituting these expressions into Eq. (1) we obtain per particle dynamics

$$\underbrace{\begin{bmatrix} d\mathbf{r}_i \\ d\mathbf{v}_i \\ dS_i \end{bmatrix}}_{d\mathbf{x}_i} = \sum_j \left(\underbrace{\frac{1}{m} \begin{bmatrix} \mathbf{0} & \mathbf{I}\delta_{ij} & \mathbf{0} \\ -\mathbf{I}\delta_{ij} & \mathbf{0} & \mathbf{0} \\ \mathbf{0} & \mathbf{0} & \mathbf{0} \end{bmatrix}}_{L_{ij}} \underbrace{\begin{bmatrix} \frac{\partial U}{\partial \mathbf{r}_j} \\ m\mathbf{v}_j \\ T_j \end{bmatrix}}_{\frac{\partial E}{\partial \mathbf{x}_j}} \right) + \underbrace{\begin{bmatrix} \mathbf{0} \\ \mathbf{0} \\ 1 \end{bmatrix}}_{\frac{\partial S}{\partial \mathbf{x}_j}} + k_B \frac{\partial}{\partial \mathbf{x}_j} \cdot \mathbf{M}_{ij} \Big) dt + \underbrace{\begin{bmatrix} d\tilde{\mathbf{r}}_i \\ d\tilde{\mathbf{v}}_i \\ d\tilde{S}_i \end{bmatrix}}_{d\tilde{\mathbf{x}}_i}. \quad (3)$$

6.2 Machine learnable parameterizations

To close this system of equations, we will introduce small neural networks shared across all particles to define:

- Particle volume $\mathcal{V}_i(\mathbf{r}_1, \dots, \mathbf{r}_N)$.
- Per particle internal energy $U_i(\mathcal{V}_i, S_i)$
- Thermal fluctuations $d\tilde{x} = QdW$.

After specifying these terms, M may be calculated from Q , providing a closed system of equations in Eq. (3). For simplicity all neural networks are taken as shallow multilayer perceptrons, unless otherwise noted. There is substantial room for improvement to adopt more sophisticated e.g. graph attention networks or transformers. We have been able to achieve state-of-the-art results with simple architectures and so choose to present this work with minimal complexity in the ML architecture; the simple MLPs adopted here have the added benefit of being amenable to finite difference calculation of gradients at inference time, allowing a fast implementation in LAMMPS.

We stress that in contrast to traditional particle methods, the operators are not constructed to discretize a known PDE; rather, we impose algebraic symmetries which impose structure preservation to build a "model skeleton", and then use observational data to "flesh out the skeleton".

6.2.1 Volume definition

To obtain a method which scales as $O(N)$ in the number of particles, we prescribe \mathcal{V} to include only contributions from particles within a neighborhood of radius h , denoted as $\mathcal{N}_i = \{j \in V, |\mathbf{r}_{ij}| < h\}$ and parameterize the volume

$$\frac{1}{\mathcal{V}_i} = \sum_{j \in \mathcal{N}_i} W_{ij} = \sum_{j \in \mathcal{N}_i} \exp \left[\text{MLP}_{\mathcal{V}} \left(\frac{|\mathbf{r}_{ij}|}{h}; \theta_{\mathcal{V}} \right) \right] \left(1 - \frac{|\mathbf{r}_{ij}|^2}{h^2} \right)_+, \quad (4)$$

where for convenience we define the inverse volume $d_i = \mathcal{V}_i^{-1}$, $\mathbf{r}_{ij} = \mathbf{r}_i - \mathbf{r}_j$ denotes the relative positions between particle i and neighboring particles $j \in \mathcal{N}_i$, and $|\cdot|$ denotes the Euclidean norm.

This amounts to a message passing/aggregation network with no attention mechanism. We require only that W be positive to ensure a positive volume for each particle. In light of Noethers theorem, we require that W be invariant under shifts in coordinate to ensure momentum conservation, which

we impose by using a radial kernel. More sophisticated graph attention mechanisms, deep message passing networks, and non-radial shift invariant architectures could be incorporated without compromising structure preservation.

We note that this architecture is inspired by classical particle methods such as SPH, where particle volume is defined via a kernel density estimate, see [69, 70], and other works which assign a "virtual" notion of volume to particles [71, 72].

6.2.2 Convexity and monotonicity of internal energy

In classical variational mechanics, the Gibbs relations mandate that internal energy must respect certain convexity and monotonicity constraints to preserve hyperbolicity in the resulting equations. Equivalently, from a simple physical perspective, pressure and temperature must be positive, requiring $\partial_V U \leq 0$ and $\partial_S U \geq 0$. The second derivatives define the isothermal compressibility and the specific heat at constant volume, respectively, and must also be positive, i.e. U is convex in both arguments. In this work, we employ the recently proposed Constrained Monotonic Neural Network [73]:

$$U_i = \text{CMNN}_U(S_i, \mathcal{V}_i; \theta_U). \quad (5)$$

guaranteeing by construction that the first and second arguments be monotonically decreasing and increasing, respectively. This is achieved by enforcing the weight signs, and ensure the convexity by using softplus activation functions so that no constrained optimizers need to be used to obtain a thermodynamically consistent internal energy. For more details, see Appendix D.

6.2.3 Stochastic fluctuations

When specializing the general ansatz (Eq. (1)) to a particle setting, additional care must be taken to ensure that forces satisfy conservation of linear and angular momentum. Motivated by [30], we assume a functional form for which random forcing in $d\tilde{\mathbf{v}}$ consists only of pairwise interactions, from which the degeneracy conditions enforce as a consequence:

$$\begin{aligned} m d\tilde{\mathbf{v}}_i &= \sqrt{2k_B} \sum_{j \in \mathcal{N}_i} \left[A_{ij} d\bar{\mathbf{W}}_{ij} + B_{ij} \frac{\mathbf{I}}{D} \text{tr}(d\mathbf{W}_{ij}) \right] \mathbf{e}_{ij}, \\ T_i d\tilde{S}_i &= -\frac{\sqrt{2k_B}}{2} \sum_{j \in \mathcal{N}_i} \left[A_{ij} d\bar{\mathbf{W}}_{ij} + B_{ij} \frac{\mathbf{I}}{D} \text{tr}(d\mathbf{W}_{ij}) \right] : \mathbf{e}_{ij} \mathbf{v}_{ij} \\ &\quad + \sqrt{2k_B} \sum_{j \in \mathcal{N}_i} C_{ij} dV_{ij}, \end{aligned} \quad (6)$$

where $A_{ij} = A_{ji}$, $B_{ij} = B_{ji}$ and $C_{ij} = C_{ji}$ are ij -symmetric functions of the position and entropy of the particles, D is the dimension of the problem and $\mathbf{e}_{ij} = \mathbf{r}_{ij}/|\mathbf{r}_{ij}|$ is the interdistance unitary vector. The Wiener differentials $d\mathbf{W}_{ij} = d\mathbf{W}_{ji}$ and $dV_{ij} = -dV_{ji}$ are symmetric and skew-symmetric, respectively, with regard to particle labels i, j . Their components are independent zero mean and unit variance Gaussian increments which are uncorrelated in components and particle index except if they belong to the same interaction (more details in Appendix A).

Unlike in [30], where A , B , and C were chosen to arrive at an accurate discretization of the fluctuating Navier-Stokes equations, we instead define shallow MLPs to identify state-dependent nonlinear scalings of the fluctuations

$$\begin{aligned} A_{ij} &= \text{MLP}_A \left(\frac{|\mathbf{r}_{ij}|}{h}, T_i; \theta_A \right) \cdot \text{MLP}_A \left(\frac{|\mathbf{r}_{ij}|}{h}, T_j; \theta_A \right), \\ B_{ij} &= \text{MLP}_B \left(\frac{|\mathbf{r}_{ij}|}{h}, T_i; \theta_B \right) \cdot \text{MLP}_B \left(\frac{|\mathbf{r}_{ij}|}{h}, T_j; \theta_B \right), \\ C_{ij} &= \text{MLP}_C \left(\frac{|\mathbf{r}_{ij}|}{h}, T_i; \theta_C \right) \cdot \text{MLP}_C \left(\frac{|\mathbf{r}_{ij}|}{h}, T_j; \theta_C \right), \end{aligned}$$

parametrized by $\theta_A, \theta_B, \theta_C$, which ensures the symmetry over particle pair indices and the functional dependency of viscosity with temperature. Additionally, we include the Boltzmann constant k_B and the particle mass m as trainable parameters to tune the relative importance of stochastic fluctuations relative to conservative dynamics. This is optional and can be replaced with their actual value, consistent with the units of the studied problem.

6.3 Dynamic equations

With the specified parameterization and using the metriplectic equation in Eq. (3), we can finally summarize the dynamic equations of the method:

$$\begin{aligned} d\mathbf{r}_i &= \mathbf{v}_i dt \\ m d\mathbf{v}_i &= -\frac{\partial U}{\partial \mathbf{r}_i} dt + \mathbf{F}_{\text{diss}}^v + \mathbf{F}_{\text{div}}^v + m d\tilde{\mathbf{v}}_i \\ T_i dS_i &= F_{\text{diss}}^S + F_{\text{div}}^S + T_i d\tilde{S}_i \end{aligned}$$

where F_{diss} are the dissipative terms and F_{div} the divergence terms of the dynamics, balanced out by the fluctuation-dissipation theorem. The developed formulation ensures the following conservation laws:

Proposition 6.2. *The metriplectic equation in Eq. (3) satisfies momentum conservation $d\mathbf{P} = \mathbf{0}$.*

Proof. See proof in Proposition B.1. \square

Proposition 6.3. *The metriplectic equation in Eq. (3) satisfies energy conservation $dE = 0$.*

Proof. See proof in Proposition B.2. \square

6.4 Self-supervision of entropy

While position and velocity are easily measurable either in experimental or by post-processed synthetic data (e.g. fully resolved MD data), calculating entropy would require an enumeration of microstates which is intractable for the vast majority of cases. To fully supervise the system, we therefore need to generate time-series labels of \mathbf{x}_{irr} . This has been a challenge for several works which have aimed to machine learn metriplectic dynamics [51, 47], limiting their applicability to small degree of freedom systems. In this work we adopt a self-supervised approach which allows scalability to massive numbers of degrees of freedom.

To generate labels for S_i , we introduce an auxiliary edge convolutional operator [74] which constructs a closure for the entropy in terms of position and velocity

$$S_i = \frac{1}{|\mathcal{N}_i|} \sum_{j \in \mathcal{N}_i} \text{MLP}_S \left(\frac{|\mathbf{r}_{ij}|}{h}, \mathbf{v}_{ij}; \theta_S \right).$$

In principle, this architecture could incorporate position-velocity information from a finite time history. For simplicity however, we present results using only information from the current timestep. In light of the fluctuation-dissipation theorem, we conjecture that knowledge of the energy dissipated (present in the position and velocity fields) is sufficient to identify the magnitude of the corresponding entropy increment.

We highlight that this architecture is *not* a closure in the dynamics—at the conclusion of training \mathcal{M} is prescribed, the self-supervision network is discarded, and at inference time entropy is instead evolved by solution of Equation 1.

6.5 Training via log-likelihood

Let $\mathcal{D} = \{(\mathbf{x}_{\text{rev}}^t, \mathbf{x}_{\text{rev}}^{t+1})\}_{t=0}^{N_{\text{train}}}$ be a dataset consisting of position-velocity pairs. To train the system, we construct a joint probability distribution $p(\mathbf{x}_{\text{rev}}^{t+1}, \mathbf{x}_{\text{irr}}^{t+1} | \mathbf{x}_{\text{rev}}^t, \mathbf{x}_{\text{irr}}^t)$ corresponding to a numerical integration of Equation 1 and train the architectures with maximum likelihood. We denote all trainable parameters via

$$\Theta = \{\theta_V, \theta_U, \theta_A, \theta_B, \theta_C, \theta_S, k_B, m\}$$

and define the maximum log-likelihood objective

$$\Theta^* = \arg \min_{\Theta} \text{NLL}(x^1, \dots, x^T).$$

Through a marginalization procedure detailed in Appendix C, Section 3, we can split the problem as per particle-wise loss corresponding to the multivariate Gaussian distribution:

$$\begin{aligned} \boldsymbol{\mu}_i^{t+1} &= \begin{bmatrix} \mathbf{v}_i^t + \frac{d\mathbf{v}_i^t}{dt} \Delta t \\ S_i^t + \frac{dS_i^t}{dt} \Delta t \end{bmatrix}, \\ \boldsymbol{\Sigma}_{ii}^{t+1} &= \begin{bmatrix} \Delta \tilde{\mathbf{v}}_i \Delta \tilde{\mathbf{v}}_i^T & \Delta \tilde{\mathbf{v}}_i \Delta \tilde{S}_i \\ \Delta \tilde{S}_i \Delta \tilde{\mathbf{v}}_i^T & \Delta \tilde{S}_i \Delta \tilde{S}_i \end{bmatrix}. \end{aligned}$$

Thus the final loss function is defined as

$$\begin{aligned} \mathcal{L} &= \frac{1}{N_{\text{train}}} \sum_{t=0}^{N_{\text{train}}} \frac{1}{N} \sum_{i=0}^N \left[\frac{1}{2} \ln |\boldsymbol{\Sigma}_{ii}^{t+1}| \right. \\ &\quad \left. + \frac{1}{2} (\mathbf{x}_i^{t+1} - \boldsymbol{\mu}_i^{t+1})^T (\boldsymbol{\Sigma}_{ii}^{t+1})^{-1} (\mathbf{x}_i^{t+1} - \boldsymbol{\mu}_i^{t+1}) \right], \end{aligned}$$

which can be minimized using standard batch gradient descent.

6.6 Test metrics

The proposed method is compared with three previous baseline methods, which include no conservation laws nor thermodynamical priors:

- GNS [58]: Message-passing graph neural network with an encoder-process-decoder structure, originally coined as "Graph Network-based Simulator".

- GNS-SDE [59]: Modification of GNS to handle stochastic dynamics by learning the drift and diffusion coefficients of a black-box stochastic differential equation.
- DPD [29]: Classic Dissipative Particle Dynamics with conservative, dissipative and random forces, ensuring the fluctuation-dissipation theorem. The fit of the DPD parameters are performed with gradient descent maximizing the log-likelihood of the predictions, providing a baseline for a well-calibrated classical model.

The benchmark algorithms are trained in fair conditions using the same training procedure and integrator as the presented method (see Appendix F for more details). All methods are tested over long rollouts over 25 times the training set, to ensure steady-state statistics are achieved. Three metrics are considered: velocity autocorrelation function, radial distribution function and mean squared displacement, defined as the following ensemble averages:

$$\begin{aligned} \text{VACF}(t) &= \langle \mathbf{v}(\tau) \cdot \mathbf{v}(\tau + t) \rangle, \\ \text{RDF}(r) &= \frac{\langle \rho(r) \rangle}{\rho}, \\ \text{MSD}(t) &= \langle |\mathbf{r}(\tau) - \mathbf{r}(\tau + t)|^2 \rangle, \end{aligned}$$

where $\rho(r)$ is the local number density of particles at distance r and τ is a dummy variable representing the initial reference time over which ensemble averages are computed. Reproducing all three correlation metrics is necessary to correctly capture the dynamic behavior of the molecular dynamic system [75]:

- VACF: This metric evaluates how the velocity of a particle at one time is correlated with its velocity at a later time, and provides insight into the momentum relaxation of the system. The integral of the function is the self-diffusion coefficient of the system.
- RDF: This metric measures how the particle density varies as a function of distance from a reference particle. It is related to the structural organization and relative arrangements of particles, and is strongly determined by the conservative forces of the system.
- MSD: This metric quantifies the average squared distance that particles travel over time. It is used to characterize the diffusive behavior of particles and distinguish between different transport regimes. It is related to the VACF via the Green-Kubo relations [76, 77].

The VACF, RDF, and MSD curves are compared with the ground truth statistics through the point-wise L2 relative error:

$$\varepsilon_{\mathbf{y}} = \frac{|\mathbf{y}_{\text{GT}} - \mathbf{y}_{\text{pred}}|}{|\mathbf{y}_{\text{GT}}|}.$$

The code was implemented using Pytorch Geometric [78], and is publicly available online at <https://github.com/PIMILab>. All the experiments were performed using Adam optimizer [79] and run on a single NVIDIA H200 GPU. The dataset generation and hyperparameter details can be found in Appendix G.

6.7 Extension to new physics

To extend the method to viscoelastic, we first need to recall the law of thermodynamics for deformed bodies [80] as $dU = TdS + \boldsymbol{\sigma} : d\boldsymbol{\varepsilon}$. By applying a volumetric and deviatoric decomposition of the stress tensor $\boldsymbol{\sigma}^{\alpha\beta} = -P\delta^{\alpha\beta} + \boldsymbol{\tau}^{\alpha\beta}$, we obtain $dU = TdS - Pd\mathcal{V} + \boldsymbol{\tau} : d\bar{\boldsymbol{\varepsilon}}$ where \mathcal{V} is the volume and $\boldsymbol{\tau}$ and $\bar{\boldsymbol{\varepsilon}}$ are the traceless stress and strain tensors. This is the same as the previous equation of state in Eq. (5) with an additional shear elastic energy component. Now we may define per particle temperature, pressure and deviatoric stress as partials of U

$$T_i = \frac{\partial U_i}{\partial S_i}, \quad P_i = -\frac{\partial U_i}{\partial \mathcal{V}_i}, \quad \boldsymbol{\tau}_i = \frac{\partial U_i}{\partial \bar{\boldsymbol{\varepsilon}}_i}.$$

To model the traceless strain tensor, we propose a similar parametrization to Eq. (4) but enforce symmetries via

$$\boldsymbol{\varepsilon}_i = \sum_{j \in \mathcal{N}_i} \mathbf{W}_{ij} = \sum_{j \in \mathcal{N}_i} \frac{1}{2} (\mathbf{l}_{ij} + \mathbf{l}_{ij}^T),$$

$$\mathbf{l}_{ij} = \text{MLP}_{\boldsymbol{\varepsilon}} \left(\frac{\mathbf{u}_{ij}}{h}, \frac{\mathbf{r}_{ij}^0}{h}; \theta_{\boldsymbol{\varepsilon}} \right) - \text{MLP}_{\boldsymbol{\varepsilon}} \left(\mathbf{0}, \frac{\mathbf{r}_{ij}^0}{h}; \theta_{\boldsymbol{\varepsilon}} \right),$$

where \mathbf{l}_{ij} is a lower triangular matrix whose entries are computed using a multilayer perceptron parametrized by $\theta_{\boldsymbol{\varepsilon}}$, $\mathbf{r}_{ij}^0 = \mathbf{r}_i^0 - \mathbf{r}_j^0$ is the undeformed configuration relative positions and $\mathbf{u}_{ij} = \mathbf{r}_{ij} - \mathbf{r}_{ij}^0$ is the displacement with respect to the reference configuration. This parametrization ensures zero strain under zero displacements and is also invariant under coordinate transformations. Finally, we subtract the trace to obtain a traceless strain tensor which will give rise to shear stresses,

$$\bar{\boldsymbol{\varepsilon}}_i = \boldsymbol{\varepsilon}_i - \frac{\mathbf{I}}{D} \text{tr}(\boldsymbol{\varepsilon}_i) = \sum_{j \in \mathcal{N}_i} \bar{\mathbf{W}}_{ij},$$

where D is the dimension of the problem. This formulation is inspired in large strain elasticity, but many other options could be considered based on classic SPH deformation gradient tensor or equivariant architectures. In regard to the internal energy model, we assume additive internal energies with similar monotonicity and convexity constraints as in the fluid model case (convex in the strain argument, as its second derivative represent the elasticity tensor):

$$U_i = U_i^{\text{vol}} + U_i^{\text{dev}} = \text{CMNN}_{U^{\text{vol}}}(S_i, \mathcal{V}_i; \theta_{U^{\text{vol}}}) + \text{CMNN}_{U^{\text{dev}}}(S_i, I(\bar{\boldsymbol{\varepsilon}}_i); \theta_{U^{\text{dev}}}),$$

where $I(\bar{\boldsymbol{\varepsilon}}_i)$ are the $D - 1$ non-zero invariants of the traceless strain tensor. The additional terms in the conservative dynamics equation can be found in .

The results are evaluated with L2 relative error in position and RDF function to evaluate the structural fidelity of the predictions. As for the dynamics, we use the non-affine displacement (D_{\min}^2) which evaluates how much the local neighbourhood of a particle deviates from an affine transformation between two time snapshots.

$$D_{\min}^2(t_1, t_2) = \min_j \langle |\mathbf{u}_i(t_1) - \mathbf{J}\mathbf{u}_j(t_2)|^2 \rangle,$$

where \mathbf{J} is the best least squares fit local deformation gradient.

Acknowledgements

We thank Pep Español and George Karniadakis for their insightful feedback and valuable discussions throughout the development of this work. We also acknowledge Joel T. Clemmer for his assistance with the LAMMPS code implementation and Aleksandra Vojvodic for the computational resources.

References

- [1] Jin Soo Lim, Diomedes Saldana-Greco, and Andrew M Rappe. Improper magnetic ferroelectricity of nearly pure electronic nature in helicoidal spiral camn 7 o 12. *Physical Review B*, 97(4):045115, 2018.
- [2] Thomas C O’Connor, Ting Ge, Michael Rubinstein, and Gary S Grest. Topological linking drives anomalous thickening of ring polymers in weak extensional flows. *Physical review letters*, 124(2):027801, 2020.
- [3] Douglas J Jerolmack and Karen E Daniels. Viewing earth’s surface as a soft-matter landscape. *Nature Reviews Physics*, 1(12):716–730, 2019.
- [4] Robert Kostynick, Hadis Matinpour, Shravan Pradeep, Sarah Haber, Alban Sauret, Eckart Meiburg, Thomas Dunne, Paulo Arratia, and Douglas Jerolmack. Rheology of debris flow materials is controlled by the distance from jamming. *Proceedings of the National Academy of Sciences*, 119(44):e2209109119, 2022.
- [5] Robert Zwanzig. Ensemble method in the theory of irreversibility. *The Journal of Chemical Physics*, 33(5):1338–1341, 1960.
- [6] Hazime Mori. Transport, collective motion, and brownian motion. *Progress of theoretical physics*, 33(3):423–455, 1965.
- [7] Hermann Grabert. *Projection operator techniques in nonequilibrium statistical mechanics*, volume 95. Springer, 2006.
- [8] Robert Zwanzig. *Nonequilibrium statistical mechanics*. Oxford university press, 2001.
- [9] Herbert B Callen and Theodore A Welton. Irreversibility and generalized noise. *Physical Review*, 83(1):34, 1951.
- [10] Rep Kubo. The fluctuation-dissipation theorem. *Reports on progress in physics*, 29(1):255, 1966.
- [11] Stefan Chmiela, Alexandre Tkatchenko, Huziel E Sauceda, Igor Poltavsky, Kristof T Schütt, and Klaus-Robert Müller. Machine learning of accurate energy-conserving molecular force fields. *Science advances*, 3(5):e1603015, 2017.
- [12] John Jumper, Richard Evans, Alexander Pritzel, Tim Green, Michael Figurnov, Olaf Ronneberger, Kathryn Tunyasuvunakool, Russ Bates, Augustin Žídek, Anna Potapenko, et al. Highly accurate protein structure prediction with alphafold. *nature*, 596(7873):583–589, 2021.

- [13] Justin Gilmer, Samuel S Schoenholz, Patrick F Riley, Oriol Vinyals, and George E Dahl. Neural message passing for quantum chemistry. In *International conference on machine learning*, pages 1263–1272. PMLR, 2017.
- [14] Anuroop Sriram, Abhishek Das, Brandon M Wood, Siddharth Goyal, and C Lawrence Zitnick. Towards training billion parameter graph neural networks for atomic simulations. *arXiv preprint arXiv:2203.09697*, 2022.
- [15] Linfeng Zhang, Jiequn Han, Han Wang, Roberto Car, and Weinan E. Deep potential molecular dynamics: a scalable model with the accuracy of quantum mechanics. *Physical review letters*, 120(14):143001, 2018.
- [16] Nathaniel Thomas, Tess Smidt, Steven Kearnes, Lusann Yang, Li Li, Kai Kohlhoff, and Patrick Riley. Tensor field networks: Rotation-and translation-equivariant neural networks for 3d point clouds. *arXiv preprint arXiv:1802.08219*, 2018.
- [17] Maurice Weiler, Mario Geiger, Max Welling, Wouter Boomsma, and Taco S Cohen. 3d steerable cnns: Learning rotationally equivariant features in volumetric data. *Advances in Neural information processing systems*, 31, 2018.
- [18] Risi Kondor, Zhen Lin, and Shubhendu Trivedi. Clebsch–gordan nets: a fully fourier space spherical convolutional neural network. *Advances in Neural Information Processing Systems*, 31, 2018.
- [19] Johannes Brandstetter, Rob Hesselink, Elise van der Pol, Erik J Bekkers, and Max Welling. Geometric and physical quantities improve e(3) equivariant message passing. *arXiv preprint arXiv:2110.02905*, 2021.
- [20] Kristof Schütt, Pieter-Jan Kindermans, Huziel Enoc Saucedo Felix, Stefan Chmiela, Alexandre Tkatchenko, and Klaus-Robert Müller. Schnet: A continuous-filter convolutional neural network for modeling quantum interactions. *Advances in neural information processing systems*, 30, 2017.
- [21] Johannes Gasteiger, Janek Groß, and Stephan Günnemann. Directional message passing for molecular graphs. *arXiv preprint arXiv:2003.03123*, 2020.
- [22] Yi Liu, Limei Wang, Meng Liu, Yuchao Lin, Xuan Zhang, Bora Oztekin, and Shuiwang Ji. Spherical message passing for 3d molecular graphs. In *International Conference on Learning Representations (ICLR)*, 2022.
- [23] Ashish Vaswani, Noam Shazeer, Niki Parmar, Jakob Uszkoreit, Llion Jones, Aidan N Gomez, Łukasz Kaiser, and Illia Polosukhin. Attention is all you need. *Advances in neural information processing systems*, 30, 2017.
- [24] Philipp Thölke and Gianni De Fabritiis. Torchmdnet: equivariant transformers for neural network based molecular potentials. *arXiv preprint arXiv:2202.02541*, 2022.
- [25] Tuan Le, Frank Noé, and Djork-Arné Clevert. Equivariant graph attention networks for molecular property prediction. *arXiv preprint arXiv:2202.09891*, 2022.
- [26] Yi-Lun Liao and Tess Smidt. Equiformer: Equivariant graph attention transformer for 3d atomistic graphs. *arXiv preprint arXiv:2206.11990*, 2022.
- [27] Bowen Jing, Hannes Stärk, Tommi Jaakkola, and Bonnie Berger. Generative modeling of molecular dynamics trajectories. *arXiv preprint arXiv:2409.17808*, 2024.
- [28] Majdi Hassan, Nikhil Shenoy, Jungyoon Lee, Hannes Stärk, Stephan Thaler, and Dominique Beaini. Et-flow: Equivariant flow-matching for molecular conformer generation. *Advances in Neural Information Processing Systems*, 37:128798–128824, 2024.
- [29] Robert D Groot and Patrick B Warren. Dissipative particle dynamics: Bridging the gap between atomistic and mesoscopic simulation. *The Journal of chemical physics*, 107(11):4423–4435, 1997.
- [30] Pep Espanol and Mariano Revenga. Smoothed dissipative particle dynamics. *Physical Review E*, 67(2):026705, 2003.
- [31] MB Liu, GR Liu, LW Zhou, and JZ3402522 Chang. Dissipative particle dynamics (dpd): an overview and recent developments. *Archives of Computational Methods in Engineering*, 22:529–556, 2015.
- [32] Domenico Davide Meringolo, Agostino Lauria, Francesco Aristodemo, and Pasquale Fabio Filianoti. Large eddy simulation within the smoothed particle hydrodynamics: Applications to multiphase flows. *Physics of Fluids*, 35(6), 2023.
- [33] Jiannong Fang, Aurèle Parriaux, Martin Rentschler, and Christophe Ancey. Improved sph methods for simulating free surface flows of viscous fluids. *Applied numerical mathematics*, 59(2):251–271, 2009.
- [34] Yining Han, Jaehyeok Jin, and Gregory A Voth. Constructing many-body dissipative particle dynamics models of fluids from bottom-up coarse-graining. *The Journal of Chemical Physics*, 154(8), 2021.
- [35] Wujie Wang and Rafael Gómez-Bombarelli. Coarse-graining auto-encoders for molecular dynamics. *npj Computational Materials*, 5(1):125, 2019.
- [36] Wujie Wang and Rafael Gómez-Bombarelli. Learning coarse-grained particle latent space with auto-encoders. *Adv. Neural Inf. Process. Syst.*, 1, 2019.
- [37] Agnieszka Ilnicka and Gisbert Schneider. Designing molecules with autoencoder networks. *Nature Computational Science*, 3(11):922–933, 2023.
- [38] Brooke E Husic, Nicholas E Charron, Dominik Lemm, Jiang Wang, Adrià Pérez, Maciej Majewski, Andreas Krämer, Yaoyi Chen, Simon Olsson, Gianni De Fabritiis, et al. Coarse graining molecular dynamics with graph neural networks. *The Journal of chemical physics*, 153(19), 2020.
- [39] Xiang Fu, Tian Xie, Nathan J Rebello, Bradley D Olsen, and Tommi Jaakkola. Simulate time-integrated coarse-grained molecular dynamics with multi-scale graph networks. *arXiv preprint arXiv:2204.10348*, 2022.

- [40] Miles Cranmer, Sam Greydanus, Stephan Hoyer, Peter Battaglia, David Spergel, and Shirley Ho. Lagrangian neural networks. *arXiv preprint arXiv:2003.04630*, 2020.
- [41] Samuel Greydanus, Misko Dzamba, and Jason Yosinski. Hamiltonian neural networks. *Advances in neural information processing systems*, 32, 2019.
- [42] Marco David and Florian Méhats. Symplectic learning for hamiltonian neural networks. *Journal of Computational Physics*, 494:112495, 2023.
- [43] Zhengdao Chen, Jianyu Zhang, Martin Arjovsky, and Léon Bottou. Symplectic recurrent neural networks. *arXiv preprint arXiv:1909.13334*, 2019.
- [44] Yaofeng Desmond Zhong, Biswadip Dey, and Amit Chakraborty. Dissipative symoden: Encoding hamiltonian dynamics with dissipation and control into deep learning. *arXiv preprint arXiv:2002.08860*, 2020.
- [45] Andrew Sosanya and Sam Greydanus. Dissipative hamiltonian neural networks: Learning dissipative and conservative dynamics separately. *arXiv preprint arXiv:2201.10085*, 2022.
- [46] Shanshan Xiao, Jiawei Zhang, and Yifa Tang. Generalized lagrangian neural networks. *arXiv preprint arXiv:2401.03728*, 2024.
- [47] Quercus Hernández, Alberto Badías, David González, Francisco Chinesta, and Elías Cueto. Structure-preserving neural networks. *Journal of Computational Physics*, 426:109950, 2021.
- [48] Quercus Hernández, Alberto Badías, Francisco Chinesta, and Elías Cueto. Thermodynamics-informed graph neural networks. *IEEE Transactions on Artificial Intelligence*, 5(3):967–976, 2022.
- [49] Zhen Zhang, Yeonjong Shin, and George Em Karniadakis. Gfnnns: Generic formalism informed neural networks for deterministic and stochastic dynamical systems. *Philosophical Transactions of the Royal Society A*, 380(2229):20210207, 2022.
- [50] Kookjin Lee, Nathaniel Trask, and Panos Stinis. Machine learning structure preserving brackets for forecasting irreversible processes. *Advances in Neural Information Processing Systems*, 34:5696–5707, 2021.
- [51] Anthony Gruber, Kookjin Lee, and Nathaniel Trask. Reversible and irreversible bracket-based dynamics for deep graph neural networks. *Advances in Neural Information Processing Systems*, 36:38454–38484, 2023.
- [52] Haijun Yu, Xinyuan Tian, Weinan E, and Qianxiao Li. Onsagernet: Learning stable and interpretable dynamics using a generalized onsager principle. *Physical Review Fluids*, 6(11):114402, 2021.
- [53] Shenglin Huang, Zequn He, and Celia Reina. Variational onsager neural networks (vonns): A thermodynamics-based variational learning strategy for non-equilibrium pdes. *Journal of the Mechanics and Physics of Solids*, 163:104856, 2022.
- [54] Miroslav Grmela and Hans Christian Öttinger. Dynamics and thermodynamics of complex fluids. i. development of a general formalism. *Physical Review E*, 56(6):6620, 1997.
- [55] Hans Christian Öttinger and Miroslav Grmela. Dynamics and thermodynamics of complex fluids. ii. illustrations of a general formalism. *Physical Review E*, 56(6):6633, 1997.
- [56] Alexander Mielke, Mark A Peletier, and Johannes Zimmer. Deriving a generic system from a hamiltonian system. *arXiv preprint arXiv:2404.09284*, 2024.
- [57] Thomas N Thiem, Mahdi Kooshkbaghi, Tom Bertalan, Carlo R Laing, and Ioannis G Kevrekidis. Emergent spaces for coupled oscillators. *Frontiers in computational neuroscience*, 14:36, 2020.
- [58] Alvaro Sanchez-Gonzalez, Jonathan Godwin, Tobias Pfaff, Rex Ying, Jure Leskovec, and Peter Battaglia. Learning to simulate complex physics with graph networks. In *International conference on machine learning*, pages 8459–8468. PMLR, 2020.
- [59] Naura Dridi, Lucas Drumetz, and Ronan Fablet. Learning stochastic dynamical systems with neural networks mimicking the euler-maruyama scheme. In *2021 29th European Signal Processing Conference (EUSIPCO)*, pages 1990–1994. IEEE, 2021.
- [60] Geoffrey Ingram Taylor and Albert Edward Green. Mechanism of the production of small eddies from large ones. *Proceedings of the Royal Society of London. Series A-Mathematical and Physical Sciences*, 158(895):499–521, 1937.
- [61] Arthur W Lees and Samuel F Edwards. The computer study of transport processes under extreme conditions. *Journal of Physics C: Solid State Physics*, 5(15):1921, 1972.
- [62] Steve Plimpton. Fast parallel algorithms for short-range molecular dynamics. *Journal of computational physics*, 117(1):1–19, 1995.
- [63] Nathan C Keim and Paulo E Arratia. Mechanical and microscopic properties of the reversible plastic regime in a 2d jammed material. *Physical review letters*, 112(2):028302, 2014.
- [64] K Lawrence Galloway, Xiaoguang Ma, Nathan C Keim, Douglas J Jerolmack, Arjun G Yodh, and Paulo E Arratia. Scaling of relaxation and excess entropy in plastically deformed amorphous solids. *Proceedings of the National Academy of Sciences*, 117(22):11887–11893, 2020.
- [65] M.L. Falk and J.S. Langer. Dynamics of viscoplastic deformation in amorphous solids. *Phys. Rev. E*, 57(6):7192–7205, 1998.
- [66] A Waswani, N Shazeer, N Parmar, J Uszkoreit, L Jones, A Gomez, L Kaiser, and I Polosukhin. Attention is all you need. In *NIPS*, 2017.
- [67] Junhyun Lee, Inyeop Lee, and Jaewoo Kang. Self-attention graph pooling. In *International conference on machine learning*, pages 3734–3743. pmlr, 2019.

- [68] Zhen Zhang, Jiajun Bu, Martin Ester, Jianfeng Zhang, Chengwei Yao, Zhi Yu, and Can Wang. Hierarchical graph pooling with structure learning. *arXiv preprint arXiv:1911.05954*, 2019.
- [69] Joe J Monaghan. Smoothed particle hydrodynamics. In: *Annual review of astronomy and astrophysics. Vol. 30 (A93-25826 09-90)*, p. 543-574., 30:543–574, 1992.
- [70] Joseph P Morris, Patrick J Fox, and Yi Zhu. Modeling low reynolds number incompressible flows using sph. *Journal of computational physics*, 136(1):214–226, 1997.
- [71] Edmond Kwan-yu Chiu, Qiqi Wang, Rui Hu, and Antony Jameson. A conservative mesh-free scheme and generalized framework for conservation laws. *SIAM Journal on Scientific Computing*, 34(6):A2896–A2916, 2012.
- [72] Nathaniel Trask, Pavel Bochev, and Mauro Perego. A conservative, consistent, and scalable meshfree mimetic method. *Journal of Computational Physics*, 409:109187, 2020.
- [73] Davor Runje and Sharath M Shankaranarayana. Constrained monotonic neural networks. In *International Conference on Machine Learning*, pages 29338–29353. PMLR, 2023.
- [74] Yue Wang, Yongbin Sun, Ziwei Liu, Sanjay E Sarma, Michael M Bronstein, and Justin M Solomon. Dynamic graph cnn for learning on point clouds. *ACM Transactions on Graphics (tog)*, 38(5):1–12, 2019.
- [75] David Chandler and Jerome K Percus. Introduction to modern statistical mechanics, 1988.
- [76] Melville S Green. Markoff random processes and the statistical mechanics of time-dependent phenomena. ii. irreversible processes in fluids. *The Journal of chemical physics*, 22(3):398–413, 1954.
- [77] Ryogo Kubo. Statistical-mechanical theory of irreversible processes. i. general theory and simple applications to magnetic and conduction problems. *Journal of the physical society of Japan*, 12(6):570–586, 1957.
- [78] Matthias Fey and Jan Eric Lenssen. Fast graph representation learning with pytorch geometric. *arXiv preprint arXiv:1903.02428*, 2019.
- [79] Diederik P Kingma. Adam: A method for stochastic optimization. *arXiv preprint arXiv:1412.6980*, 2014.
- [80] Lev Davidovich Landau, LP Pitaevskii, Arnold Markovich Kosevich, and Evgenii Mikhailovich Lifshitz. *Theory of elasticity: volume 7*, volume 7. Elsevier, 2012.
- [81] Prajit Ramachandran, Barret Zoph, and Quoc V Le. Searching for activation functions. *arXiv preprint arXiv:1710.05941*, 2017.

A Dynamical equations

This section provides derivations of the complete dynamical equations, from the starting point of the metriplectic problem to the particle discretization used in this work. By recalling the formulation of the main text, consider now a collection of N particles with positions \mathbf{r}_i and velocities $\mathbf{v}_i = \frac{d\mathbf{r}_i}{dt}$ for $i \in V = \{1, \dots, N\}$. We introduce energy and entropy functionals

$$E = \sum_i \left[\frac{1}{2} m_i \mathbf{v}_i^2 + U_i \right], \quad S = \sum_i S_i,$$

where: $m_i = m$ is a particle mass, assumed to be constant; S_i is a per particle entropy; $U_i = U(\mathcal{V}_i, S_i, \bar{\mathbf{e}}_i)$ is a function prescribing per particle internal energy; and $\mathcal{V}_i(\mathbf{r}_1, \dots, \mathbf{r}_N)$ is a per particle volume which will be prescribed as a function of neighboring particle positions. The dynamic equations of the system is described by the metriplectic equation:

$$\underbrace{\begin{bmatrix} d\mathbf{r}_i \\ d\mathbf{v}_i \\ dS_i \end{bmatrix}}_{d\mathbf{x}_i} = \sum_j \frac{1}{m} \underbrace{\begin{bmatrix} \mathbf{0} & \mathbf{I}\delta_{ij} & \mathbf{0} \\ -\mathbf{I}\delta_{ij} & \mathbf{0} & \mathbf{0} \\ \mathbf{0} & \mathbf{0} & \mathbf{0} \end{bmatrix}}_{\mathbf{L}_{ij}} \underbrace{\begin{bmatrix} \frac{\partial U}{\partial \mathbf{r}_j} \\ m\mathbf{v}_j \\ T_j \end{bmatrix}}_{\frac{\partial E}{\partial \mathbf{x}_j}} dt + \sum_j \mathbf{M}_{ij} \underbrace{\begin{bmatrix} \mathbf{0} \\ \mathbf{0} \\ 1 \end{bmatrix}}_{\frac{\partial S}{\partial \mathbf{x}_j}} dt + k_B \sum_j \frac{\partial}{\partial \mathbf{x}_j} \cdot \mathbf{M}_{ij} dt + \underbrace{\begin{bmatrix} d\tilde{\mathbf{r}}_i \\ d\tilde{\mathbf{v}}_i \\ d\tilde{S}_i \end{bmatrix}}_{d\tilde{\mathbf{x}}_i}, \quad (7)$$

subject to the fluctuation-dissipation theorem:

$$d\tilde{\mathbf{x}} d\tilde{\mathbf{x}}^T = 2k_B \mathbf{M} dt. \quad (8)$$

The stochastic differentials $d\tilde{\mathbf{v}}_i = (d\tilde{\mathbf{r}}_i, d\tilde{\mathbf{v}}_i, d\tilde{S}_i)$ are defined as:

$$\begin{aligned} d\tilde{\mathbf{r}}_i &= \mathbf{0} \\ m d\tilde{\mathbf{v}}_i &= \sqrt{2k_B} \sum_{j \in \mathcal{N}_i} \left[A_{ij} d\bar{\mathbf{W}}_{ij} + B_{ij} \frac{\mathbf{I}}{D} \text{tr}(d\mathbf{W}_{ij}) \right] \mathbf{e}_{ij}, \\ T_i d\tilde{S}_i &= -\frac{\sqrt{2k_B}}{2} \sum_{j \in \mathcal{N}_i} \left[A_{ij} d\bar{\mathbf{W}}_{ij} + B_{ij} \frac{\mathbf{I}}{D} \text{tr}(d\mathbf{W}_{ij}) \right] : \mathbf{e}_{ij} \mathbf{v}_{ij} + \sqrt{2k_B} \sum_{j \in \mathcal{N}_i} C_{ij} dV_{ij}, \end{aligned} \quad (9)$$

where $A_{ij} = A_{ji}$, $B_{ij} = B_{ji}$ and $C_{ij} = C_{ji}$ are symmetric functions of the position and entropy of the particles, D is the dimension of the problem and $\mathbf{e}_{ij} = \mathbf{r}_{ij}/|\mathbf{r}_{ij}|$ is the interdistance unitary vector. The Wiener differentials $d\mathbf{W}_{ij} = d\mathbf{W}_{ji}$ and $dV_{ij} = -dV_{ji}$ are symmetric and skew-symmetric with respect to particle labels i, j . Their components are independent zero mean and unit variance Gaussian increments which are uncorrelated in components and particle index except if they belong to the same interaction. This logic can be compactly expressed by using Kronecker deltas with the following differential rules:

$$\begin{aligned} d\mathbf{W}_{ii'}^{\alpha\alpha'} d\mathbf{W}_{jj'}^{\beta\beta'} &= (\delta_{ij}\delta_{i'j'} + \delta_{i'j}\delta_{ij'}) \delta^{\alpha\beta} \delta^{\alpha'\beta'} dt, \\ dV_{ii'} dV_{jj'} &= (\delta_{ij}\delta_{i'j'} - \delta_{i'j}\delta_{ij'}) dt, \\ d\mathbf{W}_{ii'}^{\alpha\alpha'} dV_{jj'} &= 0, \end{aligned} \quad (10)$$

where indices i, j and i', j' denote pairs of particles (latin subscripts) and α, β and α', β' denote the matrix component indices (greek superscripts). Last, we define the traceless symmetric matrix $d\bar{\mathbf{W}}_{ij}$ as

$$d\bar{\mathbf{W}}_{ij} = \frac{1}{2} (d\mathbf{W}_{ij} + d\mathbf{W}_{ij}^T) - \frac{\mathbf{I}}{D} \text{tr}(d\mathbf{W}_{ij}). \quad (11)$$

A.1 Computation of conservative terms

This section aims to derive the conservative terms of the dynamics. Isolating the reversible terms in Eq. (7), we obtain the usual Hamilton's equations in our chosen coordinates:

$$\begin{bmatrix} d\mathbf{r}_i \\ d\mathbf{v}_i \\ dS_i \end{bmatrix}_{\text{rev}} = \begin{bmatrix} \mathbf{v}_i \\ -\frac{\partial U}{\partial \mathbf{r}_i} \\ 0 \end{bmatrix} dt.$$

We now focus on the non-trivial term, which is the momentum equation. By expanding the gradient and using the chain rule:

$$-\frac{\partial U}{\partial \mathbf{r}_i} = -\sum_k \frac{\partial U_k}{\partial \mathbf{r}_i} = -\sum_k \left[\frac{\partial U_k}{\partial \mathcal{V}_k} \frac{\partial \mathcal{V}_k}{\partial \mathbf{r}_i} + \frac{\partial U_k}{\partial \bar{\mathbf{e}}_k} \frac{\partial \bar{\mathbf{e}}_k}{\partial \mathbf{r}_i} \right]. \quad (12)$$

First, the volumetric term gives rise to a hydrostatic pressure force. By using the equation of state relationships and the volume definition, we get:

$$\begin{aligned} -\sum_k \frac{\partial U_k}{\partial \mathcal{V}_k} \frac{\partial \mathcal{V}_k}{\partial \mathbf{r}_i} &= -\sum_k (-P_k) \left(-\frac{1}{d_k^2} \right) \frac{\partial d_i}{\partial \mathbf{r}_i} = -\sum_k \frac{P_k}{d_k^2} \sum_j \frac{\partial W_{kj}}{\partial \mathbf{r}_i} = -\sum_{k,j} \frac{P_k}{d_k^2} \frac{\partial W_{kj}}{\partial \mathbf{r}_{kj}} \frac{\partial \mathbf{r}_{kj}}{\partial \mathbf{r}_i} \\ &= -\sum_{k,j} \frac{P_k}{d_k^2} \frac{\partial W_{kj}}{\partial \mathbf{r}_{kj}} (\delta_{ik} - \delta_{ij}) = -\sum_j \frac{P_i}{d_i^2} \frac{\partial W_{ij}}{\partial \mathbf{r}_{ij}} + \sum_k \frac{P_k}{d_k^2} \frac{\partial W_{ki}}{\partial \mathbf{r}_{ki}} = \sum_j \left[\frac{P_j}{d_j^2} \frac{\partial W_{ji}}{\partial \mathbf{r}_{ji}} - \frac{P_i}{d_i^2} \frac{\partial W_{ij}}{\partial \mathbf{r}_{ij}} \right] \end{aligned}$$

For the elasticity extension, the deviatoric term contributes to the dynamics with a shear elastic restoring force. By using the chain rule, we obtain:

$$\begin{aligned} -\sum_k \frac{\partial U_k}{\partial \bar{\boldsymbol{\varepsilon}}_k^{\alpha\beta}} \frac{\partial \bar{\boldsymbol{\varepsilon}}_k^{\alpha\beta}}{\partial \mathbf{r}_i^\gamma} &= -\sum_k \boldsymbol{\tau}_k^{\alpha\beta} \sum_j \frac{\partial \bar{\mathbf{W}}_{kj}^{\alpha\beta}}{\partial \mathbf{r}_i^\gamma} = -\sum_k \boldsymbol{\tau}_k^{\alpha\beta} \sum_j \frac{\partial \bar{\mathbf{W}}_{kj}^{\alpha\beta}}{\partial \mathbf{u}_{kj}^\delta} \frac{\partial \mathbf{u}_{kj}^\delta}{\partial \mathbf{r}_i^\gamma} = -\sum_{k,j} \boldsymbol{\tau}_k^{\alpha\beta} \frac{\partial \bar{\mathbf{W}}_{kj}^{\alpha\beta}}{\partial \mathbf{u}_{kj}^\delta} \delta_{\delta\gamma} (\delta_{ik} - \delta_{ij}) \\ &= -\sum_j \boldsymbol{\tau}_i^{\alpha\beta} \frac{\partial \bar{\mathbf{W}}_{ij}^{\alpha\beta}}{\partial \mathbf{u}_{ij}^\gamma} + \sum_k \boldsymbol{\tau}_k^{\alpha\beta} \frac{\partial \bar{\mathbf{W}}_{ki}^{\alpha\beta}}{\partial \mathbf{u}_{ki}^\gamma} = \sum_j \left[\boldsymbol{\tau}_j^{\alpha\beta} \frac{\partial \bar{\mathbf{W}}_{ji}^{\alpha\beta}}{\partial \mathbf{u}_{ji}^\gamma} - \boldsymbol{\tau}_i^{\alpha\beta} \frac{\partial \bar{\mathbf{W}}_{ij}^{\alpha\beta}}{\partial \mathbf{u}_{ij}^\gamma} \right] \end{aligned}$$

A.2 Computation of dissipative terms

Once established $d\tilde{\mathbf{x}}$ by the ansatz in Eq. (9), the rest of the viscous dynamics can be straightforwardly computed using the fluctuation-dissipation theorem Eq. (8) and substituting the components of the friction matrix \mathbf{M} and $\nabla \cdot \mathbf{M}$:

$$\begin{aligned} \begin{bmatrix} d\mathbf{r}_i \\ d\mathbf{v}_i \\ d\mathcal{S}_i \end{bmatrix}_{\text{irr}} &= \sum_{j \in \mathcal{N}_i} \frac{d\tilde{\mathbf{x}} d\tilde{\mathbf{x}}^T}{2k_B} \begin{bmatrix} \mathbf{0} \\ \mathbf{0} \\ 1 \end{bmatrix} + k_B \sum_{j \in \mathcal{N}_i} \frac{\partial}{\partial \mathbf{x}_j} \cdot \frac{d\tilde{\mathbf{x}} d\tilde{\mathbf{x}}^T}{2k_B} + d\tilde{\mathbf{x}}_i \\ &= \frac{1}{2k_B} \sum_{j \in \mathcal{N}_i} \begin{bmatrix} \mathbf{0} & \mathbf{0} & \mathbf{0} \\ \mathbf{0} & d\tilde{\mathbf{v}}_i d\tilde{\mathbf{v}}_j^T & d\tilde{\mathbf{v}}_i d\tilde{\mathcal{S}}_j \\ \mathbf{0} & d\tilde{\mathcal{S}}_i d\tilde{\mathbf{v}}_j^T & d\tilde{\mathcal{S}}_i d\tilde{\mathcal{S}}_j \end{bmatrix} \begin{bmatrix} \mathbf{0} \\ \mathbf{0} \\ 1 \end{bmatrix} + \frac{1}{2} \sum_{j \in \mathcal{N}_i} \frac{\partial}{\partial \mathbf{x}_j} \cdot \begin{bmatrix} \mathbf{0} & \mathbf{0} & \mathbf{0} \\ \mathbf{0} & d\tilde{\mathbf{v}}_i d\tilde{\mathbf{v}}_j^T & d\tilde{\mathbf{v}}_i d\tilde{\mathcal{S}}_j \\ \mathbf{0} & d\tilde{\mathcal{S}}_i d\tilde{\mathbf{v}}_j^T & d\tilde{\mathcal{S}}_i d\tilde{\mathcal{S}}_j \end{bmatrix} + d\tilde{\mathbf{x}}_i \\ &= \frac{1}{2k_B} \sum_{j \in \mathcal{N}_i} \begin{bmatrix} \mathbf{0} \\ d\tilde{\mathbf{v}}_i d\tilde{\mathcal{S}}_j \\ d\tilde{\mathcal{S}}_i d\tilde{\mathcal{S}}_j \end{bmatrix} + \frac{1}{2} \sum_{j \in \mathcal{N}_i} \begin{bmatrix} \mathbf{0} \\ \frac{\partial}{\partial \mathbf{v}_j} \cdot d\tilde{\mathbf{v}}_i d\tilde{\mathbf{v}}_j^T + \frac{\partial}{\partial \mathcal{S}_j} \cdot d\tilde{\mathbf{v}}_i d\tilde{\mathcal{S}}_j \\ \frac{\partial}{\partial \mathbf{v}_j} \cdot d\tilde{\mathcal{S}}_i d\tilde{\mathbf{v}}_j^T + \frac{\partial}{\partial \mathcal{S}_j} \cdot d\tilde{\mathcal{S}}_i d\tilde{\mathcal{S}}_j \end{bmatrix} + \begin{bmatrix} \mathbf{0} \\ d\tilde{\mathbf{v}}_i \\ d\tilde{\mathcal{S}}_i \end{bmatrix}. \end{aligned}$$

By operating each term, we obtain the following expressions for the irreversible part of the dynamics:

$$\begin{aligned} d\mathbf{v}_i|_{\text{irr}} &= \frac{1}{2k_B} \sum_{j \in \mathcal{N}_i} d\tilde{\mathbf{v}}_i d\tilde{\mathcal{S}}_j + \frac{1}{2} \sum_{j \in \mathcal{N}_i} \left(\frac{\partial}{\partial \mathbf{v}_j} \cdot d\tilde{\mathbf{v}}_i d\tilde{\mathbf{v}}_j^T + \frac{\partial}{\partial \mathcal{S}_j} \cdot d\tilde{\mathbf{v}}_i d\tilde{\mathcal{S}}_j \right) + d\tilde{\mathbf{v}}_i, \\ d\mathcal{S}_i|_{\text{irr}} &= \frac{1}{2k_B} \sum_{j \in \mathcal{N}_i} d\tilde{\mathcal{S}}_i d\tilde{\mathcal{S}}_j + \frac{1}{2} \sum_{j \in \mathcal{N}_i} \left(\frac{\partial}{\partial \mathbf{v}_j} \cdot d\tilde{\mathcal{S}}_i d\tilde{\mathbf{v}}_j^T + \frac{\partial}{\partial \mathcal{S}_j} \cdot d\tilde{\mathcal{S}}_i d\tilde{\mathcal{S}}_j \right) + d\tilde{\mathcal{S}}_i. \end{aligned}$$

In this section we focus in the derivation of each term. First, we need to establish some important identities.

Lemma A.1. *Given $d\mathbf{W}_{ii'}$ and $d\mathbf{W}_{jj'}$ two matrix-valued Wiener processes with the properties stated in Eq. (10), the following identities hold:*

1. $\text{tr}(d\mathbf{W}_{ii'}) \text{tr}(d\mathbf{W}_{jj'}) = D(\delta_{ij}\delta_{i'j'} + \delta_{i'j}\delta_{ij'}) dt.$
2. $\text{tr}(d\mathbf{W}_{ii'}) d\bar{\mathbf{W}}_{jj'} = 0.$
3. $d\bar{\mathbf{W}}_{ii'}^{\alpha\alpha'} d\bar{\mathbf{W}}_{jj'}^{\beta\beta'} = (\delta_{ij}\delta_{i'j'} + \delta_{i'j}\delta_{ij'}) \left[\frac{1}{2}(\delta^{\alpha\beta}\delta^{\alpha'\beta'} + \delta^{\alpha'\beta}\delta^{\alpha\beta'}) - \frac{1}{D}\delta^{\alpha\alpha'}\delta^{\beta\beta'} \right] dt.$
4. $\left[A_{ii'} d\bar{\mathbf{W}}_{ii'}^{\alpha\alpha'} + B_{ii'} \frac{\delta^{\alpha\alpha'}}{D} \text{tr}(d\mathbf{W}_{ii'}) \right] \left[A_{jj'} d\bar{\mathbf{W}}_{jj'}^{\beta\beta'} + B_{jj'} \frac{\delta^{\beta\beta'}}{D} \text{tr}(d\mathbf{W}_{jj'}) \right]$
 $= (\delta_{ij}\delta_{i'j'} + \delta_{i'j}\delta_{ij'}) \left[\frac{1}{2} A_{ii'} A_{jj'} (\delta^{\alpha\beta}\delta^{\alpha'\beta'} + \delta^{\alpha'\beta}\delta^{\alpha\beta'}) + (B_{ii'} B_{jj'} - A_{ii'} A_{jj'}) \frac{1}{D} \delta^{\alpha\alpha'} \delta^{\beta\beta'} \right] dt.$

Proof. First, it is important to remember some of the properties of Kronecker delta operations, which are intimately related to the properties of identity matrices:

- Symmetric property: $\delta^{\alpha\beta} = \delta^{\beta\alpha}$
- Summation property: $\sum_{\sigma} \delta^{\alpha\sigma} \delta^{\sigma\beta} = \delta^{\alpha\beta}$
- Cumulative summation: $\sum_{\alpha,\beta} \delta^{\alpha\beta} = D$ where D is the dimension of the problem.
- Conmutativity: $\delta^{\alpha\alpha'} \delta^{\beta\beta'} = \delta^{\beta\beta'} \delta^{\alpha\alpha'}$

By recalling the definition of $d\overline{\mathbf{W}}_{ij}$ in Eq. (11) and the correlation rules of the Wiener processes defined in Eq. (10), the proofs are completed with straightforward algebraic manipulations:

$$\begin{aligned}
 \text{tr}(d\mathbf{W}_{ii'}) \text{tr}(d\mathbf{W}_{jj'}) &= \sum_{\alpha} d\mathbf{W}_{ii'}^{\alpha\alpha} \sum_{\beta} d\mathbf{W}_{jj'}^{\beta\beta} = \sum_{\alpha,\beta} d\mathbf{W}_{ii'}^{\alpha\alpha} d\mathbf{W}_{jj'}^{\beta\beta} \\
 &= \sum_{\alpha,\beta} (\delta_{ij} \delta_{i'j'} + \delta_{i'j} \delta_{ij'}) \delta^{\alpha\beta} \delta^{\alpha\beta} dt \\
 &= (\delta_{ij} \delta_{i'j'} + \delta_{i'j} \delta_{ij'}) \sum_{\alpha,\beta} \delta^{\alpha\beta} dt \\
 &= D(\delta_{ij} \delta_{i'j'} + \delta_{i'j} \delta_{ij'}) dt.
 \end{aligned}$$

$$\begin{aligned}
 \text{tr}(d\mathbf{W}_{ii'}) d\overline{\mathbf{W}}_{jj'} &= \text{tr}(d\mathbf{W}_{ii'}) \left[\frac{1}{2} (d\mathbf{W}_{jj'}^{\alpha\beta} + d\mathbf{W}_{jj'}^{\beta\alpha}) - \frac{\delta^{\alpha\beta}}{D} \text{tr}(d\mathbf{W}_{jj'}) \right] \\
 &= \text{tr}(d\mathbf{W}_{ii'}) \frac{1}{2} (d\mathbf{W}_{jj'}^{\alpha\beta} + d\mathbf{W}_{jj'}^{\beta\alpha}) - \frac{\delta^{\alpha\beta}}{D} \text{tr}(d\mathbf{W}_{ii'}) \text{tr}(d\mathbf{W}_{jj'}) \\
 &= \sum_{\sigma} \left[d\mathbf{W}_{ii'}^{\sigma\sigma} \frac{1}{2} (d\mathbf{W}_{jj'}^{\alpha\beta} + d\mathbf{W}_{jj'}^{\beta\alpha}) \right] - \frac{\delta^{\alpha\beta}}{D} \text{tr}(d\mathbf{W}_{ii'}) \text{tr}(d\mathbf{W}_{jj'}) \\
 &\stackrel{(1)}{=} \frac{1}{2} \sum_{\sigma} \left[d\mathbf{W}_{ii'}^{\sigma\sigma} d\mathbf{W}_{jj'}^{\alpha\beta} + d\mathbf{W}_{ii'}^{\sigma\sigma} d\mathbf{W}_{jj'}^{\beta\alpha} \right] - \frac{\delta^{\alpha\beta}}{D} D(\delta_{ij} \delta_{i'j'} + \delta_{i'j} \delta_{ij'}) dt \\
 &= \frac{1}{2} \sum_{\sigma} \left[(\delta_{ij} \delta_{i'j'} + \delta_{i'j} \delta_{ij'}) (\delta^{\sigma\alpha} \delta^{\sigma\beta} + \delta^{\sigma\beta} \delta^{\sigma\alpha}) \right] dt - \delta^{\alpha\beta} (\delta_{ij} \delta_{i'j'} + \delta_{i'j} \delta_{ij'}) dt \\
 &= (\delta_{ij} \delta_{i'j'} + \delta_{i'j} \delta_{ij'}) \left[\frac{1}{2} \sum_{\sigma} 2\delta^{\sigma\alpha} \delta^{\sigma\beta} - \delta^{\alpha\beta} \right] dt \\
 &= (\delta_{ij} \delta_{i'j'} + \delta_{i'j} \delta_{ij'}) (\delta^{\alpha\beta} - \delta^{\alpha\beta}) dt = 0.
 \end{aligned}$$

$$\begin{aligned}
 d\overline{\mathbf{W}}_{ii'}^{\alpha\alpha'} d\overline{\mathbf{W}}_{jj'}^{\beta\beta'} &= \left[\frac{1}{2} (d\mathbf{W}_{ii'}^{\alpha\alpha'} + d\mathbf{W}_{ii'}^{\alpha'\alpha}) - \frac{\delta^{\alpha\alpha'}}{D} \text{tr}(d\mathbf{W}_{ii'}) \right] d\overline{\mathbf{W}}_{jj'}^{\beta\beta'} \\
 &\stackrel{(2)}{=} \frac{1}{2} (d\mathbf{W}_{ii'}^{\alpha\alpha'} + d\mathbf{W}_{ii'}^{\alpha'\alpha}) \left[\frac{1}{2} (d\mathbf{W}_{jj'}^{\beta\beta'} + d\mathbf{W}_{jj'}^{\beta'\beta}) - \frac{\delta^{\beta\beta'}}{D} \text{tr}(d\mathbf{W}_{jj'}) \right] \\
 &= \frac{1}{4} (d\mathbf{W}_{ii'}^{\alpha\alpha'} d\mathbf{W}_{jj'}^{\beta\beta'} + d\mathbf{W}_{ii'}^{\alpha\alpha'} d\mathbf{W}_{jj'}^{\beta'\beta} + d\mathbf{W}_{ii'}^{\alpha'\alpha} d\mathbf{W}_{jj'}^{\beta\beta'} + d\mathbf{W}_{ii'}^{\alpha'\alpha} d\mathbf{W}_{jj'}^{\beta'\beta}) \\
 &\quad - \frac{\delta^{\beta\beta'}}{2D} (d\mathbf{W}_{ii'}^{\alpha\alpha'} + d\mathbf{W}_{ii'}^{\alpha'\alpha}) \text{tr}(d\mathbf{W}_{jj'}) \\
 &\stackrel{(1)}{=} (\delta_{ij} \delta_{i'j'} + \delta_{i'j} \delta_{ij'}) \left[\frac{1}{4} (\delta^{\alpha\beta} \delta^{\alpha'\beta'} + \delta^{\alpha\beta'} \delta^{\alpha'\beta} + \delta^{\alpha'\beta} \delta^{\alpha\beta'} + \delta^{\alpha'\beta'} \delta^{\alpha\beta}) \right] dt \\
 &\quad - \frac{\delta^{\beta\beta'}}{2D} \sum_{\sigma} (d\mathbf{W}_{ii'}^{\alpha\alpha'} d\mathbf{W}_{jj'}^{\sigma\sigma} + d\mathbf{W}_{ii'}^{\alpha'\alpha} d\mathbf{W}_{jj'}^{\sigma\sigma}) \\
 &= (\delta_{ij} \delta_{i'j'} + \delta_{i'j} \delta_{ij'}) \left[\frac{1}{4} (2\delta^{\alpha\beta} \delta^{\alpha'\beta'} + 2\delta^{\alpha'\beta} \delta^{\alpha\beta'}) - \frac{\delta^{\beta\beta'}}{2D} \sum_{\sigma} (\delta^{\alpha\sigma} \delta^{\alpha'\sigma} + \delta^{\alpha'\sigma} \delta^{\alpha\sigma}) \right] dt \\
 &= (\delta_{ij} \delta_{i'j'} + \delta_{i'j} \delta_{ij'}) \left[\frac{1}{2} (\delta^{\alpha\beta} \delta^{\alpha'\beta'} + \delta^{\alpha'\beta} \delta^{\alpha\beta'}) - \frac{\delta^{\beta\beta'}}{2D} \sum_{\sigma} 2\delta^{\alpha\sigma} \delta^{\alpha'\sigma} \right] dt
 \end{aligned}$$

$$= (\delta_{ij}\delta_{i'j'} + \delta_{i'j}\delta_{ij'}) \left[\frac{1}{2}(\delta^{\alpha\beta}\delta^{\alpha'\beta'} + \delta^{\alpha'\beta}\delta^{\alpha\beta'}) - \frac{1}{D}\delta^{\alpha\alpha'}\delta^{\beta\beta'} \right] dt.$$

$$\begin{aligned} & \left[A_{ii'}d\overline{\mathbf{W}}_{ii'}^{\alpha\alpha'} + B_{ii'}\frac{\delta^{\alpha\alpha'}}{D}\text{tr}(d\mathbf{W}_{ii'}) \right] \left[A_{jj'}d\overline{\mathbf{W}}_{jj'}^{\beta\beta'} + B_{jj'}\frac{\delta^{\beta\beta'}}{D}\text{tr}(d\mathbf{W}_{jj'}) \right] \\ &= A_{ii'}A_{jj'}d\overline{\mathbf{W}}_{ii'}^{\alpha\alpha'}d\overline{\mathbf{W}}_{jj'}^{\beta\beta'} + A_{ii'}B_{jj'}\frac{\delta^{\beta\beta'}}{D}d\overline{\mathbf{W}}_{ii'}^{\alpha\alpha'}\text{tr}(d\mathbf{W}_{jj'}) \\ & \quad + B_{ii'}A_{jj'}\frac{\delta^{\alpha\alpha'}}{D}\text{tr}(d\mathbf{W}_{ii'})d\overline{\mathbf{W}}_{jj'}^{\beta\beta'} + B_{ii'}B_{jj'}\frac{\delta^{\alpha\alpha'}\delta^{\beta\beta'}}{D^2}\text{tr}(d\mathbf{W}_{ii'})\text{tr}(d\mathbf{W}_{jj'}) \\ & \stackrel{(2)}{=} A_{ii'}A_{jj'}d\overline{\mathbf{W}}_{ii'}^{\alpha\alpha'}d\overline{\mathbf{W}}_{jj'}^{\beta\beta'} + B_{ii'}B_{jj'}\frac{\delta^{\alpha\alpha'}\delta^{\beta\beta'}}{D^2}\text{tr}(d\mathbf{W}_{ii'})\text{tr}(d\mathbf{W}_{jj'}) \\ & \stackrel{(1,3)}{=} (\delta_{ij}\delta_{i'j'} + \delta_{i'j}\delta_{ij'}) \left[\frac{A_{ii'}A_{jj'}}{2}(\delta^{\alpha\beta}\delta^{\alpha'\beta'} + \delta^{\alpha'\beta}\delta^{\alpha\beta'}) - \frac{A_{ii'}A_{jj'}}{D}\delta^{\alpha\alpha'}\delta^{\beta\beta'} + \frac{B_{ii'}B_{jj'}}{D^2}\delta^{\alpha\alpha'}\delta^{\beta\beta'} D \right] dt \\ &= (\delta_{ij}\delta_{i'j'} + \delta_{i'j}\delta_{ij'}) \left[\frac{A_{ii'}A_{jj'}}{2}(\delta^{\alpha\beta}\delta^{\alpha'\beta'} + \delta^{\alpha'\beta}\delta^{\alpha\beta'}) + \frac{B_{ii'}B_{jj'} - A_{ii'}A_{jj'}}{D}\delta^{\alpha\alpha'}\delta^{\beta\beta'} \right] dt. \end{aligned}$$

□

Now we can compute the M matrix by blocks using the fluctuation-dissipation theorem in Eq. (8),

$$\mathbf{M}_{ij}dt = \frac{d\tilde{\mathbf{x}}_i d\tilde{\mathbf{x}}_j^T}{2k_B} = \frac{1}{2k_B} \begin{bmatrix} \mathbf{0} & \mathbf{0} & \mathbf{0} \\ \mathbf{0} & d\tilde{\mathbf{v}}_i d\tilde{\mathbf{v}}_j^T & d\tilde{\mathbf{v}}_i d\tilde{S}_j \\ \mathbf{0} & d\tilde{S}_i d\tilde{\mathbf{v}}_j^T & d\tilde{S}_i d\tilde{S}_j \end{bmatrix}.$$

Note that the complete M matrix is symmetric, but the individual blocks M_{ij} are not. We first need to apply the ansatz of $d\tilde{\mathbf{x}}$ in Eq. (9). For convenience, we will compute the individual components of the vectorial quantities, such as \mathbf{v}^α or \mathbf{e}^α , by using the Einstein summation convention (only for the greek superscripts). We will need the following summation rules for the Kronecker deltas:

- Index contraction: $\delta^{\alpha\beta}\mathbf{v}^\alpha = \sum_\alpha \delta^{\alpha\beta}\mathbf{v}^\alpha = \mathbf{v}^\beta$
- Dot product: $\mathbf{v}^\alpha \delta^{\alpha\beta} \mathbf{e}^\beta = \sum_{\alpha,\beta} \mathbf{v}^\alpha \delta^{\alpha\beta} \mathbf{e}^\beta = \sum_\alpha \mathbf{v}^\alpha \mathbf{e}^\alpha = \mathbf{v} \cdot \mathbf{e}$

We will also need to apply the symmetry of the coefficients $A_{ij} = A_{ji}$, $B_{ij} = B_{ji}$ and $C_{ij} = C_{ji}$, the skew-symmetry of $\mathbf{e}_{ij} = -\mathbf{e}_{ji}$ and the unitary modulus of $\mathbf{e}_{ij} \cdot \mathbf{e}_{ij} = 1$. Now, we can compute the individual components by using Lemma A.1. First, we will contract the Greek superscripts and then the Roman subscripts.

$$\begin{aligned} m^2 \frac{d\tilde{\mathbf{v}}_i^\alpha d\tilde{\mathbf{v}}_j^\beta}{2k_B} &= \sum_{i',j'} \left[A_{ii'}d\overline{\mathbf{W}}_{ii'}^{\alpha\alpha'} + B_{ii'}\frac{\delta^{\alpha\alpha'}}{D}\text{tr}(d\mathbf{W}_{ii'}) \right] \mathbf{e}_{ii'}^{\alpha'} \left[A_{jj'}d\overline{\mathbf{W}}_{jj'}^{\beta\beta'} + B_{jj'}\frac{\delta^{\beta\beta'}}{D}\text{tr}(d\mathbf{W}_{jj'}) \right] \mathbf{e}_{jj'}^{\beta'} \\ &= \sum_{i',j'} (\delta_{ij}\delta_{i'j'} + \delta_{i'j}\delta_{ij'}) \left[\frac{A_{ii'}A_{jj'}}{2}(\delta^{\alpha\beta}\delta^{\alpha'\beta'} + \delta^{\alpha'\beta}\delta^{\alpha\beta'}) + \frac{B_{ii'}B_{jj'} - A_{ii'}A_{jj'}}{D}\delta^{\alpha\alpha'}\delta^{\beta\beta'} \right] \mathbf{e}_{ii'}^{\alpha'} \mathbf{e}_{jj'}^{\beta'} dt \\ &= \sum_{i',j'} (\delta_{ij}\delta_{i'j'} + \delta_{i'j}\delta_{ij'}) \left[\frac{A_{ii'}A_{jj'}}{2}(\delta^{\alpha\beta} \mathbf{e}_{ii'} \cdot \mathbf{e}_{jj'} + \mathbf{e}_{ii'}^\beta \mathbf{e}_{jj'}^\alpha) + \frac{B_{ii'}B_{jj'} - A_{ii'}A_{jj'}}{D} \mathbf{e}_{ii'}^\alpha \mathbf{e}_{jj'}^\beta \right] dt \\ &= \delta_{ij} \sum_{k \in \mathcal{N}_i} \left[\frac{A_{ik}A_{jk}}{2}(\delta^{\alpha\beta} \mathbf{e}_{ik} \cdot \mathbf{e}_{jk} + \mathbf{e}_{ik}^\beta \mathbf{e}_{jk}^\alpha) + \frac{B_{ik}B_{jk} - A_{ik}A_{jk}}{D} \mathbf{e}_{ik}^\alpha \mathbf{e}_{jk}^\beta \right] dt \\ & \quad + \left[\frac{A_{ij}A_{ji}}{2}(\delta^{\alpha\beta} \mathbf{e}_{ij} \cdot \mathbf{e}_{ji} + \mathbf{e}_{ij}^\beta \mathbf{e}_{ji}^\alpha) + \frac{B_{ij}B_{ji} - A_{ij}A_{ji}}{D} \mathbf{e}_{ij}^\alpha \mathbf{e}_{ji}^\beta \right] dt \\ &= \delta_{ij} \sum_{k \in \mathcal{N}_i} \left[\frac{A_{ik}^2}{2}(\delta^{\alpha\beta} + \mathbf{e}_{ik}^\alpha \mathbf{e}_{ik}^\beta) + \frac{B_{ik}^2 - A_{ik}^2}{D} \mathbf{e}_{ik}^\alpha \mathbf{e}_{ik}^\beta \right] dt - \left[\frac{A_{ij}^2}{2}(\delta^{\alpha\beta} + \mathbf{e}_{ij}^\alpha \mathbf{e}_{ij}^\beta) + \frac{B_{ij}^2 - A_{ij}^2}{D} \mathbf{e}_{ij}^\alpha \mathbf{e}_{ij}^\beta \right] dt. \end{aligned}$$

We can use very similar proofs for the remaining terms. Remember that the Wiener processes dV_{ij} are independent of $d\mathbf{W}_{ij}$ by Eq. (10), so the C_{ij} terms only appear in the entropic term of the matrix. Also, we will need to use the skew-symmetry of $\mathbf{v}_{ij} = -\mathbf{v}_{ji}$.

$$\begin{aligned}
 mT_j \frac{d\tilde{\mathbf{v}}_i^\alpha d\tilde{S}_j}{2k_B} &= \sum_{i',j'} \left[A_{ii'} d\overline{\mathbf{W}}_{ii'}^{\alpha\alpha'} + B_{ii'} \frac{\delta^{\alpha\alpha'}}{D} \text{tr}(d\mathbf{W}_{ii'}) \right] \mathbf{e}_{ii'}^\alpha \left(-\frac{1}{2} \left[A_{jj'} d\overline{\mathbf{W}}_{jj'}^{\beta\beta'} + B_{jj'} \frac{\delta^{\beta\beta'}}{D} \text{tr}(d\mathbf{W}_{jj'}) \right] \mathbf{e}_{jj'}^\beta \mathbf{v}_{jj'}^\beta \right. \\
 &\quad \left. + C_{jj'} dV_{jj'} \right) \\
 &= -\sum_{i',j'} (\delta_{ij} \delta_{i'j'} + \delta_{i'j} \delta_{ij'}) \left[\frac{A_{ii'} A_{jj'}}{2} (\delta^{\alpha\beta} \delta^{\alpha'\beta'} + \delta^{\alpha'\beta} \delta^{\alpha\beta'}) + \frac{B_{ii'} B_{jj'} - A_{ii'} A_{jj'}}{D} \delta^{\alpha\alpha'} \delta^{\beta\beta'} \right] \mathbf{e}_{ii'}^\alpha \mathbf{e}_{jj'}^\beta \frac{\mathbf{v}_{jj'}^\beta}{2} dt \\
 &= -\sum_{i',j'} (\delta_{ij} \delta_{i'j'} + \delta_{i'j} \delta_{ij'}) \left[\frac{A_{ii'} A_{jj'}}{2} \left(\frac{\mathbf{v}_{jj'}^\alpha}{2} \mathbf{e}_{ii'} \cdot \mathbf{e}_{jj'} + \mathbf{e}_{ii'} \cdot \frac{\mathbf{v}_{jj'}^\alpha}{2} \mathbf{e}_{jj'} \right) + \frac{B_{ii'} B_{jj'} - A_{ii'} A_{jj'}}{D} \mathbf{e}_{ii'}^\alpha \mathbf{e}_{jj'} \cdot \frac{\mathbf{v}_{jj'}}{2} \right] dt \\
 &= -\delta_{ij} \sum_{k \in \mathcal{N}_i} \left[\frac{A_{ik} A_{jk}}{2} \left(\frac{\mathbf{v}_{jk}^\alpha}{2} \mathbf{e}_{ik} \cdot \mathbf{e}_{jk} + \mathbf{e}_{ik} \cdot \frac{\mathbf{v}_{jk}^\alpha}{2} \mathbf{e}_{jk} \right) + \frac{B_{ik} B_{jk} - A_{ik} A_{jk}}{D} \mathbf{e}_{ik}^\alpha \mathbf{e}_{jk} \cdot \frac{\mathbf{v}_{jk}}{2} \right] dt \\
 &\quad - \left[\frac{A_{ij} A_{ji}}{2} \left(\frac{\mathbf{v}_{ji}^\alpha}{2} \mathbf{e}_{ij} \cdot \mathbf{e}_{ji} + \mathbf{e}_{ij} \cdot \frac{\mathbf{v}_{ji}^\alpha}{2} \mathbf{e}_{ji} \right) + \frac{B_{ij} B_{ji} - A_{ij} A_{ji}}{D} \mathbf{e}_{ij}^\alpha \mathbf{e}_{ji} \cdot \frac{\mathbf{v}_{ji}}{2} \right] dt \\
 &= -\delta_{ij} \sum_{k \in \mathcal{N}_i} \left[\frac{A_{ik}^2}{2} \left(\frac{\mathbf{v}_{ik}^\alpha}{2} + \mathbf{e}_{ik} \cdot \frac{\mathbf{v}_{ik}^\alpha}{2} \mathbf{e}_{ik} \right) + \frac{B_{ik}^2 - A_{ik}^2}{D} \mathbf{e}_{ik}^\alpha \mathbf{e}_{ik} \cdot \frac{\mathbf{v}_{ik}}{2} \right] dt \\
 &\quad - \left[\frac{A_{ij}^2}{2} \left(\frac{\mathbf{v}_{ij}^\alpha}{2} + \mathbf{e}_{ij} \cdot \frac{\mathbf{v}_{ij}^\alpha}{2} \mathbf{e}_{ij} \right) + \frac{B_{ij}^2 - A_{ij}^2}{D} \mathbf{e}_{ij}^\alpha \mathbf{e}_{ij} \cdot \frac{\mathbf{v}_{ij}}{2} \right] dt.
 \end{aligned}$$

$$\begin{aligned}
 mT_i \frac{d\tilde{S}_i d\tilde{\mathbf{v}}_j^\alpha}{2k_B} &= \sum_{i',j'} \left(-\frac{1}{2} \left[A_{ii'} d\overline{\mathbf{W}}_{ii'}^{\beta\beta'} + B_{ii'} \frac{\delta^{\beta\beta'}}{D} \text{tr}(d\mathbf{W}_{ii'}) \right] \mathbf{e}_{ii'}^\beta \mathbf{v}_{ii'}^\beta + C_{ii'} dV_{ii'} \right) \left[A_{jj'} d\overline{\mathbf{W}}_{jj'}^{\alpha\alpha'} + B_{jj'} \frac{\delta^{\alpha\alpha'}}{D} \text{tr}(d\mathbf{W}_{jj'}) \right] \mathbf{e}_{jj'}^\alpha \\
 &= -\sum_{i',j'} (\delta_{ij} \delta_{i'j'} + \delta_{ij'} \delta_{i'j}) \left[\frac{A_{ii'} A_{jj'}}{2} (\delta^{\alpha\beta} \delta^{\alpha'\beta'} + \delta^{\alpha'\beta} \delta^{\alpha\beta'}) + \frac{B_{ii'} B_{jj'} - A_{ii'} A_{jj'}}{D} \delta^{\alpha\alpha'} \delta^{\beta\beta'} \right] \mathbf{e}_{ii'}^\beta \frac{\mathbf{v}_{ii'}^\beta}{2} \mathbf{e}_{jj'}^\alpha dt \\
 &= -\sum_{i',j'} (\delta_{ij} \delta_{i'j'} + \delta_{ij'} \delta_{i'j}) \left[\frac{A_{ii'} A_{jj'}}{2} \left(\frac{\mathbf{v}_{ii'}^\alpha}{2} \mathbf{e}_{ii'} \cdot \mathbf{e}_{jj'} + \mathbf{e}_{ii'} \cdot \frac{\mathbf{v}_{ii'}^\alpha}{2} \mathbf{e}_{jj'} \right) + \frac{B_{ii'} B_{jj'} - A_{ii'} A_{jj'}}{D} \mathbf{e}_{jj'}^\alpha \mathbf{e}_{ii'} \cdot \frac{\mathbf{v}_{ii'}}{2} \right] dt \\
 &= -\delta_{ij} \sum_{k \in \mathcal{N}_i} \left[\frac{A_{ik} A_{jk}}{2} \left(\frac{\mathbf{v}_{jk}^\alpha}{2} \mathbf{e}_{ik} \cdot \mathbf{e}_{jk} + \mathbf{e}_{jk} \cdot \frac{\mathbf{v}_{jk}^\alpha}{2} \mathbf{e}_{ik} \right) + \frac{B_{ik} B_{jk} - A_{ik} A_{jk}}{D} \mathbf{e}_{jk}^\alpha \mathbf{e}_{ik} \cdot \frac{\mathbf{v}_{ik}}{2} \right] dt \\
 &\quad - \left[\frac{A_{ij} A_{ji}}{2} \left(\frac{\mathbf{v}_{ij}^\alpha}{2} \mathbf{e}_{ij} \cdot \mathbf{e}_{ji} + \mathbf{e}_{ji} \cdot \frac{\mathbf{v}_{ij}^\alpha}{2} \mathbf{e}_{ij} \right) + \frac{B_{ij} B_{ji} - A_{ij} A_{ji}}{D} \mathbf{e}_{ji}^\alpha \mathbf{e}_{ij} \cdot \frac{\mathbf{v}_{ij}}{2} \right] dt \\
 &= -\delta_{ij} \sum_{k \in \mathcal{N}_i} \left[\frac{A_{ik}^2}{2} \left(\frac{\mathbf{v}_{ik}^\alpha}{2} + \mathbf{e}_{ik} \cdot \frac{\mathbf{v}_{ik}^\alpha}{2} \mathbf{e}_{ik} \right) + \frac{B_{ik}^2 - A_{ik}^2}{D} \mathbf{e}_{ik}^\alpha \mathbf{e}_{ik} \cdot \frac{\mathbf{v}_{ik}}{2} \right] dt \\
 &\quad + \left[\frac{A_{ij}^2}{2} \left(\frac{\mathbf{v}_{ij}^\alpha}{2} + \mathbf{e}_{ij} \cdot \frac{\mathbf{v}_{ij}^\alpha}{2} \mathbf{e}_{ij} \right) + \frac{B_{ij}^2 - A_{ij}^2}{D} \mathbf{e}_{ij}^\alpha \mathbf{e}_{ij} \cdot \frac{\mathbf{v}_{ij}}{2} \right] dt.
 \end{aligned}$$

$$\begin{aligned}
 T_i T_j \frac{d\tilde{S}_i d\tilde{S}_j}{2k_B} &= \sum_{i',j'} \left(-\frac{1}{2} \left[A_{ii'} d\overline{\mathbf{W}}_{ii'}^{\alpha\alpha'} + B_{ii'} \frac{\delta^{\alpha\alpha'}}{D} \text{tr}(d\mathbf{W}_{ii'}) \right] \mathbf{e}_{ii'}^\alpha \mathbf{v}_{ii'}^\alpha + C_{ii'} dV_{ii'} \right) \left(-\frac{1}{2} \left[A_{jj'} d\overline{\mathbf{W}}_{jj'}^{\beta\beta'} \right. \right. \\
 &\quad \left. \left. + B_{jj'} \frac{\delta^{\beta\beta'}}{D} \text{tr}(d\mathbf{W}_{jj'}) \right] \mathbf{e}_{jj'}^\beta \mathbf{v}_{jj'}^\beta + C_{jj'} dV_{jj'} \right) \\
 &= \sum_{i,j'} (\delta_{ij} \delta_{i'j'} + \delta_{ij'} \delta_{i'j}) \left[\frac{A_{ii'} A_{jj'}}{2} (\delta^{\alpha\beta} \delta^{\alpha'\beta'} + \delta^{\alpha'\beta} \delta^{\alpha\beta'}) + \frac{B_{ii'} B_{jj'} - A_{ii'} A_{jj'}}{D} \delta^{\alpha\alpha'} \delta^{\beta\beta'} \right] \mathbf{e}_{ii'}^\alpha \frac{\mathbf{v}_{ii'}^\alpha}{2} \mathbf{e}_{jj'}^\beta \frac{\mathbf{v}_{jj'}^\beta}{2} dt \\
 &\quad + \sum_{i',j'} (\delta_{ij} \delta_{i'j'} - \delta_{ij'} \delta_{i'j}) C_{ii'} C_{jj'} dt
 \end{aligned}$$

$$\begin{aligned}
 &= \sum_{i,j'} (\delta_{ij} \delta_{i'j'} + \delta_{ij'} \delta_{i'j}) \left(\frac{A_{ii'} A_{jj'}}{2} \left[\left(\frac{\mathbf{v}_{ii'}}{2} \cdot \frac{\mathbf{v}_{jj'}}{2} \right) \mathbf{e}_{ii'} \cdot \mathbf{e}_{jj'} + \left(\mathbf{e}_{ii'} \cdot \frac{\mathbf{v}_{jj'}}{2} \right) \left(\mathbf{e}_{jj'} \cdot \frac{\mathbf{v}_{ii'}}{2} \right) \right] \right. \\
 &\quad \left. + \frac{B_{ii'} B_{jj'} - A_{ii'} A_{jj'}}{D} \left(\mathbf{e}_{ii'} \cdot \frac{\mathbf{v}_{ii'}}{2} \right) \left(\mathbf{e}_{jj'} \cdot \frac{\mathbf{v}_{jj'}}{2} \right) \right) dt + \sum_{i',j'} (\delta_{ij} \delta_{i'j'} - \delta_{ij'} \delta_{i'j}) C_{ii'} C_{jj'} dt \\
 &= \delta_{ij} \sum_{k \in \mathcal{N}_i} \left(\frac{A_{ik} A_{jk}}{2} \left[\left(\frac{\mathbf{v}_{ik}}{2} \cdot \frac{\mathbf{v}_{jk}}{2} \right) \mathbf{e}_{ik} \cdot \mathbf{e}_{jk} + \left(\mathbf{e}_{ik} \cdot \frac{\mathbf{v}_{jk}}{2} \right) \left(\mathbf{e}_{jk} \cdot \frac{\mathbf{v}_{ik}}{2} \right) \right] \right. \\
 &\quad \left. + \frac{B_{ik} B_{jk} - A_{ik} A_{jk}}{D} \left(\mathbf{e}_{ik} \cdot \frac{\mathbf{v}_{ik}}{2} \right) \left(\mathbf{e}_{jk} \cdot \frac{\mathbf{v}_{jk}}{2} \right) \right) dt \\
 &\quad + \frac{A_{ij} A_{ji}}{2} \left[\left(\frac{\mathbf{v}_{ij}}{2} \cdot \frac{\mathbf{v}_{ji}}{2} \right) \mathbf{e}_{ij} \cdot \mathbf{e}_{ji} + \left(\mathbf{e}_{ij} \cdot \frac{\mathbf{v}_{ji}}{2} \right) \left(\mathbf{e}_{ji} \cdot \frac{\mathbf{v}_{ij}}{2} \right) \right] + \frac{B_{ij} B_{ji} - A_{ij} A_{ji}}{D} \left(\mathbf{e}_{ij} \cdot \frac{\mathbf{v}_{ij}}{2} \right) \left(\mathbf{e}_{ji} \cdot \frac{\mathbf{v}_{ji}}{2} \right) dt \\
 &\quad + \delta_{ij} \sum_{k \in \mathcal{N}_i} C_{ik} C_{jk} dt - C_{ij} C_{ji} dt \\
 &= \delta_{ij} \sum_{k \in \mathcal{N}_i} \left(\frac{A_{ik}^2}{2} \left[\left(\frac{\mathbf{v}_{ik}}{2} \right)^2 + \left(\mathbf{e}_{ik} \cdot \frac{\mathbf{v}_{ik}}{2} \right)^2 \right] + \frac{B_{ik}^2 - A_{ik}^2}{D} \left(\mathbf{e}_{ik} \cdot \frac{\mathbf{v}_{ik}}{2} \right)^2 + C_{ik}^2 \right) dt \\
 &\quad + \left(\frac{A_{ij}^2}{2} \left[\left(\frac{\mathbf{v}_{ij}}{2} \right)^2 + \left(\mathbf{e}_{ij} \cdot \frac{\mathbf{v}_{ij}}{2} \right)^2 \right] + \frac{B_{ij}^2 - A_{ij}^2}{D} \left(\mathbf{e}_{ij} \cdot \frac{\mathbf{v}_{ij}}{2} \right)^2 - C_{ij}^2 \right) dt.
 \end{aligned}$$

First, lets compute the M contributions to the dynamics:

$$\begin{aligned}
 m \sum_{j \in \mathcal{N}_i} \frac{d\tilde{\mathbf{v}}_i d\tilde{\mathbf{S}}_j}{2k_B} &= - \sum_{j \in \mathcal{N}_i} \frac{1}{T_j} \delta_{ij} \sum_{k \in \mathcal{N}_i} \left[\frac{A_{ik}^2}{2} \left(\frac{\mathbf{v}_{ik}}{2} + \mathbf{e}_{ik} \cdot \frac{\mathbf{v}_{ik}}{2} \mathbf{e}_{ik} \right) + \frac{B_{ik}^2 - A_{ik}^2}{D} \mathbf{e}_{ik} \mathbf{e}_{ik} \cdot \frac{\mathbf{v}_{ik}}{2} \right] dt \\
 &\quad - \sum_{j \in \mathcal{N}_i} \frac{1}{T_j} \left[\frac{A_{ij}^2}{2} \left(\frac{\mathbf{v}_{ij}}{2} + \mathbf{e}_{ij} \cdot \frac{\mathbf{v}_{ij}}{2} \mathbf{e}_{ij} \right) + \frac{B_{ij}^2 - A_{ij}^2}{D} \mathbf{e}_{ij} \mathbf{e}_{ij} \cdot \frac{\mathbf{v}_{ij}}{2} \right] dt \\
 &= - \frac{1}{2T_i} \sum_{j \in \mathcal{N}_i} \left[\frac{A_{ij}^2}{2} (\mathbf{v}_{ij} + \mathbf{e}_{ij} \cdot \mathbf{v}_{ij} \mathbf{e}_{ij}) + \frac{B_{ij}^2 - A_{ij}^2}{D} \mathbf{e}_{ij} \mathbf{e}_{ij} \cdot \mathbf{v}_{ij} \right] dt \\
 &\quad - \frac{1}{2} \sum_{j \in \mathcal{N}_i} \frac{1}{T_j} \left[\frac{A_{ij}^2}{2} (\mathbf{v}_{ij} + \mathbf{e}_{ij} \cdot \mathbf{v}_{ij} \mathbf{e}_{ij}) + \frac{B_{ij}^2 - A_{ij}^2}{D} \mathbf{e}_{ij} \mathbf{e}_{ij} \cdot \mathbf{v}_{ij} \right] dt \\
 &= - \frac{1}{2} \sum_{j \in \mathcal{N}_i} \left(\frac{1}{T_i} + \frac{1}{T_j} \right) \left[\frac{A_{ij}^2}{2} (\mathbf{v}_{ij} + \mathbf{e}_{ij} \cdot \mathbf{v}_{ij} \mathbf{e}_{ij}) + \frac{B_{ij}^2 - A_{ij}^2}{D} \mathbf{e}_{ij} \mathbf{e}_{ij} \cdot \mathbf{v}_{ij} \right] dt \\
 &= - \frac{1}{2} \sum_{j \in \mathcal{N}_i} \left(\frac{1}{T_i} + \frac{1}{T_j} \right) \left[\frac{A_{ij}^2}{2} \mathbf{v}_{ij} + \left(\frac{A_{ij}^2}{2} + \frac{B_{ij}^2 - A_{ij}^2}{D} \right) \mathbf{e}_{ij} \cdot \mathbf{v}_{ij} \mathbf{e}_{ij} \right] dt.
 \end{aligned}$$

$$\begin{aligned}
 T_i \sum_{j \in \mathcal{N}_i} \frac{d\tilde{\mathbf{S}}_i d\tilde{\mathbf{S}}_j}{2k_B} &= \sum_{j \in \mathcal{N}_i} \frac{1}{T_j} \delta_{ij} \sum_{k \in \mathcal{N}_i} \left(\frac{A_{ik}^2}{2} \left[\left(\frac{\mathbf{v}_{ik}}{2} \right)^2 + \left(\mathbf{e}_{ik} \cdot \frac{\mathbf{v}_{ik}}{2} \right)^2 \right] + \frac{B_{ik}^2 - A_{ik}^2}{D} \left(\mathbf{e}_{ik} \cdot \frac{\mathbf{v}_{ik}}{2} \right)^2 + C_{ik}^2 \right) dt \\
 &\quad + \sum_{j \in \mathcal{N}_i} \frac{1}{T_j} \left(\frac{A_{ij}^2}{2} \left[\left(\frac{\mathbf{v}_{ij}}{2} \right)^2 + \left(\mathbf{e}_{ij} \cdot \frac{\mathbf{v}_{ij}}{2} \right)^2 \right] + \frac{B_{ij}^2 - A_{ij}^2}{D} \left(\mathbf{e}_{ij} \cdot \frac{\mathbf{v}_{ij}}{2} \right)^2 - C_{ij}^2 \right) dt \\
 &= \frac{1}{T_i} \sum_{j \in \mathcal{N}_i} \left(\frac{A_{ij}^2}{2} \left[\left(\frac{\mathbf{v}_{ij}}{2} \right)^2 + \left(\mathbf{e}_{ij} \cdot \frac{\mathbf{v}_{ij}}{2} \right)^2 \right] + \frac{B_{ij}^2 - A_{ij}^2}{D} \left(\mathbf{e}_{ij} \cdot \frac{\mathbf{v}_{ij}}{2} \right)^2 + C_{ij}^2 \right) dt \\
 &\quad + \sum_{j \in \mathcal{N}_i} \frac{1}{T_j} \left(\frac{A_{ij}^2}{2} \left[\left(\frac{\mathbf{v}_{ij}}{2} \right)^2 + \left(\mathbf{e}_{ij} \cdot \frac{\mathbf{v}_{ij}}{2} \right)^2 \right] + \frac{B_{ij}^2 - A_{ij}^2}{D} \left(\mathbf{e}_{ij} \cdot \frac{\mathbf{v}_{ij}}{2} \right)^2 - C_{ij}^2 \right) dt \\
 &= \frac{1}{4} \sum_{j \in \mathcal{N}_i} \left(\frac{1}{T_i} + \frac{1}{T_j} \right) \left(\frac{A_{ij}^2}{2} [\mathbf{v}_{ij}^2 + (\mathbf{v}_{ij} \cdot \mathbf{e}_{ij})^2] + \frac{B_{ij}^2 - A_{ij}^2}{D} (\mathbf{v}_{ij} \cdot \mathbf{e}_{ij})^2 \right) dt + \sum_{j \in \mathcal{N}_i} \left(\frac{1}{T_i} - \frac{1}{T_j} \right) C_{ij}^2 dt
 \end{aligned}$$

$$= \frac{1}{4} \sum_{j \in \mathcal{N}_i} \left(\frac{1}{T_i} + \frac{1}{T_j} \right) \left[\frac{A_{ij}^2}{2} \mathbf{v}_{ij}^2 + \left(\frac{A_{ij}^2}{2} + \frac{B_{ij}^2 - A_{ij}^2}{D} \right) (\mathbf{v}_{ij} \cdot \mathbf{e}_{ij})^2 \right] dt + \sum_{j \in \mathcal{N}_i} \left(\frac{1}{T_i} - \frac{1}{T_j} \right) C_{ij}^2 dt.$$

Last, we derive the divergence terms $\nabla \cdot \mathbf{M}$. Note that we need to define the heat capacity at constant volume C_i as the following expression:

$$\frac{\partial T_i}{\partial S_i} = \frac{T_i}{C_i}.$$

We also need to establish the following divergence identities

$$\begin{aligned} \frac{\partial}{\partial \mathbf{v}_i} \cdot \mathbf{v}_{ij} &= \frac{\partial}{\partial \mathbf{v}_i} \cdot (\mathbf{v}_i - \mathbf{v}_j) = \frac{\partial}{\partial \mathbf{v}_i} \cdot \mathbf{v}_i = D, \\ \frac{\partial}{\partial \mathbf{v}_j} \cdot \mathbf{v}_{ij} &= \frac{\partial}{\partial \mathbf{v}_j} \cdot (\mathbf{v}_i - \mathbf{v}_j) = -\frac{\partial}{\partial \mathbf{v}_j} \cdot \mathbf{v}_j = -D, \\ \frac{\partial}{\partial \mathbf{v}_j} \cdot (\mathbf{e}_{ij} \cdot \mathbf{v}_{ij} \mathbf{e}_{ij}) &= \frac{\partial}{\partial \mathbf{v}_j^\beta} e_{ij}^\alpha v_{ij}^\alpha e_{ij}^\beta = -\frac{\partial}{\partial \mathbf{v}_j^\beta} e_{ij}^\alpha v_{ij}^\alpha e_{ij}^\beta = -\mathbf{e}_{ij}^\beta e_{ij}^\beta = -1, \end{aligned}$$

and usual derivatives

$$\frac{\partial}{\partial S_i} \left(\frac{1}{T_i} \right) = -\frac{1}{T_i C_i}, \quad \frac{\partial}{\partial S_i} \left(\frac{1}{T_i^2} \right) = -\frac{2}{T_i^2 C_i}, \quad \frac{\partial A_{ij}}{\partial S_i} = \frac{\partial A_{ij}}{\partial T_i} \frac{\partial T_i}{\partial S_i} = \frac{\partial A_{ij}}{\partial T_i} \frac{T_i}{C_i}.$$

Now we can compute the remaining terms:

$$\begin{aligned} m^2 \sum_{j \in \mathcal{N}_i} \frac{\partial}{\partial \mathbf{v}_j} \cdot \frac{d\tilde{\mathbf{v}}_i d\tilde{\mathbf{v}}_j^T}{2k_B} &= \sum_{j \in \mathcal{N}_i} \frac{\partial}{\partial \mathbf{v}_j} \cdot \delta_{ij} \sum_{k \in \mathcal{N}_i} \left[\frac{A_{ik}^2}{2} (\mathbf{I} + \mathbf{e}_{ik} \mathbf{e}_{ik}^T) + \frac{B_{ik}^2 - A_{ik}^2}{D} \mathbf{e}_{ik} \mathbf{e}_{ik}^T \right] dt \\ &\quad - \sum_{j \in \mathcal{N}_i} \frac{\partial}{\partial \mathbf{v}_j} \cdot \left[\frac{A_{ij}^2}{2} (\mathbf{I} + \mathbf{e}_{ij} \mathbf{e}_{ij}^T) + \frac{B_{ij}^2 - A_{ij}^2}{D} \mathbf{e}_{ij} \mathbf{e}_{ij}^T \right] dt = \mathbf{0}. \end{aligned}$$

$$\begin{aligned} m \sum_{j \in \mathcal{N}_i} \frac{\partial}{\partial S_j} \cdot \frac{d\tilde{\mathbf{v}}_i d\tilde{S}_j}{2k_B} &= - \sum_{j \in \mathcal{N}_i} \frac{\partial}{\partial S_j} \cdot \frac{1}{T_j} \delta_{ij} \sum_{k \in \mathcal{N}_i} \left[\frac{A_{ik}^2}{2} \left(\frac{\mathbf{v}_{ik}}{2} + \mathbf{e}_{ik} \cdot \frac{\mathbf{v}_{ik}}{2} \mathbf{e}_{ik} \right) + \frac{B_{ik}^2 - A_{ik}^2}{D} \mathbf{e}_{ik} \mathbf{e}_{ik} \cdot \frac{\mathbf{v}_{ik}}{2} \right] dt \\ &\quad - \sum_{j \in \mathcal{N}_i} \frac{\partial}{\partial S_j} \cdot \frac{1}{T_j} \left[\frac{A_{ij}^2}{2} \left(\frac{\mathbf{v}_{ij}}{2} + \mathbf{e}_{ij} \cdot \frac{\mathbf{v}_{ij}}{2} \mathbf{e}_{ij} \right) + \frac{B_{ij}^2 - A_{ij}^2}{D} \mathbf{e}_{ij} \mathbf{e}_{ij} \cdot \frac{\mathbf{v}_{ij}}{2} \right] dt \\ &= -\frac{1}{2} \frac{\partial}{\partial S_i} \cdot \frac{1}{T_i} \sum_{j \in \mathcal{N}_i} \left[\frac{A_{ij}^2}{2} (\mathbf{v}_{ij} + \mathbf{e}_{ij} \cdot \mathbf{v}_{ij} \mathbf{e}_{ij}) + \frac{B_{ij}^2 - A_{ij}^2}{D} \mathbf{e}_{ij} \mathbf{e}_{ij} \cdot \mathbf{v}_{ij} \right] dt \\ &\quad - \frac{1}{2} \sum_{j \in \mathcal{N}_i} \frac{\partial}{\partial S_j} \cdot \frac{1}{T_j} \left[\frac{A_{ij}^2}{2} (\mathbf{v}_{ij} + \mathbf{e}_{ij} \cdot \mathbf{v}_{ij} \mathbf{e}_{ij}) + \frac{B_{ij}^2 - A_{ij}^2}{D} \mathbf{e}_{ij} \mathbf{e}_{ij} \cdot \mathbf{v}_{ij} \right] dt \\ &= \frac{1}{2} \sum_{j \in \mathcal{N}_i} \left(\frac{1}{T_i C_i} + \frac{1}{T_j C_j} \right) \left[\frac{A_{ij}^2}{2} \mathbf{v}_{ij} + \left(\frac{A_{ij}^2}{2} + \frac{B_{ij}^2 - A_{ij}^2}{D} \right) \mathbf{e}_{ij} \cdot \mathbf{v}_{ij} \mathbf{e}_{ij} \right] dt \\ &\quad - \frac{1}{2} \sum_{j \in \mathcal{N}_i} \frac{1}{T_i} \left[A_{ij} \frac{\partial A_{ij}}{\partial S_i} \mathbf{v}_{ij} + \left(A_{ij} \frac{\partial A_{ij}}{\partial S_i} + \frac{2}{D} B_{ij} \frac{\partial B_{ij}}{\partial S_i} - \frac{2}{D} A_{ij} \frac{\partial A_{ij}}{\partial S_i} \right) \mathbf{e}_{ij} \cdot \mathbf{v}_{ij} \mathbf{e}_{ij} \right] dt \\ &\quad - \frac{1}{2} \sum_{j \in \mathcal{N}_i} \frac{1}{T_j} \left[A_{ij} \frac{\partial A_{ij}}{\partial S_j} \mathbf{v}_{ij} + \left(A_{ij} \frac{\partial A_{ij}}{\partial S_j} + \frac{2}{D} B_{ij} \frac{\partial B_{ij}}{\partial S_j} - \frac{2}{D} A_{ij} \frac{\partial A_{ij}}{\partial S_j} \right) \mathbf{e}_{ij} \cdot \mathbf{v}_{ij} \mathbf{e}_{ij} \right] dt \\ &= \frac{1}{2} \sum_{j \in \mathcal{N}_i} \left(\frac{1}{T_i C_i} + \frac{1}{T_j C_j} \right) \left[\frac{A_{ij}^2}{2} \mathbf{v}_{ij} + \left(\frac{A_{ij}^2}{2} + \frac{B_{ij}^2 - A_{ij}^2}{D} \right) \mathbf{e}_{ij} \cdot \mathbf{v}_{ij} \mathbf{e}_{ij} \right] dt \\ &\quad - \frac{1}{2} \sum_{j \in \mathcal{N}_i} \frac{1}{C_i} \left[A_{ij} \frac{\partial A_{ij}}{\partial T_i} \mathbf{v}_{ij} + \left(A_{ij} \frac{\partial A_{ij}}{\partial T_i} + \frac{2}{D} B_{ij} \frac{\partial B_{ij}}{\partial T_i} - \frac{2}{D} A_{ij} \frac{\partial A_{ij}}{\partial T_i} \right) \mathbf{e}_{ij} \cdot \mathbf{v}_{ij} \mathbf{e}_{ij} \right] dt \end{aligned}$$

$$-\frac{1}{2} \sum_{j \in \mathcal{N}_i} \frac{1}{C_j} \left[A_{ij} \frac{\partial A_{ij}}{\partial T_j} \mathbf{v}_{ij} + \left(A_{ij} \frac{\partial A_{ij}}{\partial T_j} + \frac{2}{D} B_{ij} \frac{\partial B_{ij}}{\partial T_j} - \frac{2}{D} A_{ij} \frac{\partial A_{ij}}{\partial T_j} \right) \mathbf{e}_{ij} \cdot \mathbf{v}_{ij} \mathbf{e}_{ij} \right] dt$$

$$\begin{aligned} T_i \sum_{j \in \mathcal{N}_i} \frac{\partial}{\partial \mathbf{v}_j} \cdot \frac{d\tilde{S}_i d\tilde{\mathbf{v}}_j^T}{2k_B} &= - \sum_{j \in \mathcal{N}_i} \frac{\partial}{\partial \mathbf{v}_j} \cdot \frac{1}{m} \delta_{ij} \sum_{k \in \mathcal{N}_i} \left[\frac{A_{ik}^2}{2} \left(\frac{\mathbf{v}_{ik}}{2} + \mathbf{e}_{ik} \cdot \frac{\mathbf{v}_{ik}}{2} \mathbf{e}_{ik} \right) + \frac{B_{ik}^2 - A_{ik}^2}{D} \mathbf{e}_{ik} \mathbf{e}_{ik} \cdot \frac{\mathbf{v}_{ik}}{2} \right] dt \\ &+ \sum_{j \in \mathcal{N}_i} \frac{\partial}{\partial \mathbf{v}_j} \cdot \frac{1}{m} \left[\frac{A_{ij}^2}{2} \left(\frac{\mathbf{v}_{ij}}{2} + \mathbf{e}_{ij} \cdot \frac{\mathbf{v}_{ij}}{2} \mathbf{e}_{ij} \right) + \frac{B_{ij}^2 - A_{ij}^2}{D} \mathbf{e}_{ij} \mathbf{e}_{ij} \cdot \frac{\mathbf{v}_{ij}}{2} \right] dt \\ &= -\frac{1}{2m} \frac{\partial}{\partial \mathbf{v}_i} \cdot \sum_{j \in \mathcal{N}_i} \left[\frac{A_{ij}^2}{2} (\mathbf{v}_{ij} + \mathbf{e}_{ij} \cdot \mathbf{v}_{ij} \mathbf{e}_{ij}) + \frac{B_{ij}^2 - A_{ij}^2}{D} \mathbf{e}_{ij} \mathbf{e}_{ij} \cdot \mathbf{v}_{ij} \right] dt \\ &+ \frac{1}{2m} \sum_{j \in \mathcal{N}_i} \frac{\partial}{\partial \mathbf{v}_j} \cdot \left[\frac{A_{ij}^2}{2} (\mathbf{v}_{ij} + \mathbf{e}_{ij} \cdot \mathbf{v}_{ij} \mathbf{e}_{ij}) + \frac{B_{ij}^2 - A_{ij}^2}{D} \mathbf{e}_{ij} \mathbf{e}_{ij} \cdot \mathbf{v}_{ij} \right] dt \\ &= -\frac{1}{m} \sum_{j \in \mathcal{N}_i} \left[(D+1) \frac{A_{ij}^2}{2} + \frac{B_{ij}^2 - A_{ij}^2}{D} \right] dt. \end{aligned}$$

$$\begin{aligned} \sum_{j \in \mathcal{N}_i} \frac{\partial}{\partial S_j} \cdot \frac{d\tilde{S}_i d\tilde{S}_j}{2k_B} &= \sum_{j \in \mathcal{N}_i} \frac{\partial}{\partial S_j} \cdot \frac{1}{T_i T_j} \delta_{ij} \sum_{k \in \mathcal{N}_i} \left(\frac{A_{ik}^2}{2} \left[\left(\frac{\mathbf{v}_{ik}}{2} \right)^2 + \left(\mathbf{e}_{ik} \cdot \frac{\mathbf{v}_{ik}}{2} \right)^2 \right] + \frac{B_{ik}^2 - A_{ik}^2}{D} \left(\mathbf{e}_{ik} \cdot \frac{\mathbf{v}_{ik}}{2} \right)^2 + C_{ik}^2 \right) dt \\ &+ \sum_{j \in \mathcal{N}_i} \frac{\partial}{\partial S_j} \cdot \frac{1}{T_i T_j} \left(\frac{A_{ij}^2}{2} \left[\left(\frac{\mathbf{v}_{ij}}{2} \right)^2 + \left(\mathbf{e}_{ij} \cdot \frac{\mathbf{v}_{ij}}{2} \right)^2 \right] + \frac{B_{ij}^2 - A_{ij}^2}{D} \left(\mathbf{e}_{ij} \cdot \frac{\mathbf{v}_{ij}}{2} \right)^2 - C_{ij}^2 \right) dt \\ &= \frac{\partial}{\partial S_i} \cdot \frac{1}{T_i^2} \sum_{j \in \mathcal{N}_i} \left(\frac{A_{ij}^2}{2} \left[\left(\frac{\mathbf{v}_{ij}}{2} \right)^2 + \left(\mathbf{e}_{ij} \cdot \frac{\mathbf{v}_{ij}}{2} \right)^2 \right] + \frac{B_{ij}^2 - A_{ij}^2}{D} \left(\mathbf{e}_{ij} \cdot \frac{\mathbf{v}_{ij}}{2} \right)^2 + C_{ij}^2 \right) dt \\ &+ \sum_{j \in \mathcal{N}_i} \frac{\partial}{\partial S_j} \cdot \frac{1}{T_i T_j} \left(\frac{A_{ij}^2}{2} \left[\left(\frac{\mathbf{v}_{ij}}{2} \right)^2 + \left(\mathbf{e}_{ij} \cdot \frac{\mathbf{v}_{ij}}{2} \right)^2 \right] + \frac{B_{ij}^2 - A_{ij}^2}{D} \left(\mathbf{e}_{ij} \cdot \frac{\mathbf{v}_{ij}}{2} \right)^2 - C_{ij}^2 \right) dt \\ &= -\frac{1}{4T_i} \sum_{j \in \mathcal{N}_i} \left(\frac{2}{T_i C_i} + \frac{1}{T_j C_j} \right) \left[\frac{A_{ij}^2}{2} \mathbf{v}_{ij}^2 + \left(\frac{A_{ij}^2}{2} + \frac{B_{ij}^2 - A_{ij}^2}{D} \right) (\mathbf{v}_{ij} \cdot \mathbf{e}_{ij})^2 \right] dt \\ &- \frac{1}{T_i} \sum_{j \in \mathcal{N}_i} \left(\frac{2}{T_i C_i} - \frac{1}{T_j C_j} \right) C_{ij}^2 dt \\ &+ \frac{1}{4T_i} \sum_{j \in \mathcal{N}_i} \frac{1}{T_i} \left[A_{ij} \frac{\partial A_{ij}}{\partial S_i} \mathbf{v}_{ij}^2 + \left(A_{ij} \frac{\partial A_{ij}}{\partial S_i} + \frac{2}{D} B_{ij} \frac{\partial B_{ij}}{\partial S_i} - \frac{2}{D} A_{ij} \frac{\partial A_{ij}}{\partial S_i} \right) (\mathbf{v}_{ij} \cdot \mathbf{e}_{ij})^2 \right] dt \\ &+ \frac{1}{4T_i} \sum_{j \in \mathcal{N}_i} \frac{1}{T_j} \left[A_{ij} \frac{\partial A_{ij}}{\partial S_j} \mathbf{v}_{ij}^2 + \left(A_{ij} \frac{\partial A_{ij}}{\partial S_j} + \frac{2}{D} B_{ij} \frac{\partial B_{ij}}{\partial S_j} - \frac{2}{D} A_{ij} \frac{\partial A_{ij}}{\partial S_j} \right) (\mathbf{v}_{ij} \cdot \mathbf{e}_{ij})^2 \right] dt \\ &+ \frac{1}{T_i} \sum_{j \in \mathcal{N}_i} \left(\frac{1}{T_i} 2C_{ij} \frac{\partial C_{ij}}{\partial S_i} - \frac{1}{T_j} 2C_{ij} \frac{\partial C_{ij}}{\partial S_j} \right) dt \\ &= -\frac{1}{4T_i} \sum_{j \in \mathcal{N}_i} \left(\frac{2}{T_i C_i} + \frac{1}{T_j C_j} \right) \left[\frac{A_{ij}^2}{2} \mathbf{v}_{ij}^2 + \left(\frac{A_{ij}^2}{2} + \frac{B_{ij}^2 - A_{ij}^2}{D} \right) (\mathbf{v}_{ij} \cdot \mathbf{e}_{ij})^2 \right] dt \\ &- \frac{1}{T_i} \sum_{j \in \mathcal{N}_i} \left(\frac{2}{T_i C_i} - \frac{1}{T_j C_j} \right) C_{ij}^2 dt \\ &+ \frac{1}{4T_i} \sum_{j \in \mathcal{N}_i} \frac{1}{C_i} \left[A_{ij} \frac{\partial A_{ij}}{\partial T_i} \mathbf{v}_{ij}^2 + \left(A_{ij} \frac{\partial A_{ij}}{\partial T_i} + \frac{2}{D} B_{ij} \frac{\partial B_{ij}}{\partial T_i} - \frac{2}{D} A_{ij} \frac{\partial A_{ij}}{\partial T_i} \right) (\mathbf{v}_{ij} \cdot \mathbf{e}_{ij})^2 \right] dt \\ &+ \frac{1}{4T_i} \sum_{j \in \mathcal{N}_i} \frac{1}{C_j} \left[A_{ij} \frac{\partial A_{ij}}{\partial T_j} \mathbf{v}_{ij}^2 + \left(A_{ij} \frac{\partial A_{ij}}{\partial T_j} + \frac{2}{D} B_{ij} \frac{\partial B_{ij}}{\partial T_j} - \frac{2}{D} A_{ij} \frac{\partial A_{ij}}{\partial T_j} \right) (\mathbf{v}_{ij} \cdot \mathbf{e}_{ij})^2 \right] dt \end{aligned}$$

$$+ \frac{2}{T_i} \sum_{j \in \mathcal{N}_i} \left(\frac{1}{C_i} C_{ij} \frac{\partial C_{ij}}{\partial T_i} - \frac{1}{C_j} C_{ij} \frac{\partial C_{ij}}{\partial T_j} \right) dt.$$

A.3 Complete equations

With the parameterization specified we finally can summarize the dynamic equations of the method.

$$\begin{aligned} d\mathbf{r}_i &= \mathbf{v}_i dt, \\ m d\mathbf{v}_i &= \sum_{j \in \mathcal{N}_i} \left[\frac{P_j}{d_j^2} \frac{\partial W_{ji}}{\partial \mathbf{r}_{ji}} - \frac{P_i}{d_i^2} \frac{\partial W_{ij}}{\partial \mathbf{r}_{ij}} \right] dt + \sum_j \left[\tau_j \frac{\partial \bar{W}_{ji}}{\partial \mathbf{u}_{ji}} - \tau_i \frac{\partial \bar{W}_{ij}}{\partial \mathbf{u}_{ij}} \right] \\ &\quad - \frac{1}{2} \sum_{j \in \mathcal{N}_i} \left(\frac{1}{T_i} + \frac{1}{T_j} \right) \left[\frac{A_{ij}^2}{2} \mathbf{v}_{ij} + \left(\frac{A_{ij}^2}{2} + \frac{B_{ij}^2 - A_{ij}^2}{D} \right) \mathbf{e}_{ij} \cdot \mathbf{v}_{ij} \mathbf{e}_{ij} \right] dt \\ &\quad + \frac{k_B}{2} \sum_{j \in \mathcal{N}_i} \left(\frac{1}{T_i C_i} + \frac{1}{T_j C_j} \right) \left[\frac{A_{ij}^2}{2} \mathbf{v}_{ij} + \left(\frac{A_{ij}^2}{2} + \frac{B_{ij}^2 - A_{ij}^2}{D} \right) \mathbf{e}_{ij} \cdot \mathbf{v}_{ij} \mathbf{e}_{ij} \right] dt \\ &\quad - \frac{k_B}{2} \sum_{j \in \mathcal{N}_i} \frac{1}{C_i} \left[A_{ij} \frac{\partial A_{ij}}{\partial T_i} \mathbf{v}_{ij} + \left(A_{ij} \frac{\partial A_{ij}}{\partial T_i} + \frac{2}{D} B_{ij} \frac{\partial B_{ij}}{\partial T_i} - \frac{2}{D} A_{ij} \frac{\partial A_{ij}}{\partial T_i} \right) \mathbf{e}_{ij} \cdot \mathbf{v}_{ij} \mathbf{e}_{ij} \right] dt \\ &\quad - \frac{k_B}{2} \sum_{j \in \mathcal{N}_i} \frac{1}{C_j} \left[A_{ij} \frac{\partial A_{ij}}{\partial T_j} \mathbf{v}_{ij} + \left(A_{ij} \frac{\partial A_{ij}}{\partial T_j} + \frac{2}{D} B_{ij} \frac{\partial B_{ij}}{\partial T_j} - \frac{2}{D} A_{ij} \frac{\partial A_{ij}}{\partial T_j} \right) \mathbf{e}_{ij} \cdot \mathbf{v}_{ij} \mathbf{e}_{ij} \right] dt \\ &\quad + \sqrt{2k_B} \sum_{j \in \mathcal{N}_i} \left[A_{ij} d\bar{W}_{ij} + B_{ij} \frac{1}{D} \text{tr}(d\mathbf{W}_{ij}) \right] \mathbf{e}_{ij}, \\ T_i dS_i &= \frac{1}{4} \sum_{j \in \mathcal{N}_i} \left(\frac{1}{T_i} + \frac{1}{T_j} \right) \left[\frac{A_{ij}^2}{2} \mathbf{v}_{ij}^2 + \left(\frac{A_{ij}^2}{2} + \frac{B_{ij}^2 - A_{ij}^2}{D} \right) (\mathbf{v}_{ij} \cdot \mathbf{e}_{ij})^2 \right] dt + \sum_{j \in \mathcal{N}_i} \left(\frac{1}{T_i} - \frac{1}{T_j} \right) C_{ij}^2 dt \\ &\quad - \frac{k_B}{m} \sum_{j \in \mathcal{N}_i} \left[(D+1) \frac{A_{ij}^2}{2} + \frac{B_{ij}^2 - A_{ij}^2}{D} \right] dt \\ &\quad - \frac{k_B}{4} \sum_{j \in \mathcal{N}_i} \left(\frac{2}{T_i C_i} + \frac{1}{T_j C_j} \right) \left[\frac{A_{ij}^2}{2} \mathbf{v}_{ij}^2 + \left(\frac{A_{ij}^2}{2} + \frac{B_{ij}^2 - A_{ij}^2}{D} \right) (\mathbf{v}_{ij} \cdot \mathbf{e}_{ij})^2 \right] dt - k_B \sum_{j \in \mathcal{N}_i} \left(\frac{2}{T_i C_i} - \frac{1}{T_j C_j} \right) C_{ij}^2 dt \\ &\quad + \frac{k_B}{4} \sum_{j \in \mathcal{N}_i} \frac{1}{C_i} \left[A_{ij} \frac{\partial A_{ij}}{\partial T_i} \mathbf{v}_{ij}^2 + \left(A_{ij} \frac{\partial A_{ij}}{\partial T_i} + \frac{2}{D} B_{ij} \frac{\partial B_{ij}}{\partial T_i} - \frac{2}{D} A_{ij} \frac{\partial A_{ij}}{\partial T_i} \right) (\mathbf{v}_{ij} \cdot \mathbf{e}_{ij})^2 \right] dt \\ &\quad + \frac{k_B}{4} \sum_{j \in \mathcal{N}_i} \frac{1}{C_j} \left[A_{ij} \frac{\partial A_{ij}}{\partial T_j} \mathbf{v}_{ij}^2 + \left(A_{ij} \frac{\partial A_{ij}}{\partial T_j} + \frac{2}{D} B_{ij} \frac{\partial B_{ij}}{\partial T_j} - \frac{2}{D} A_{ij} \frac{\partial A_{ij}}{\partial T_j} \right) (\mathbf{v}_{ij} \cdot \mathbf{e}_{ij})^2 \right] dt \\ &\quad + 2k_B \sum_{j \in \mathcal{N}_i} \left(\frac{1}{C_i} C_{ij} \frac{\partial C_{ij}}{\partial T_i} - \frac{1}{C_j} C_{ij} \frac{\partial C_{ij}}{\partial T_j} \right) dt \\ &\quad - \frac{\sqrt{2k_B}}{2} \sum_{j \in \mathcal{N}_i} \left[A_{ij} d\bar{W}_{ij} + B_{ij} \frac{1}{D} \text{tr}(d\mathbf{W}_{ij}) \right] : \mathbf{e}_{ij} \mathbf{v}_{ij} + \sqrt{2k_B} \sum_{j \in \mathcal{N}_i} C_{ij} dV_{ij}. \end{aligned}$$

In the next section we prove that the proposed methodology fulfills the required thermodynamics and conservation laws.

B Conservation laws

Proposition B.1. *The metriplectic equation in Eq. (3) satisfies momentum conservation $d\mathbf{P} = \mathbf{0}$.*

Proof. This is a direct consequence of the skew-symmetry of the particle pair forces over index swapping. The total deterministic momentum over all particles is $\mathbf{P} = \sum_i m \mathbf{v}_i$. By using Itô's lemma, we have that:

$$d\mathbf{P} = \frac{\partial \mathbf{P}}{\partial \mathbf{x}} \cdot d\mathbf{x} + \frac{1}{2} \frac{\partial^2 \mathbf{P}}{\partial \mathbf{x}^2} : d\tilde{\mathbf{x}} d\tilde{\mathbf{x}}^T,$$

which is equivalent, by using the fluctuation dissipation theorem, to

$$d\mathbf{P} = \frac{\partial \mathbf{P}}{\partial \mathbf{x}} \cdot d\mathbf{x} + k_B \frac{\partial^2 \mathbf{P}}{\partial \mathbf{x}^2} : \mathbf{M} = \frac{\partial \mathbf{P}}{\partial \mathbf{x}} \cdot \left[\left(\mathbf{L} \frac{\partial E}{\partial \mathbf{x}} + \mathbf{M} \frac{\partial S}{\partial \mathbf{x}} + k_B \frac{\partial}{\partial \mathbf{x}} \cdot \mathbf{M} \right) dt + d\tilde{\mathbf{x}} \right] + k_B \frac{\partial^2 \mathbf{P}}{\partial \mathbf{x}^2} : \mathbf{M}.$$

We now show each summand is zero. The first term, by expanding the gradient of the internal energy from Eq. (12):

$$\frac{\partial \mathbf{P}}{\partial \mathbf{x}} \cdot \mathbf{L} \frac{\partial E}{\partial \mathbf{x}} = \sum_i [0, m\mathbf{1}, 0] \frac{1}{m} \begin{bmatrix} m\mathbf{v}_i \\ -\frac{\partial U}{\partial \mathbf{r}_i} \\ 0 \end{bmatrix} = \sum_i -\frac{\partial U}{\partial \mathbf{r}_i} = \sum_i \sum_{j \in \mathcal{N}_i} \left[\frac{P_j}{d_j^2} \frac{\partial W_{ji}}{\partial \mathbf{r}_{ji}} - \frac{P_i}{d_i^2} \frac{\partial W_{ij}}{\partial \mathbf{r}_{ij}} + \boldsymbol{\tau}_j : \frac{\partial \bar{\mathbf{W}}_{ji}}{\partial \mathbf{u}_{ji}} - \boldsymbol{\tau}_i : \frac{\partial \bar{\mathbf{W}}_{ij}}{\partial \mathbf{u}_{ij}} \right].$$

As the particle interactions are defined within a fixed neighbourhood \mathcal{N}_i for each particle, we can split the set of interactions in three subsets: $\{(i, j)\} = \{(i', j')\} \cup \{(j', i')\} \cup \{(i', i')\}$. This means that every particle interaction (i', j') has a mirror interaction with swapped indices (j', i') for $i' \neq j'$, as well as self interactions of a particle with itself (i', i') when $i' = j'$. The position vectors are $\mathbf{r}_{i'j'} = -\mathbf{r}_{j'i'}$ and $\mathbf{r}_{i'i'} = \mathbf{0}$ respectively. By applying the index swapping to the derivative and the condition of a spherical symmetric kernel $\nabla W(\mathbf{0}) = \mathbf{0}$, we get the following split sum:

$$\begin{aligned} \frac{\partial \mathbf{P}}{\partial \mathbf{x}} \cdot \mathbf{L} \frac{\partial E}{\partial \mathbf{x}} &= \sum_{i', j'} \left[\frac{P_{j'}}{d_{j'}^2} \frac{\partial W_{j'i'}}{\partial \mathbf{r}_{j'i'}} - \frac{P_{i'}}{d_{i'}^2} \frac{\partial W_{i'j'}}{\partial \mathbf{r}_{i'j'}} \right] + \sum_{j', i'} \left[\frac{P_{i'}}{d_{i'}^2} \frac{\partial W_{i'j'}}{\partial \mathbf{r}_{i'j'}} - \frac{P_{j'}}{d_{j'}^2} \frac{\partial W_{j'i'}}{\partial \mathbf{r}_{j'i'}} \right] + \sum_{i', i'} 2 \frac{P_{i'}}{d_{i'}^2} \frac{\partial W_{i'i'}}{\partial \mathbf{r}_{i'i'}} \\ &+ \sum_{i', j'} \left[\boldsymbol{\tau}_{j'} : \frac{\partial \bar{\mathbf{W}}_{j'i'}}{\partial \mathbf{u}_{j'i'}} - \boldsymbol{\tau}_{i'} : \frac{\partial \bar{\mathbf{W}}_{i'j'}}{\partial \mathbf{u}_{i'j'}} \right] + \sum_{j', i'} \left[\boldsymbol{\tau}_{i'} : \frac{\partial \bar{\mathbf{W}}_{i'j'}}{\partial \mathbf{u}_{i'j'}} - \boldsymbol{\tau}_{j'} : \frac{\partial \bar{\mathbf{W}}_{j'i'}}{\partial \mathbf{u}_{j'i'}} \right] + \mathbf{0} = \mathbf{0}. \end{aligned}$$

We can gather the divergence and second order term into a single divergence term

$$\frac{\partial \mathbf{P}}{\partial \mathbf{x}} \cdot k_B \frac{\partial}{\partial \mathbf{x}} \cdot \mathbf{M} + k_B \frac{\partial^2 \mathbf{P}}{\partial \mathbf{x}^2} : \mathbf{M} = k_B \frac{\partial}{\partial \mathbf{x}} \cdot \left(\mathbf{M} \frac{\partial \mathbf{P}}{\partial \mathbf{x}} \right) = \mathbf{0}.$$

By decomposing \mathbf{M} on its dyadic $d\mathbf{x}d\mathbf{x}^T = 2k_B \mathbf{M} dt$ we get that the sufficient condition is that $\frac{\partial \mathbf{P}}{\partial \mathbf{x}} \cdot d\tilde{\mathbf{x}} = \mathbf{0}$. By expanding and using the noise ansatz,

$$\frac{\partial \mathbf{P}}{\partial \mathbf{x}} \cdot d\tilde{\mathbf{x}} = \sum_i [0, m\mathbf{1}, 0] \begin{bmatrix} \mathbf{0} \\ d\tilde{\mathbf{v}}_i \\ d\tilde{S}_i \end{bmatrix} = \sum_i m d\tilde{\mathbf{v}}_i = \sum_i \sqrt{2k_B} \sum_{j \in \mathcal{N}_i} \left[A_{ij} d\bar{\mathbf{W}}_{ij} + B_{ij} \frac{1}{D} \text{tr}(d\mathbf{W}_{ij}) \right] \mathbf{e}_{ij}.$$

We obtain the desired cancellation by a similar reasoning as before: pairwise interactions cancel out due to the symmetries of A_{ij} , B_{ij} and $d\mathbf{W}_{ij}$ and skew-symmetry of the interdistance unit vectors $\mathbf{e}_{ij} = -\mathbf{e}_{ji}$ and $\mathbf{e}_{ii} = \mathbf{0}$. Thus, the fluctuating velocities do not contribute to the total momentum.

$$\begin{aligned} \frac{\partial \mathbf{P}}{\partial \mathbf{x}} \cdot d\tilde{\mathbf{x}} &= \sqrt{2k_B} \sum_{i', j'} \left[A_{i'j'} d\bar{\mathbf{W}}_{i'j'} + B_{i'j'} \frac{1}{D} \text{tr}(d\mathbf{W}_{i'j'}) \right] \mathbf{e}_{i'j'} + \sqrt{2k_B} \sum_{j', i'} \left[A_{j'i'} d\bar{\mathbf{W}}_{j'i'} + B_{j'i'} \frac{1}{D} \text{tr}(d\mathbf{W}_{j'i'}) \right] \mathbf{e}_{j'i'} \\ &+ \sqrt{2k_B} \sum_{i', i'} \left[A_{i'i'} d\bar{\mathbf{W}}_{i'i'} + B_{i'i'} \frac{1}{D} \text{tr}(d\mathbf{W}_{i'i'}) \right] \mathbf{e}_{i'i'} \\ &= \sqrt{2k_B} \sum_{i', j'} \left[A_{i'j'} d\bar{\mathbf{W}}_{i'j'} + B_{i'j'} \frac{1}{D} \text{tr}(d\mathbf{W}_{i'j'}) \right] \mathbf{e}_{i'j'} - \sqrt{2k_B} \sum_{i', j'} \left[A_{i'j'} d\bar{\mathbf{W}}_{i'j'} + B_{i'j'} \frac{1}{D} \text{tr}(d\mathbf{W}_{i'j'}) \right] \mathbf{e}_{i'j'} = \mathbf{0}. \end{aligned}$$

The second and fourth terms are $\mathbf{M} \frac{\partial \mathbf{P}}{\partial \mathbf{x}}$ and $\frac{\partial \mathbf{P}}{\partial \mathbf{x}} \cdot d\tilde{\mathbf{x}}$ respectively, already proven to be zero. □

Proposition B.2. Eq. (3) satisfies energy conservation $dE = 0$ if $\mathbf{M} \nabla E = \mathbf{0}$ and $d\tilde{\mathbf{x}} \cdot \nabla E = 0$.

Proof. By Itô's lemma, we have that

$$dE = \frac{\partial E}{\partial \mathbf{x}} \cdot d\mathbf{x} + \frac{1}{2} \frac{\partial^2 E}{\partial \mathbf{x}^2} : d\tilde{\mathbf{x}}d\tilde{\mathbf{x}}^T,$$

which is equivalent, by using the fluctuation dissipation theorem, to

$$dE = \frac{\partial E}{\partial \mathbf{x}} \cdot d\mathbf{x} + k_B \frac{\partial^2 E}{\partial \mathbf{x}^2} : \mathbf{M} = \frac{\partial E}{\partial \mathbf{x}} \cdot \left[\left(\mathbf{L} \frac{\partial E}{\partial \mathbf{x}} + \mathbf{M} \frac{\partial S}{\partial \mathbf{x}} + k_B \frac{\partial}{\partial \mathbf{x}} \cdot \mathbf{M} \right) dt + d\tilde{\mathbf{x}} \right] + k_B \frac{\partial^2 E}{\partial \mathbf{x}^2} : \mathbf{M}.$$

We now show each summand is zero.

Due to the skew-symmetry of \mathbf{L} we have that the first summand is

$$\frac{\partial E}{\partial \mathbf{x}} \cdot \mathbf{L} \frac{\partial E}{\partial \mathbf{x}} = 0.$$

For the second, following the symmetric positive semi-definiteness and degeneracy condition for \mathbf{M}

$$\frac{\partial E}{\partial \mathbf{x}} \cdot \mathbf{M} \frac{\partial S}{\partial \mathbf{x}} = \frac{\partial S}{\partial \mathbf{x}} \cdot \mathbf{M} \frac{\partial E}{\partial \mathbf{x}} = 0.$$

We can gather the divergence and second order term into a single divergence which can be cancelled via the degeneracy condition

$$\frac{\partial E}{\partial \mathbf{x}} \cdot k_B \frac{\partial}{\partial \mathbf{x}} \cdot \mathbf{M} + k_B \frac{\partial^2 E}{\partial \mathbf{x}^2} : \mathbf{M} = k_B \frac{\partial}{\partial \mathbf{x}} \cdot \left(\mathbf{M} \frac{\partial E}{\partial \mathbf{x}} \right) = 0.$$

The final stochastic differential term is zero by assumption:

$$\frac{\partial E}{\partial \mathbf{x}} \cdot d\tilde{\mathbf{x}} = d\tilde{\mathbf{x}} \cdot \frac{\partial E}{\partial \mathbf{x}} = 0.$$

□

Proposition B.3. *The metriplectic equation in Eq. (3) satisfies the degeneracy conditions $\mathbf{L}\nabla S = \mathbf{M}\nabla E = \mathbf{0}$ and $d\tilde{\mathbf{x}} \cdot \nabla E = 0$, thus it satisfies energy conservation.*

Proof. The first degeneracy condition is satisfied trivially by the definition of the entropy as a state variable and the zero block structure of the Poisson matrix,

$$\mathbf{L} \frac{\partial S}{\partial \mathbf{x}} = \sum_{j \in \mathcal{N}_i} \frac{1}{m} \begin{bmatrix} \mathbf{0} & -\mathbf{I}\delta_{ij} & \mathbf{0} \\ \mathbf{I}\delta_{ij} & \mathbf{0} & \mathbf{0} \\ \mathbf{0} & \mathbf{0} & \mathbf{0} \end{bmatrix} \begin{bmatrix} \mathbf{0} \\ \mathbf{0} \\ 1 \end{bmatrix} = \mathbf{0}.$$

For the second degeneracy, we need to use the factorization of the friction matrix into the dyadic of the noise differentials $d\mathbf{x}d\mathbf{x}^T = 2k_B\mathbf{M}dt$ in the following way,

$$d\tilde{\mathbf{x}}d\tilde{\mathbf{x}}^T \frac{\partial E}{\partial \mathbf{x}} = 2k_B\mathbf{M}dt \frac{\partial E}{\partial \mathbf{x}}.$$

Now we can prove that the left term is equal to zero, which also holds for the right term. Considering that $2k_Bdt \neq 0$, it implies that the second degeneracy is zero. By applying the definition of ∇E and expanding the relative velocity $\mathbf{v}_{ij} = \mathbf{v}_i - \mathbf{v}_j$ we get

$$\begin{aligned} d\tilde{\mathbf{x}} \cdot \frac{\partial E}{\partial \mathbf{x}} &= \sum_i \left[\mathbf{0}, d\tilde{\mathbf{v}}_i, d\tilde{S}_i \right] \begin{bmatrix} -\frac{\partial U}{\partial \mathbf{r}_i} \\ m\mathbf{v}_i \\ T_i \end{bmatrix} = \sum_i (m\mathbf{v}_i \cdot d\tilde{\mathbf{v}}_i + T_i d\tilde{S}_i) = \sum_i \mathbf{v}_i \cdot \sqrt{2k_B} \sum_{j \in \mathcal{N}_i} [A_{ij}d\bar{\mathbf{W}}_{ij} + B_{ij} \frac{1}{D} \text{tr}(d\mathbf{W}_{ij})] \mathbf{e}_{ij} \\ &\quad + \sum_i -\frac{\sqrt{2k_B}}{2} \sum_{j \in \mathcal{N}_i} \left[A_{ij}d\bar{\mathbf{W}}_{ij} + B_{ij} \frac{1}{D} \text{tr}(d\mathbf{W}_{ij}) \right] : \mathbf{e}_{ij} \mathbf{v}_{ij} + \sum_i \sqrt{2k_B} \sum_{j \in \mathcal{N}_i} C_{ij} dV_{ij} \\ &= \sqrt{2k_B} \sum_{i,j} \left[A_{ij}d\bar{\mathbf{W}}_{ij} + B_{ij} \frac{1}{D} \text{tr}(d\mathbf{W}_{ij}) \right] \mathbf{e}_{ij} \cdot \mathbf{v}_i - \frac{\sqrt{2k_B}}{2} \sum_{i,j} \left[A_{ij}d\bar{\mathbf{W}}_{ij} + B_{ij} \frac{1}{D} \text{tr}(d\mathbf{W}_{ij}) \right] \mathbf{e}_{ij} \cdot \mathbf{v}_i \\ &\quad + \frac{\sqrt{2k_B}}{2} \sum_{i,j} \left[A_{ij}d\bar{\mathbf{W}}_{ij} + B_{ij} \frac{1}{D} \text{tr}(d\mathbf{W}_{ij}) \right] \mathbf{e}_{ij} \cdot \mathbf{v}_j \\ &= \sqrt{2k_B} \sum_{i,j} \left[A_{ij}d\bar{\mathbf{W}}_{ij} + B_{ij} \frac{1}{D} \text{tr}(d\mathbf{W}_{ij}) \right] \mathbf{e}_{ij} \cdot \mathbf{v}_i - \sqrt{2k_B} \sum_{i,j} \left[A_{ij}d\bar{\mathbf{W}}_{ij} + B_{ij} \frac{1}{D} \text{tr}(d\mathbf{W}_{ij}) \right] \mathbf{e}_{ij} \cdot \mathbf{v}_i = 0. \end{aligned}$$

We have used the same index swapping cancellations between pairwise particles as in Proposition B.1. The independent term vanishes due to the skew-symmetry of dV_{ij} and symmetry of C_{ij} , which makes a cancellation for each pair of particles. Similarly, we have performed an index swap by exploiting the symmetries of A_{ij} , B_{ij} , C_{ij} and $d\mathbf{W}_{ij}$.

□

Proposition B.4. *The degeneracies $\mathbf{M}\nabla E = \mathbf{0}$ and $d\tilde{\mathbf{x}} \cdot \nabla E = 0$ are satisfied if $Q_{ji} = C_{ijk} \frac{\partial E}{\partial \mathbf{x}_k}$ where C_{ijk} is a 3-tensor with the following skew-symmetry $C_{ijk} = -C_{ikj}$.*

Proof. The noise vector is described by $d\tilde{x} = QdW$ where dW denotes a vector of independent and identically distributed (IID) increments of a Wiener process. From the degeneracy $d\tilde{x} \cdot \nabla E = dW^T Q^T \nabla E = \mathbf{0}$ we obtain the constraint that $Q^T \nabla E = \mathbf{0}$ implies $d\tilde{x} \cdot \nabla E = 0$ for any sample dW . The other degeneracy condition follows immediately $M \nabla E = QQ^T \nabla E = \mathbf{0}$.

Now we proof the condition $Q^T \nabla E = \mathbf{0}$. By using the 3-tensor skew-symmetric parametrization we get:

$$Q_{ji} \frac{\partial E}{\partial x_j} = C_{ijk} \frac{\partial E}{\partial x_k} \frac{\partial E}{\partial x_j} = C_{ikj} \frac{\partial E}{\partial x_j} \frac{\partial E}{\partial x_k} = -C_{ijk} \frac{\partial E}{\partial x_k} \frac{\partial E}{\partial x_j} = -Q_{ji} \frac{\partial E}{\partial x_j}.$$

By rearranging the first and last terms of the equality, we have

$$Q_{ji} \frac{\partial E}{\partial x_j} + Q_{ji} \frac{\partial E}{\partial x_j} = 2Q_{ji} \frac{\partial E}{\partial x_j} = 0 \rightarrow Q_{ji} \frac{\partial E}{\partial x_j} = 0.$$

□

Remark. The proposed parametrization can be constructed in several ways, designing specific parameters θ in increasing level of complexity and respecting the required skew-symmetry:

- Nodal parameters + edge skew-symmetry: $C_{ijk} = \theta_i(\theta'_{jk} - \theta'_{kj})$.
- Edge parameters + edge skew-symmetry: $C_{ijk} = \theta_{ij}(\theta'_{jk} - \theta'_{kj})$.
- General tensor skew-symmetry: $C_{ijk} = \theta_{ijk} - \theta_{ikj}$.

Remark. This parametrization can also be extended in case there are more than one entropic variables: S_1, \dots, S_N by using a higher rank tensor with similar symmetries $C_{ijk_1 \dots k_N} = -C_{ik_a k_1 \dots j \dots k_N}$ for all extra indices and defining $Q_{ji} = C_{ijk_1 \dots k_N} \frac{\partial E}{\partial x_{k_1}} \dots \frac{\partial E}{\partial x_{k_N}}$.

C Derivation of log-likelihood

Let $\mathcal{D} = \{(\mathbf{x}_{\text{rev}}^t, \mathbf{x}_{\text{rev}}^{t+1})\}_{t=0}^{N_{\text{train}}}$ be a dataset consisting of position-velocity pairs. To train the system, we construct a joint probability distribution $p(\mathbf{x}_{\text{rev}}^{t+1}, \mathbf{x}_{\text{irr}}^{t+1} | \mathbf{x}_{\text{rev}}^t, \mathbf{x}_{\text{irr}}^t)$ corresponding to a numerical integration of Eq. (3) and train the architectures with maximum likelihood. Recall that for a general drift-diffusion SDE

$$d\mathbf{x} = f(\mathbf{x}, t)dt + g(\mathbf{x}, t)dW,$$

application of the Euler-Maruyama integrator provides a Gaussian increment

$$\mathbf{x}^{t+1} | \mathbf{x}^t \sim \mathcal{N}(\boldsymbol{\mu}^{t+1} = \mathbf{x}^t + f(\mathbf{x}^t, t)\Delta t, \boldsymbol{\Sigma}^{t+1} = g(\mathbf{x}^t, t)^2 \Delta t). \quad (13)$$

Under a Markovian assumption, we can thus define a joint distribution for the complete time series and derive the negative log-likelihood.

$$\text{NLL}(x^1, \dots, x^T) = - \sum_{t=1}^T \log p(x^t | x^{t-1}).$$

To obtain robust long-term rollouts, we specialize this candidate log-likelihood function to Eq. (3) and modify the transition probabilities slightly to develop a semi-implicit Euler scheme. We denote all trainable parameters via

$$\Theta = \{\theta_V, \theta_U, \theta_A, \theta_B, \theta_C, \theta_S, k_B, m\}$$

and define the maximum log-likelihood objective

$$\Theta^* = \arg \min_{\Theta} \text{NLL}(x^1, \dots, x^T).$$

To modify Eq. (13), we identify a transition probability $p(x^t | x^{t-1})$ consistent with the update rule.

$$\begin{aligned} \mathbf{v}^{t+1} &= \mathbf{v}^t + \frac{d\mathbf{v}^t}{dt} \Delta t + \Delta \tilde{\mathbf{v}}^t, \\ \mathbf{r}^{t+1} &= \mathbf{r}^t + \mathbf{v}^{t+1} \Delta t, \\ S^{t+1} &= S^t + \frac{dS^t}{dt} \Delta t + \Delta \tilde{S}^t. \end{aligned}$$

For small Δt , this is provided by the multivariate normal distribution $\mathbf{x}^{t+1}|\mathbf{x}^t \sim N(\boldsymbol{\mu}^{t+1}, \boldsymbol{\Sigma}^{t+1})$ with mean and covariance

$$\boldsymbol{\mu}^{t+1} = \begin{bmatrix} \mathbf{r}^t + \mathbf{v}^t \Delta t + \frac{d\mathbf{v}^t}{dt} \Delta t^2 \\ \mathbf{v}^t + \frac{d\mathbf{v}^t}{dt} \Delta t \\ S^t + \frac{dS^t}{dt} \Delta t \end{bmatrix}, \quad \boldsymbol{\Sigma}^{t+1} = \begin{bmatrix} \Delta \tilde{\mathbf{v}} \Delta \tilde{\mathbf{v}}^T \Delta t^2 & \Delta \tilde{\mathbf{v}} \Delta \tilde{\mathbf{v}}^T \Delta t & \Delta \tilde{\mathbf{v}} \Delta \tilde{S} \Delta t \\ \Delta \tilde{\mathbf{v}} \Delta \tilde{\mathbf{v}}^T \Delta t & \Delta \tilde{\mathbf{v}} \Delta \tilde{\mathbf{v}}^T & \Delta \tilde{\mathbf{v}} \Delta \tilde{S} \\ \Delta \tilde{S} \Delta \tilde{\mathbf{v}}^T \Delta t & \Delta \tilde{S} \Delta \tilde{\mathbf{v}}^T & \Delta \tilde{S} \Delta \tilde{S} \end{bmatrix}.$$

Now we can define the loss function to be the standard negative log-likelihood of the observations as

$$\mathcal{L} = \sum_{t=0}^{N_{\text{train}}} \left[\frac{1}{2} \ln |\boldsymbol{\Sigma}^{t+1}| + \frac{1}{2} (\mathbf{x}^{t+1} - \boldsymbol{\mu}^{t+1})^T (\boldsymbol{\Sigma}^{t+1})^{-1} (\mathbf{x}^{t+1} - \boldsymbol{\mu}^{t+1}) \right].$$

There are two problems with this approach. First, the computation of $\boldsymbol{\Sigma}$ involves the explicit construction of the global M matrix which has a space complexity scaling of $O(N^2)$, so it is very expensive in terms of memory usage and computation time for the determinant and inverse operations. We can overcome this problem by using only the marginal covariances $\boldsymbol{\Sigma}_{ii}$ of each particle, which scales linearly with the number of particles $O(N)$. Second, the covariance matrix $\boldsymbol{\Sigma}$ is singular because the position has a deterministic relationship with the velocity up to a linear scaling of Δt . We overcome this by also marginalizing over the dependent position variable, which solves the rank deficiency.

Now we can split the problem as a particle-wise problem with the following statistical properties:

$$\boldsymbol{\mu}_i^{t+1} = \begin{bmatrix} \mathbf{v}_i^t + \frac{d\mathbf{v}_i^t}{dt} \Delta t \\ S_i^t + \frac{dS_i^t}{dt} \Delta t \end{bmatrix}, \quad \boldsymbol{\Sigma}_{ii}^{t+1} = \begin{bmatrix} \Delta \tilde{\mathbf{v}}_i \Delta \tilde{\mathbf{v}}_i^T & \Delta \tilde{\mathbf{v}}_i \Delta \tilde{S}_i \\ \Delta \tilde{S}_i \Delta \tilde{\mathbf{v}}_i^T & \Delta \tilde{S}_i \Delta \tilde{S}_i \end{bmatrix}.$$

Thus the final loss function is defined as

$$\mathcal{L} = \frac{1}{N_{\text{train}}} \sum_{t=0}^{N_{\text{train}}} \frac{1}{N} \sum_{i=0}^N \left[\frac{1}{2} \ln |\boldsymbol{\Sigma}_{ii}^{t+1}| + \frac{1}{2} (\mathbf{x}_i^{t+1} - \boldsymbol{\mu}_i^{t+1})^T (\boldsymbol{\Sigma}_{ii}^{t+1})^{-1} (\mathbf{x}_i^{t+1} - \boldsymbol{\mu}_i^{t+1}) \right].$$

C.1 Computation of marginal covariances

For the marginal covariances, we need to get the $i = j$ components of the complete covariance matrix M , whose components were already computed in the previous section. By the following properties $\delta_{ii} = 1$, $\mathbf{e}_{ii} = \mathbf{v}_{ii} = 0$ and the fact the the summation over $j \in \mathcal{N}_i$ only contains nodes different than i , we obtain the following contributions:

$$\begin{aligned} m^2 \frac{d\tilde{\mathbf{v}}_i d\tilde{\mathbf{v}}_i^T}{2k_B} &= \delta_{ii} \sum_{k \in \mathcal{N}_i} \left[\frac{A_{ik}^2}{2} (\mathbf{I} + \mathbf{e}_{ik} \mathbf{e}_{ik}^T) + \frac{B_{ik}^2 - A_{ik}^2}{D} \mathbf{e}_{ik} \mathbf{e}_{ik}^T \right] dt - \left[\frac{A_{ii}^2}{2} (\mathbf{I} + \mathbf{e}_{ii} \mathbf{e}_{ii}^T) + \frac{B_{ii}^2 - A_{ii}^2}{D} \mathbf{e}_{ii} \mathbf{e}_{ii}^T \right] dt \\ &= \sum_{j \in \mathcal{N}_i} \left[\frac{A_{ij}^2}{2} \mathbf{I} + \left(\frac{A_{ij}^2}{2} + \frac{B_{ij}^2 - A_{ij}^2}{D} \right) \mathbf{e}_{ij} \mathbf{e}_{ij}^T \right] dt. \end{aligned}$$

$$\begin{aligned} mT_i \frac{d\tilde{\mathbf{v}}_i d\tilde{S}_i}{2k_B} &= -\delta_{ii} \sum_{k \in \mathcal{N}_i} \left[\frac{A_{ik}^2}{2} \left(\frac{\mathbf{v}_{ik}}{2} + \mathbf{e}_{ik} \cdot \frac{\mathbf{v}_{ik}}{2} \mathbf{e}_{ik} \right) + \frac{B_{ik}^2 - A_{ik}^2}{D} \mathbf{e}_{ik} \mathbf{e}_{ik} \cdot \frac{\mathbf{v}_{ik}}{2} \right] dt \\ &\quad - \left[\frac{A_{ii}^2}{2} \left(\frac{\mathbf{v}_{ii}}{2} + \mathbf{e}_{ii} \cdot \frac{\mathbf{v}_{ii}}{2} \mathbf{e}_{ii} \right) + \frac{B_{ii}^2 - A_{ii}^2}{D} \mathbf{e}_{ii} \mathbf{e}_{ii} \cdot \frac{\mathbf{v}_{ii}}{2} \right] dt \\ &= -\frac{1}{2} \sum_{j \in \mathcal{N}_i} \left[\frac{A_{ij}^2}{2} \mathbf{v}_{ij} + \left(\frac{A_{ij}^2}{2} + \frac{B_{ij}^2 - A_{ij}^2}{D} \right) \mathbf{e}_{ij} \cdot \mathbf{v}_{ij} \mathbf{e}_{ij} \right] dt. \end{aligned}$$

$$\begin{aligned} mT_i \frac{d\tilde{S}_i d\tilde{\mathbf{v}}_i^T}{2k_B} &= -\delta_{ii} \sum_{k \in \mathcal{N}_i} \left[\frac{A_{ik}^2}{2} \left(\frac{\mathbf{v}_{ik}^T}{2} + \mathbf{e}_{ik} \cdot \frac{\mathbf{v}_{ik}}{2} \mathbf{e}_{ik}^T \right) + \frac{B_{ik}^2 - A_{ik}^2}{D} \mathbf{e}_{ik}^T \mathbf{e}_{ik} \cdot \frac{\mathbf{v}_{ik}}{2} \right] dt \\ &\quad + \left[\frac{A_{ii}^2}{2} \left(\frac{\mathbf{v}_{ii}^T}{2} + \mathbf{e}_{ii} \cdot \frac{\mathbf{v}_{ii}}{2} \mathbf{e}_{ii}^T \right) + \frac{B_{ii}^2 - A_{ii}^2}{D} \mathbf{e}_{ii}^T \mathbf{e}_{ii} \cdot \frac{\mathbf{v}_{ii}}{2} \right] dt \end{aligned}$$

$$= -\frac{1}{2} \sum_{j \in \mathcal{N}_i} \left[\frac{A_{ij}^2}{2} \mathbf{v}_{ij}^T + \left(\frac{A_{ij}^2}{2} + \frac{B_{ij}^2 - A_{ij}^2}{D} \right) \mathbf{e}_{ij} \cdot \mathbf{v}_{ij} \mathbf{e}_{ij}^T \right] dt.$$

$$\begin{aligned} T_i^2 \frac{d\tilde{S}_i d\tilde{S}_i}{2k_B} &= \delta_{ii} \sum_{k \in \mathcal{N}_i} \left(\frac{A_{ik}^2}{2} \left[\left(\frac{\mathbf{v}_{ik}}{2} \right)^2 + \left(\mathbf{e}_{ik} \cdot \frac{\mathbf{v}_{ik}}{2} \right)^2 \right] + \frac{B_{ik}^2 - A_{ik}^2}{D} \left(\mathbf{e}_{ik} \cdot \frac{\mathbf{v}_{ik}}{2} \right)^2 + C_{ik}^2 \right) dt \\ &+ \left(\frac{A_{ii}^2}{2} \left[\left(\frac{\mathbf{v}_{ii}}{2} \right)^2 + \left(\mathbf{e}_{ii} \cdot \frac{\mathbf{v}_{ii}}{2} \right)^2 \right] + \frac{B_{ii}^2 - A_{ii}^2}{D} \left(\mathbf{e}_{ii} \cdot \frac{\mathbf{v}_{ii}}{2} \right)^2 - C_{ii}^2 \right) dt \\ &= \sum_{j \in \mathcal{N}_i} \left(\frac{A_{ij}^2}{2} \left[\left(\frac{\mathbf{v}_{ij}}{2} \right)^2 + \left(\mathbf{e}_{ij} \cdot \frac{\mathbf{v}_{ij}}{2} \right)^2 \right] + \frac{B_{ij}^2 - A_{ij}^2}{D} \left(\mathbf{e}_{ij} \cdot \frac{\mathbf{v}_{ij}}{2} \right)^2 + C_{ij}^2 \right) dt \\ &= \frac{1}{4} \sum_{j \in \mathcal{N}_i} \left[\frac{A_{ij}^2}{2} \mathbf{v}_{ij}^2 + \left(\frac{A_{ij}^2}{2} + \frac{B_{ij}^2 - A_{ij}^2}{D} \right) \left(\mathbf{e}_{ij} \cdot \mathbf{v}_{ij} \right)^2 \right] dt + \sum_{j \in \mathcal{N}_i} C_{ij}^2 dt. \end{aligned}$$

Note that the resulting marginal covariance matrices are symmetric, as expected. Furthermore, as the complete covariance matrix \mathbf{M} is positive semidefinite by construction, all its leading minors are also positive semidefinite matrices. Thus, all the marginal covariance matrices are valid.

D Constrained monotonic neural networks

The purpose of Constrained Monotonic Neural Networks [73] is to construct a universal approximator with a precondition of (partial) monotonicity and/or convexity of a multivariate, multidimensional function. The basic building block is a monotone constrained fully connected layer:

$$\mathbf{h} = \rho^s(|\mathbf{W}^T|_{\mathbf{t}} \mathbf{x} + \mathbf{b})$$

where $\mathbf{x} \in \mathbb{R}^n$ is the input vector, $\mathbf{h} \in \mathbb{R}^m$ is the output vector, $\mathbf{W} \in \mathbb{R}^{n \times m}$ and $\mathbf{b} \in \mathbb{R}^m$ are the weights and biases, ρ^s is the combined activation function, and \mathbf{t} is the monotonicity indicator vector. This is a usual MLP architecture whose weights and activation functions are specifically chosen to ensure monotonicity and convexity of the output results.

In particular, we need to model the internal energy $U_i = U(S_i, \mathcal{V}_i)$ scalar function which is increasing in entropy S_i and decreasing in volume \mathcal{V}_i , both scalar quantities. Thus, the monotonicity indicator vector is $\mathbf{t} = [1, -1]$ and the weight matrix is modified by the operation $|\mathbf{W}^T|_{\mathbf{t}}$ which assigns the following sign change:

$$w'_{ji} = \begin{cases} |w_{ji}| & \text{if } t_i = 1 \\ -|w_{ji}| & \text{if } t_i = -1 \\ w_{ji} & \text{otherwise} \end{cases}.$$

For the subsequent hidden layers, monotonic dense units with the indicator vector \mathbf{t} always being set to 1 are used in order to preserve monotonicity. Last, we enforce convexity with respect to both inputs by using a convex activation function ρ^s . In our experiments, we have used a softmax activation. It is noteworthy that even with the imposed constraints on weights and activation functions, the network retains its universal approximation property. The complete proof is provided in [73].

E Training and testing algorithms

Algorithm 1 Training algorithm for the proposed method.

Input: State variables: $(\mathbf{r}^t, \mathbf{v}^t)$
for each particle i **do**
 Compute neighbour particles $j \in \mathcal{N}_i$
 Estimate entropy S_i :
 $S_i = \text{NN}(\mathbf{r}_{ij}, \mathbf{v}_{ij})$
 Compute particle volume \mathcal{V}_i and traceless strain tensor $\bar{\boldsymbol{\varepsilon}}_i$:
 $d_i = \text{NN}(\mathbf{r}_{ij})$
 $\bar{\boldsymbol{\varepsilon}}_i = \text{NN}(\mathbf{r}_{ij}, \mathbf{r}_{ij}^0)$
 Compute internal energy U_i :
 $U_i = \text{NN}(S_i, \mathcal{V}_i, \bar{\boldsymbol{\varepsilon}}_i)$
 $P_i = -\frac{\partial U_i}{\partial \mathcal{V}_i}, T_i = \frac{\partial U_i}{\partial S_i}, \boldsymbol{\tau}_i = \frac{\partial U_i}{\partial \bar{\boldsymbol{\varepsilon}}_i}$
 Compute prediction statistics:
 $A_{ij}, B_{ij}, C_{ij} = \text{NN}(\mathbf{r}_{ij}, T_i, T_j)$
 Compute Σ_{ii}^{t+1} and $\boldsymbol{\mu}_i^{t+1}$
end for
 Compute negative log-likelihood loss \mathcal{L}

Algorithm 2 Testing algorithm for the proposed method.

Input: Initial conditions: $(\mathbf{r}^0, \mathbf{v}^0)$
 Estimate initial entropy $S^0 = \text{NN}(\mathbf{r}_{ij}^0, \mathbf{v}_{ij}^0)$
for each snapshot t **do**
 for each particle i **do**
 Compute neighbour particles $j \in \mathcal{N}_i$
 Compute particle volume \mathcal{V}_i and traceless strain tensor $\bar{\boldsymbol{\varepsilon}}_i$:
 $d_i = \text{NN}(\mathbf{r}_{ij})$
 $\bar{\boldsymbol{\varepsilon}}_i = \text{NN}(\mathbf{r}_{ij}, \mathbf{r}_{ij}^0)$
 Compute internal energy U_i :
 $U_i = \text{NN}(S_i, \mathcal{V}_i, \bar{\boldsymbol{\varepsilon}}_i)$
 $P_i = -\frac{\partial U_i}{\partial \mathcal{V}_i}, T_i = \frac{\partial U_i}{\partial S_i}, \boldsymbol{\tau}_i = \frac{\partial U_i}{\partial \bar{\boldsymbol{\varepsilon}}_i}$
 Compute stochastic increments $d\tilde{\mathbf{x}}_i$:
 $A_{ij}, B_{ij}, C_{ij} = \text{NN}(\mathbf{r}_{ij}, T_i, T_j)$
 Random numbers $d\mathbf{W}_{ij}$ and dV_{ij}
 Compute $d\tilde{\mathbf{x}}_i = (\mathbf{0}, d\tilde{\mathbf{v}}_i, d\tilde{S}_i)$
 end for
 Solve dynamics \mathbf{x}^{t+1} via GENERIC
 Update state vector: $\mathbf{x}^t \leftarrow \mathbf{x}^{t+1}$
end for

F Alternative architectures

F.1 GNS

Graph Network-based Simulator (GNS) [58] is a deep learning architecture specifically designed for capturing the dynamical behaviour of complex fluids. For GNS, we use the original deterministic acceleration prediction based on positions and velocities. We use the following encoder-processor-decoder message-passing structure:

- Encoder: Following the original paper, the nodal features are chosen to be the velocities of the particles \mathbf{v}_i , and the edge features the relative positions \mathbf{r}_{ij} and distances $|\mathbf{r}_{ij}|$. Those are encoded in node \mathbf{z}_i and edge \mathbf{z}_{ij} latent vectors by using two networks:

$$\mathbf{z}_{ij} = \text{MLP}_e \left(\frac{\mathbf{r}_{ij}}{h}, \frac{|\mathbf{r}_{ij}|}{h} \right), \quad \mathbf{z}_i = \text{MLP}_v(\mathbf{v}_i).$$

- Processor: The latent nodes and edges are then processed with a message passing layer with mean aggregation function. This scheme is repeated M times with residual connections in order for the information to transverse the complete graph.

$$\mathbf{z}_{ij}^{l+1} = \mathbf{z}_{ij}^l + \text{MLP}_m^l(\mathbf{z}_i^l, \mathbf{z}_j^l, \mathbf{z}_{ij}^l), \quad \mathbf{z}_i^{l+1} = \mathbf{z}_i^l + \text{MLP}_v^l\left(\mathbf{z}_i^l, \frac{1}{|\mathcal{N}_i|} \sum_{j \in \mathcal{N}_i} \mathbf{z}_{ij}^{l+1}\right).$$

- Decoder: The decoder extracts the dynamic information from the latent nodes as an acceleration prediction:

$$\mathbf{a}_i = \text{MLP}_d(\mathbf{z}_i^M) dt.$$

The dynamic equations are then the following:

$$\begin{aligned} d\mathbf{r}_i &= \mathbf{v}_i dt \\ d\mathbf{v}_i &= \text{GNS}(\mathbf{r}_i, \mathbf{v}_i) dt = \mathbf{a}_i dt \end{aligned}$$

F.2 GNS-SDE

The original GNS paper does not account for stochastic effects. We have adapted the methodology to account for stochastic effects in a second architecture which we refer to as GNS-SDE [59]. The idea is to have two independent GNS which account for the drift and diffusion terms of a generic stochastic differential equation as follows:

$$\begin{aligned} d\mathbf{r}_i &= \mathbf{v}_i dt, \\ d\mathbf{v}_i &= \text{GNS}_{\text{drift}}(\mathbf{r}_i, \mathbf{v}_i) dt + \text{GNS}_{\text{diff}}(\mathbf{r}_i, \mathbf{v}_i) d\mathbf{w} \end{aligned}$$

where $\text{GNS}_{\text{drift}}(\mathbf{x})$ and $\text{GNS}_{\text{diff}}(\mathbf{x})$ are the drift and diffusion coefficients respectively and $d\mathbf{w}$ is a Wiener process with zero mean and unit variance.

F.3 DPD

As a traditional coarse-graining baseline, we use the standard Dissipative Particle Dynamics (DPD) force decomposition in conservative, dissipative and random forces between particles as:

$$\begin{aligned} d\mathbf{r}_i &= \mathbf{v}_i dt, \\ m d\mathbf{v}_i &= \sum_{j \in \mathcal{N}_i} (\mathbf{F}_{ij}^C dt + \mathbf{F}_{ij}^D dt + \mathbf{F}_{ij}^R d\mathbf{w}) \end{aligned}$$

where each force is computed using:

$$\begin{aligned} \mathbf{F}_{ij}^C &= \alpha w^C(|\mathbf{r}_{ij}|) \mathbf{e}_{ij}, \\ \mathbf{F}_{ij}^D &= -\gamma w^D(|\mathbf{r}_{ij}|) (\mathbf{e}_{ij} \cdot \mathbf{v}_{ij}) \mathbf{e}_{ij}, \\ \mathbf{F}_{ij}^R &= \sigma w^R(|\mathbf{r}_{ij}|) \mathbf{e}_{ij}. \end{aligned}$$

The conservative and random pairwise weight function is chosen to be the usual linear function of the normalized distance

$$w^C(|\mathbf{r}_{ij}|) = w^R(|\mathbf{r}_{ij}|) = 1 - \frac{|\mathbf{r}_{ij}|}{h}.$$

The dissipative forces are fully determined by the fluctuation-dissipation theorem:

$$\begin{aligned} \sigma^2 &= 2\gamma k_B T, \\ w^D(|\mathbf{r}_{ij}|) &= w^R(|\mathbf{r}_{ij}|)^2. \end{aligned}$$

To sum up, this model has 4 trainable parameters: the force amplitudes α and σ , the particle mass m and the thermal energy $k_B T$.

G Hyperparameters

G.1 Datasets

The datasets were generated using the following hyperparameters:

- Number of CG particles (N): Discretization of the domain in coarse-grained particles.
- Length of the domain (L): Length of the cubic box in 2D and 3D. For molecular dynamics examples, the periodic boundary conditions are applied.
- Cutoff radius (h): The radius which determines the neighbourhood from which the interactions are active, following the minimum image convention for periodic boundary conditions.
- Time step (Δt): Time step of the coarse-grained learnt simulation. In molecular dynamics examples, several orders of magnitude bigger than the original time scale. In solid mechanics example, it is determined by the CFL condition and the measured data availability.

Table 3: Dataset hyperparameters.

	N	L	h	Δt
IDEAL GAS	500	1.00 (3D periodic)	0.20	5.0e-4
STAR POLYMER 11	1000	30.18 (3D periodic)	4.75	2.5e-2
STAR POLYMER 51	2000	63.41 (3D periodic)	7.61	4.0e-2
VISCOELASTIC	900	2 (2D)	0.13	1.0e-2
NEEDLE	1135	2 (2D)	0.11	5.0e-4

G.1.1 IDEAL GAS

The first example is the simulation of $N = 500$ coarse-grained particles in a 3D periodic box of length $L = 1$. The fluid has a shear and bulk viscosity of $\eta = \zeta = 0.1$ and thermal conductivity of $\kappa = 0.1$. The equation of state is assumed to be an monoatomic ideal gas,

$$U(S, \mathcal{V}) = \frac{3h_p^2 N_p^2}{4\pi m} \left(\frac{N_p}{\mathcal{V}} \right)^{\frac{2}{3}} \exp \left(\frac{2S}{3k_B N_p} - \frac{5}{3} \right),$$

where h_p is the Planck constant and N_p the number of particles per fluid particle. We select units in which $N_p h_p = 1$, $N_p k_B = 10$ and $m = 1$. The dataset was generated directly in the coarse-grained domain using the methodology described in [30].

G.1.2 STAR POLYMER 11 and STAR POLYMER 51

The second example is a polymer melt in a 3D periodic box. Each polymer is composed of a core atom and 10 arms bonded by a FENE potential, whereas the interaction between polymers is modelled by a Lennard-Jones potential. Two different internal configurations are considered: 1 and 5 beads per arm, which results in less and higher coarse-graining levels. The fully resolved datasets are generated using LAMMPS [62] and then coarse-grained by computing the center of mass position and velocity of each polymer.

G.1.3 VISCOELASTIC

The 2D solid square domain of length $L = 2$ with a imposed shear displacement of $\Delta L_x = 1$ in the X axis. The material is chosen to be a Mooney-Rivlin model with density $\rho = 1000$ and parameters $C_{10} = 1.5 \cdot 10^6$, $C_{01} = 5 \cdot 10^5$ and $D_1 = 10^{-7}$. A time-dependant viscoelastic behaviour was included as a two-term Prony series with shear relaxation modulus ratio and relaxation time of $G_1 = 0.5$, $\tau_1 = 0.2$ and $G_2 = 0.49$, $\tau_2 = 0.3$ respectively. The system is discretized in $N = 900$ coarse graining particles. The reference solution was computed using the finite element solver Abaqus.

G.1.4 NEEDLE

The last example is a real measured dataset of a jammed 2D monolayer of repulsive microspheres under cyclic shear forcing. The system consists of sulfate latex particles adsorbed at a water-decane interface, forming a soft jammed material due to electrostatic dipole-dipole repulsion. The material is sheared using an interfacial stress rheometer (ISR), where a magnetized needle applies oscillatory shear stress within a confined channel [63, 64]. High-resolution optical microscopy is used to capture

the positions of each particle, processed with a computer vision particle tracking algorithm, and the velocities are obtained with finite differences. The system is discretized in $N = 1135$ coarse graining particles.

G.2 Training

The hyperparameters used to train the models are the following:

- Number of training snapshots (N_{train}): Time horizon considered for the training from the initial conditions. They are shuffled in 75% train and 25% validation split.
- Number of extrapolation snapshots (N_{extrap}): Sequential rollout of the model from the initial conditions. In molecular dynamics, the model is extrapolated to $N_{\text{extrap}} = 25N_{\text{train}}$ to reach the steady-state statistics.
- Learning rate (l_r): Initial learning rate for training.
- Number of epochs (N_{epoch}): Number of total training epochs.
- Number of hidden layers (N_h): Number of hidden layers of the MLPs. All the MLPs used are 2 hidden layers with SiLU activation functions [81].

Table 4: Training hyperparameters.

	N_{train}	N_{extrap}	l_r	N_{epoch}	N_h
IDEAL GAS	300	7.5e3	1.0e-2	5.0e3	50
STAR POLYMER 11	400	1.0e4	1.0e-3	5.0e3	100
STAR POLYMER 51	400	1.0e4	1.0e-3	1.0e4	50
VISCOELASTIC	800	1000	1.0e-3	2.0e3	100
NEEDLE	2000	3500	1.0e-3	2.0e3	100

H Additional figures

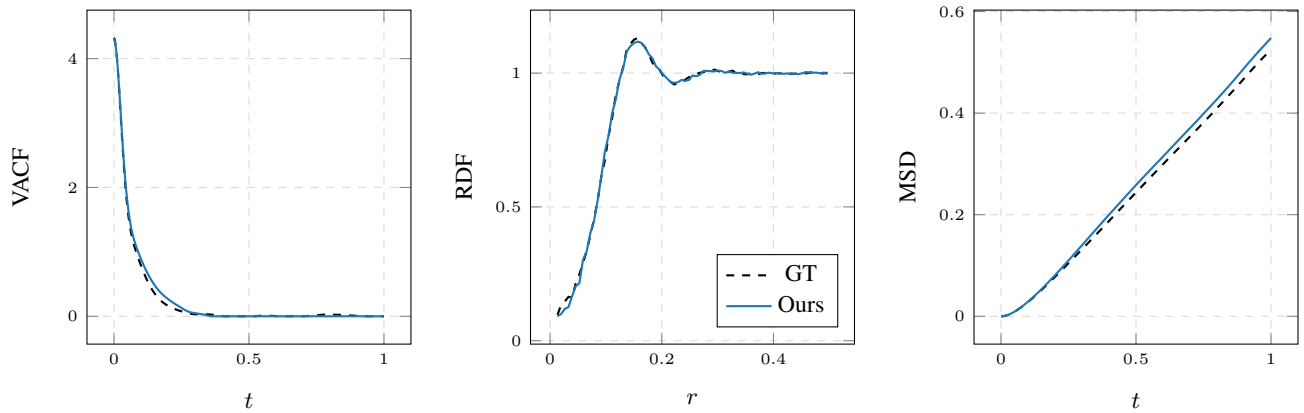


Figure 9: Correlation metrics for the TAYLOR-GREEN dataset.

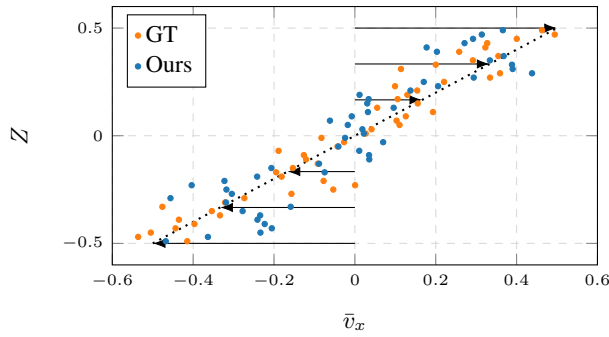


Figure 10: Velocity profile of the SHEAR FLOW test dataset averaged over the X axis. The forced boundary condition is represented as a dotted line.

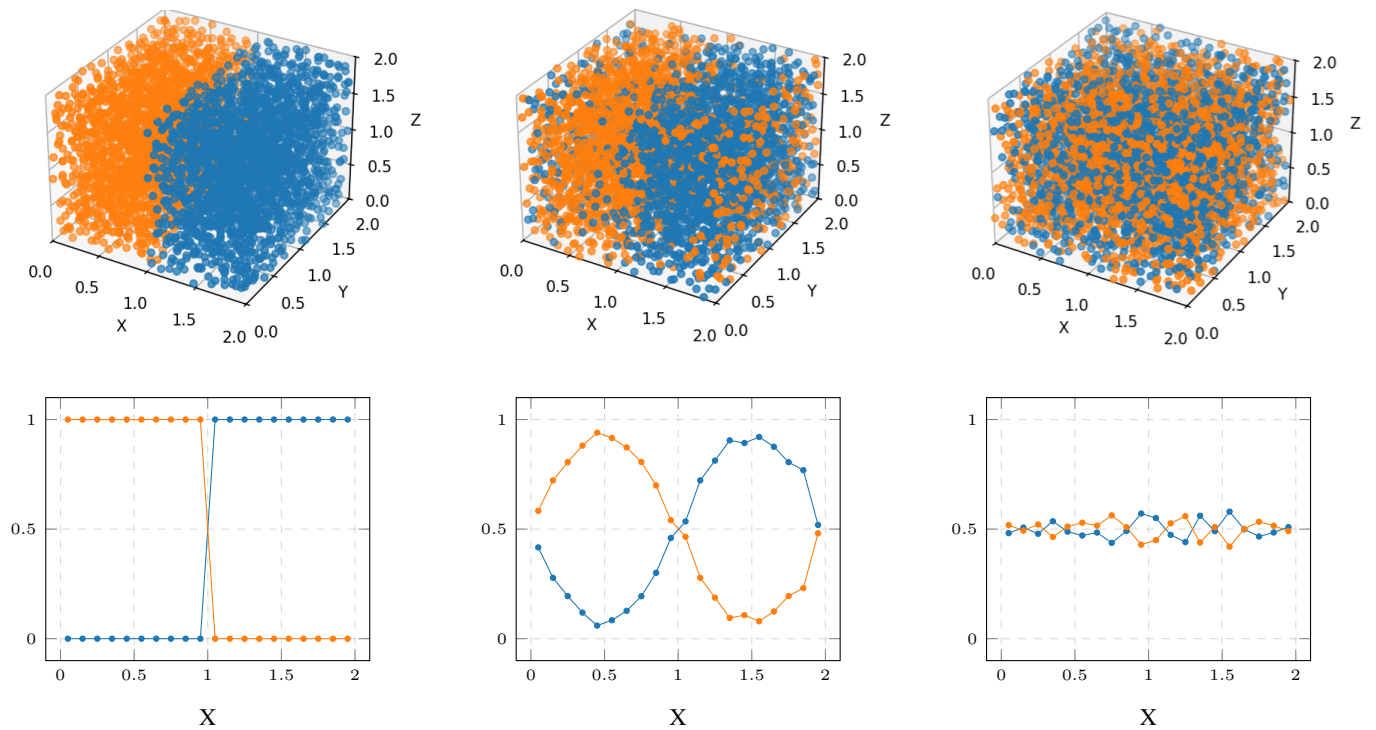


Figure 11: Visualization of the neural network inference simulation of the SELF DIFFUSION case with a bigger domain $L = 2$ at same density. The upper panels show several snapshots of the mixing of particles due to the thermal fluctuations. The lower panels represent the corresponding spatial concentration of red and blue particle profiles averaged over the X axis.

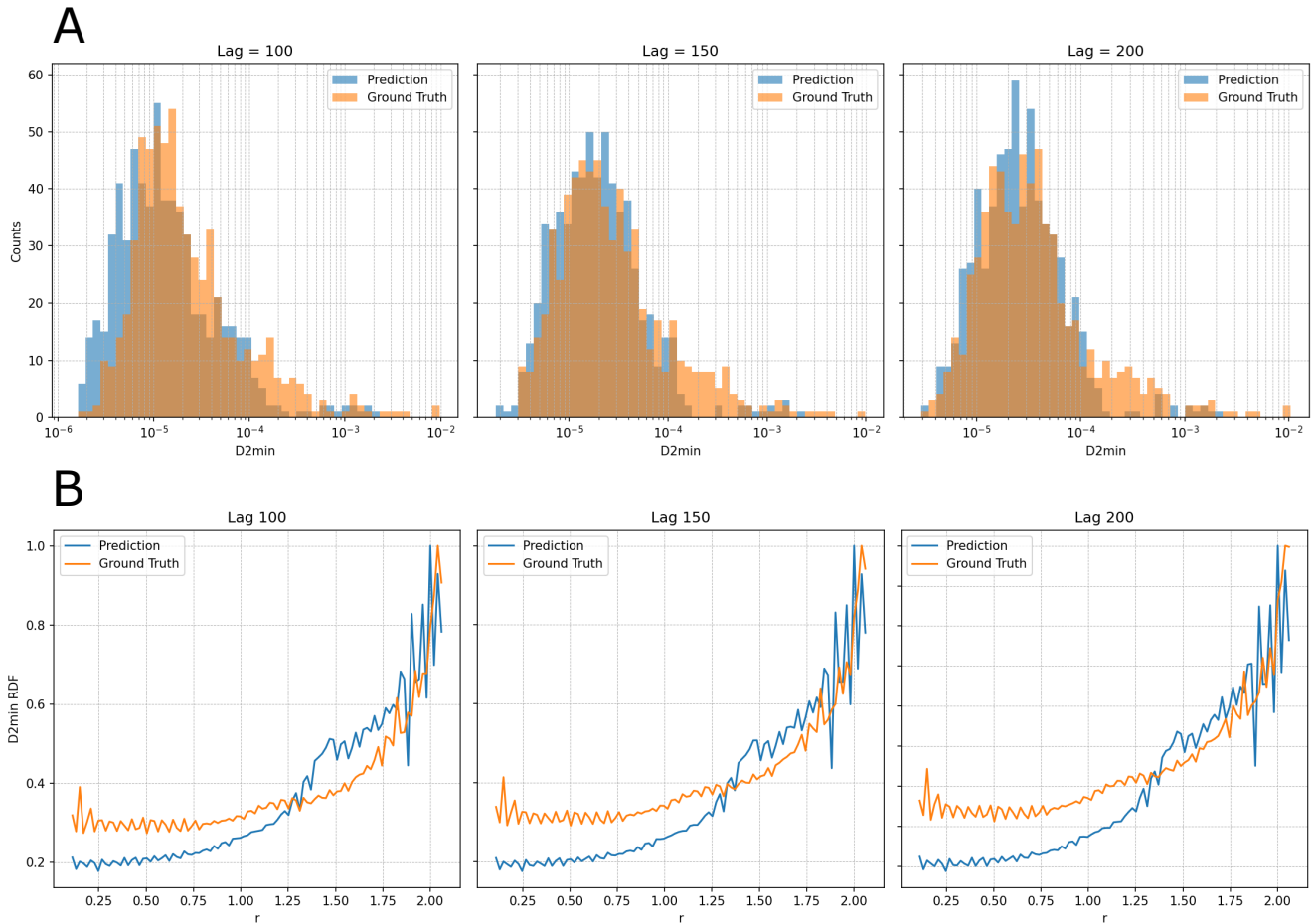


Figure 12: Dynamical properties for the NEEDLE dataset with lag times 100, 150 and 200. (A) Histograms of non-affine displacements D_{\min}^2 for all the domain particles of the prediction and the reference solution. (B) Normalized radial distribution function of the local non-affine displacements.